MPHIL

Electrochemical detection of cancer biomarkers

Zhurauski, Pavel

Award date:
2017

Awarding institution:
University of Bath

Electrochemical detection of cancer biomarkers

Pavel Zhurauski

A thesis submitted for the degree of Master of Philosophy

University of Bath

Department of Electronic and Electrical Engineering

May 2017

Table of contents

Alla mia amatissima Famiglia……

Anastasia, Giacomo ed Elena!

Acknowledgements

I would have a very long list of people to thank and to include in this list, but I feel this time, to be honest with myself and to express the gratitude maybe for few but absolutely crucial people for me to achieve this goal. The most important for different reasons and which are not absolutely just academically professional my supervisor, project leader, friend and definitely a person who I will bring in the heart for the rest of my life, Dr Pedro Estrela. I will never forget my super, Indian friends Pawan and Nikhil who represented the smile and constant support in every kind of situation. Our relation from colleagues became immediately a deep friendship. Thank you, guys! Thanks to my friend Jules always exemplary, my friend Sunil always wise and definitely my lovely girls Marina and Sherife. Thanks, Nello, nice, nice moments together! Thank you to all other guys from Bath.

Special thanks to my lovely PROSENSE group. I met really fantastic people who I will never forget and will always be grateful for fantastic moments passed together.

At last but not least I would like to thank Kim and Pete, the fantastic family who treated me as a prince during my stay in Bath. My darling Simone, I am not forgetting you, don’t be worried.

Thank you all, Grazie tutti. Spasibo vsem, Obrigado todos.!

Pavel

List of Publications

1. Jolly, P., Batistuti, M.R., Miodek, A., **Zhurauski, P.,** Mulato, M., Lindsay, M.A. and Estrela, P., 2017. Corrigendum: Highly sensitive dual mode electrochemical platform for microRNA detection. *Scientific reports*, 7, p.41110.
2. Jolly, P., **Zhurauski, P.,** Hammond, J., Miodek, A., Liébana, S., Bertok, T., Drago, G-A., Tkac, J., & Estrela, P., 2017. Self-assembled aptamer modified redox activated gold nanoparticles for cancer biomarker detection. *Sensors and Actuators B: Chemical.* vol 251, pp 637-643.
3. Arya, S., **Zhurauski, P.,** Jolly P., Batistuti, M., Mulato, M., & Estrela, P., 2017. Capacitive aptasensor based on interdigitated electrode for breast cancer detection in undiluted human serum. Submitted to *Biosensors and Bioelectronics*.
4. **Zhurauski, P.,** Arya, S., P., Jolly P., Tiede, C., Tomlinson, D. C., Ferrigno, P. K., & Estrela, P., 2017. Sensitive and selective Affimer-modified interdigitated electrode-based capacitive biosensor for tumour markers. Submitted to *ACS Sensors*.

Abstract

Early diagnosis of cancer is crucial for the successful treatment of the disease. Highly sensitive methods are urgently needed for measuring cancer diagnosis markers present at ultra-low levels during early stages of the disease. Such methods should facilitate early detection and an adequate selection of the treatment of diseases in order to achieve increased patient survival rates. Existing diagnostic tests (e.g., ELISA) are not sensitive enough, detecting proteins at levels corresponding to advanced stages of the disease. Smaller, faster, and cheaper (one-step) devices are highly desired for replacing time-consuming laboratory analyses. Making analytical results available at the patient's bedside within a few minutes will greatly improve the monitoring of cancer progress and patient therapy.

Advances in molecular biology have led to a deeper understanding of potential biomarkers that can be used for cancer diagnosis. The realisation of point-of-care cancer diagnostics thus requires proper attention to the major challenge of multi-target detection. Arrays of biosensors, detecting protein signature patterns or multiple DNA mutations, can be used to help screening and guide treatment. Innovative biosensor strategies would allow cancer testing to be performed more rapidly, inexpensively, and reliably in a decentralised setting. This particular thesis will discuss the use of electrochemical biosensors for molecular detection and the prospects and challenges of using such devices for point-of-care (POC) cancer diagnostics.

List of abbreviations

AFM	Atomic Force Microscopy
AuNPs	Au nanoparticles
CPE	Constant phase element
CV	Cyclic voltammetry
DNA	Deoxyribonucleic acid
DPV	Differential pulse voltammetry
EDL	Electrochemical double layer
EIS	Electrochemical impedance spectroscopy
ELISA	Enzyme-linked immunosorbent assay
Fc	6-(ferrocenyl)hexanethiol
FRA	Frequency-response analyser
GNP	Gold nanoparticle
GIST	Gastrointentinal Stromal Tumour
HSA	Human serum albumin
IDE	Interdigitated electrodes
IHP	Inner Helmholtz plane
LOD	Limit of detection
LOQ	Limit of quantitation
MCH	6-mercapto-1-hexanol
OHP	Outer Helmholtz plane
PBS	Phosphate-buffered saline
PEG	Polyethylene-glycol
PSA	Prostate specific antigen
SAM	Self-assembled monolayer
SEM	Scanning electron microscopy
SPR	Surface plasmon resonance

Chapter 1. Introduction

A significant increase in interest related to biosensors has been observed since the end of the 1980s. Biosensors are small intricate devices utilising biochemical recognition for the selective analysis of specific molecules. The key roles of a biosensor include: recognition of analytes, signal transduction and electronic signal readout. Biosensors are an exciting area of opportunity; promising advanced specificity, speed, portability and low cost. This offers an important opportunity for multiple decentralised clinical tests, e.g., physician's offices, emergency clinics, bedside monitoring and self-testing.

Research in the field of biosensors has seen a literature bias specifically towards electrochemical sensors (Turner et al., 1986; Wang, 2000a). Possibly due to the inexpensive nature of the device, while offering a superior accuracy and sensitivity for efficient patient diagnoses. An electrochemical biosensor is any device that utilises a combination of a biological recognition event and electrode transducer, in order to produce a useful electrical signal. The most frequently used transducers found in combination with electrochemical devices are amperometric and potentiometric. In an amperometric device, a signal is obtained by applying a constant potential and observing the current associated with the reduction or oxidation of a reactive species involved in a bio-recognition event. A potentiometric transducer converts a bio-recognition event into a potential signal related to the use of ion-selective electrodes (ISE). Amperometric devices are likely to be viewed as a more efficient option due to higher sensitivity and a wider linear range. Leading research on sensing concepts along with recent technological advancements has made possible the wide range of clinical applications of amperometric devices (Wang, 1999). The advantages of electrical bioassays in modern use allow a strong potential rivalry between the most advanced optical protocols already in place. For example, miniaturisation allows for the high-density packing of microscopic electrode transducers on such a small footprint as a biochip device, giving higher-density arrays.

This thesis will focus on the development of multiple electrochemical devices utilising a number of bio-recognition molecules as DNA aptamers and affimers for label-free

detection of cancer biomarkers. Significant detection results were obtained by optimising the recognition layer surface chemistry of these devices. Specifically focusing on the structure of the self-assembled monolayer (SAM) and the distribution of molecular probes on the electrodes surface.

Primarily, this work details the development of the binding structures in order to prevent non-specific binding during analyte detection. The key electrochemical assays used for analysis were electrochemical impedance spectroscopy (EIS) (Faradaic and non-Faradaic configurations) for impedimetric detection as well as square wave voltammetry (SWV) for amperometric detection. Additionally, cyclic voltammetry (CV) was utilised for the analysis of the formation of layers and quantification of the volume of the probe on the surface of an electrode. Two sensing electrodes were used within this research, covered with a gold surface, including interdigitated electrodes and macroelectrodes.

The contained chapters will comprise the work of several scientific publications which is the result of previously carried out research. The first investigates the redox activated self-assembled monolayers which have always been a key idea in the fabrication of biosensors. To make the biosensor more effective and sensitive, a number of nanoparticles, such as Au nanoparticles (AuNPs) have been utilised. Given that the optimisation of redox marker species and probes has been a key focus for the detection of analytes, there has been a continuing interest in methods implementing redox markers. Here, a novel method for the assembly of a label-free impedimetric and amperometric aptasensors will be reported, using surface chemistry to utilise AuNPs and attach them to a Au planar surface.

Outline:

As mentioned earlier, this thesis is a presentation of the development of multiple electrochemical detection platforms for molecular diagnostic applications. This project is a sub-project of the Marie Curie Initial Training Network-PROSENSE, where the focus is on parallel sensing for cancer diagnostics. The thesis could be

broadly divided into three major sections describing three different biosensors for the detection of three different biomarkers for either prostate and breast cancer.

The main objectives of the thesis are:

1. Development of an impedimetric aptamer-based biosensor for the detection of prostate specific antigen; a biomarker for prostate cancer.

2. Development of an aptamer-based biosensor for the detection of Her2; a biomarker for breast cancer

3. Development of an affimer-based biosensor for the detection of Her4; a biomarker for gastrointestinal stromal tumour

To begin with, the current chapter will detail and describe the fundamentals and theory of biosensing. It will present all the techniques that have been utilised for the development of biosensors. It will also highlight the types of bio-recognition probes that have been utilised along with surface chemistry techniques.

Both DNA aptamers and affimers are synthetic alternatives to antibodies, which can be generated with high affinity and specificity to a wide range of molecules. Chapter 3 will discuss the development of an impedimetric aptasensor for the detection of prostate specific antigen (PSA), a biomarker for prostate cancer. This particular study is a progressive study from the previously reported aptasensor that was based on a standard binary SAM on planar Au surface. An anti-PSA DNA aptamer was co-immobilised with either 6-mercapto-1-hexanol (MCH) or 6-(ferrocenyl) hexanethiol (FcSH) for both impedimetric or amperometric detection, respectively. It was shown that the use of AuNPs enables a significant improvement in the limit of impedimetric detection as compared to a standard binary self-assembled monolayer aptasensor. A PSA detection of as low as 10 pg/ml was achieved with a dynamic range from 10 pg/ml to 10 ng/ml, well within the clinically relevant values, whilst retaining the high specificity of analysis in both physiological buffer and human plasma spiked samples. A new approach can, therefore, be reported to pattern ferrocene crowned Au nanoparticles to create redox environments for the development of aptasensors.

The following two chapters will detail electrochemical detection by monitoring the changes in the capacitance of the system. Such an approach was realised by performing electrochemical impedance spectroscopy (EIS) technique. Special attention is given to the surface chemistry, which has a very simple configuration involving DNA aptamers and affimers as probes. New DNA aptamer-modified and affimer-modified interdigitated electrodes for use as capacitive biosensors have been developed for detection of Her2 (breast cancer biomarker) and Her4 (gastrointestinal stromal tumour biomarker) in undiluted serum. It is important to mention that unlike the previous chapters, these two chapters are based on the use of interdigitated electrodes for increased sensitivity.

A thiol-terminated DNA aptamer with an affinity for Her2 and a pre-modified cysteine-terminated affimer with a high affinity for Her4 were used as bio-recognition probes via self-assembly on interdigitated Au electrodes. Non-specific binding was prevented by blocking free spaces on the surface, starting with phosphate-buffered saline-tween20 blocker. Sensors were characterised using cyclic voltammetry (CV), electrochemical impedance spectroscopy (EIS), atomic force microscopy (AFM) and contact angle studies. Non-Faradic EIS measurements were utilised to investigate the sensor performance by monitoring the changes in capacitance.

The aptasensor exhibited linear detection for Her2 from 1 pM to 100 nM in physiological buffer and undiluted serum with a limit of detection of 0.86 pM and 0.89 pM in buffer and serum, respectively. An association constant of 0.066 $(pM)^{-1}$ indicated high affinity of the surface bound aptamer for Her2.

The affi-sensor demonstrated high sensitivity with a broad dynamic range from 1 pM to 100 nM with a limit of detection of 0.33 pM and 0.97 pM in buffer and serum, respectively. Furthermore, the affi-sensor demonstrated excellent specificity for other serum proteins, suggesting possible resilience to non-specific binding. The sensing ability of the affi-sensor in undiluted serum suggests its potential for a new range of affimer based sensors.

The results may open the way to develop other DNA aptamer- and affimer-based biosensors for protein biomarker detection in undiluted serum. The results and the

advantages of the adopted systems will be discussed in detail and will also be discussed alongside possible solutions for future work and utility of these electrochemical sensors.

The final chapter will summarise the work presented in this thesis and will draw light on the future work.

1.1 Electrochemical biosensors

In general, a device that registers and converts physical, biological or chemical changes into a measurable signal is called a sensor. A sensor typically contains a recognition element that enables a very selective response to a target, or at least with minimal interferences from other sample components. The transducer or a detector device is a primary component of a sensor that registers the recognition event and converts it into a signal. Lastly, a signal processor processes the signal and often amplifies it before converting and displaying a user-friendly data output.

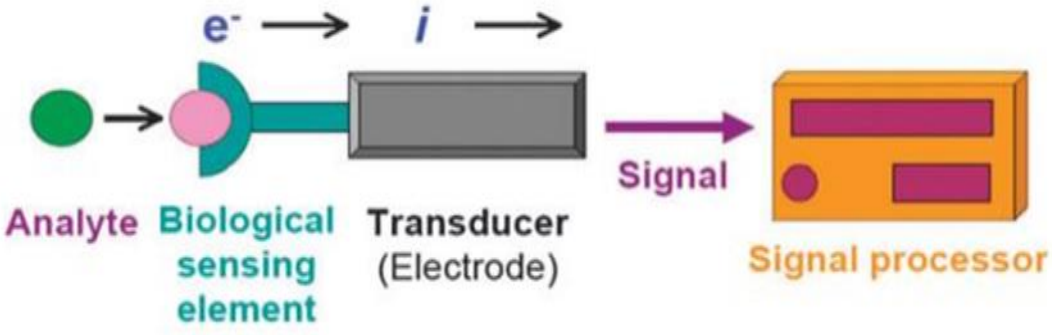

Figure 1.1 A schematic of a biosensor with an electrochemical transducer

Among various kinds of sensor, the electrochemical sensor can be considered a subclass of chemical sensors. An electrochemical sensor coupled with a biological recognition unit (Figure 1.1) is usually employed to enhance the sensitivity with the high specificity of biological recognition processes. Such a device is termed an 'electrochemical biosensor'. These biosensors contain a specific biological recognition element (which can comprise of enzymes, proteins, antibodies, nucleic acids, cells, tissues or receptors) that can selectively react or bind with their respective

target analyte in the sample solution and produce an electrochemical signal that can be directly or indirectly related to the concentration of the analyte under study.

Based on the kind of biological recognition event, electrochemical biosensors could be further subdivided into two main categories; biocatalytic devices and affinity sensors. For instance, biocatalytic-based biosensors consist of enzymes, whole cells or tissue slices as a recognition element that can selectively recognise the target analyte and produce electroactive species as a product of the reaction. A well-established example of an enzyme-based biosensor is the glucose sensor. Here the enzyme 'glucose oxidase' oxidises the glucose such that hydrogen peroxide is released as a product of the reaction which in turn are oxidised on the surface of the electrode, producing electrons which are detected as an electrical current (Hammond et al. 2016). On the other hand, affinity-based biosensors rely on biological components such as an antibody, nucleic acid, or a receptor that can selectively interact and bind with its specific target with high affinity. Some examples of affinity-based sensors are Immunosensors and DNA hybridization biosensors. This thesis will focus on affinity-based sensors with two different kinds of receptors, namely aptamers and affimers. As a field of study, biosensors comprise of an interdisciplinary field of study that is currently one of the most active areas of research in analytical chemistry. There are many advantages of employing a biosensor. For instance, biosensors could eliminate the need for pre-sample preparation and therefore, reduce both time and cost. In general, the performance of a biosensor is experimentally evaluated based on its sensitivity, limit of detection, linear and dynamic ranges, reproducibility or precision of the response, selectivity and its response in the presence of interferences.

1.2 Electrochemical detection techniques

This section will present the different types of electrochemical techniques that have been employed in the biosensor development. Although electrochemical impedance spectroscopy has been used as the main detection technique, other techniques such as square wave voltammetry (SWV) and cyclic voltammetry (CV) has also been presented.

1.2.1 Electrochemical Impedance Spectroscopy (EIS)

Electrochemical impedance spectroscopy (EIS) is a label-free and sensitive electrochemical technique that has been extensively used as a detection technique to develop novel biosensors for various applications including molecular diagnostics. In brief, it measures the changes in the impedance caused by the binding event that occurs at the interface of the electrode surface and the electrolyte caused by the change in electrical properties due to the target. (Bond and Scholz 2010; Lasia 2002).

EIS measurements are based on Faradaic processes that employ a redox couple in an equimolar concentration of both reduced and oxidised forms in order to simplify the analysis. In principle, a Faradaic process is one where an electrochemical reaction results in the transfer of charge (electrons) across the interface of the working electrode and the bulk electrolyte solution. Typically, to perform an EIS measurement, a small alternating current (AC) voltage is applied which is superimposed onto a formal potential of the respective redox couple.

By utilising a redox couple, charge transfer resistance can be measured using EIS. This is an indicator of how easily the redox couple can reach the electrode surface from the electrolyte solution. An EIS measurement is usually performed by scanning in a broad range of frequencies. In this thesis, we have used a frequency range spanning from 100 mHz to 100 kHz. Such a measurement was performed using a potentiostat comprising of a frequency response analyser (FRA). It is worth mentioning that although EIS measurements presented in this thesis investigates the full frequency span response, it is possible to monitor a single frequency which could be easily implemented in a practical low-cost biosensor.

EIS is a measure of the current flowing between the electrodes (working electrode and the counter electrode) into the electrolyte solution of the cell. Moreover, ‘spectroscopy’ is a term that refers to the measurements that have been recorded by scanning a range of frequencies of the AC signal. As mentioned earlier, a small AC voltage (equal to the formal potential of the redox couple) is applied between the electrodes, to maintain a thermodynamic equilibrium at the electrochemical interface.

As a result, there is an easy separation of the contributions from mass transfer and electron transfer. A typical sinusoidal voltage signal as a function of time (*V(t)*) and can be expressed as:

$$V(t) = V_0 \sin(\omega t)$$

Equation 1.1

Where, V_0 is the amplitude of the voltage and ω is the angular frequency ($\omega = 2\pi f$, where f refers to the frequency in Hertz (Hz)). Because of the applied voltage V(t), an AC current signal is produced and recorded (*I(t)*) as a function of time. *I(t)* recorded can be further expressed as:

$$I(t) = I_0 \sin(\omega t + \varphi)$$

Equation 1.2

Where I_0 is the amplitude of the current and φ is the phase angle which depends on the respective impedance of the system under investigation. Moreover, the process of applied voltage and the measured current output can be represented as shown in Figure 1.2:

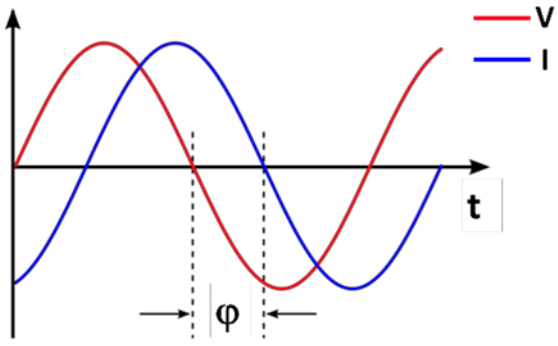

Figure 1.2 AC signal of applied voltage and obtained current response

The impedance measured is represented by both the real and the imaginary parts of the impedance. Using Ohms' law, the impedance (Z) can be determined from Equation 1.1.and Equation 1.2:

$$Z = \frac{V_t}{I_t} = \frac{V_0 \sin(\omega t)}{I_0 \sin(\omega t + \varphi)} = Z_0 \frac{\sin(\omega t)}{\sin(\omega t + \varphi)}$$

Equation 1.3

However, since the impedance measured is a complex impedance, Euler's expression is employed as:

$$\exp(j\varphi) = cos\varphi + jsin(\varphi)$$

Equation 1.4

Where j is an imaginary number equal to $(-1)^{1/2}$. Furthermore, both Equation 1.1 and Equation 1.2 can be further processed as a function of time and represented as:

$$V(t) = V_0 exp(j\omega t)$$

Equation 1.5

$$I(t) = I_0 exp(j\omega t + j\varphi)$$

Equation 1.6

As a result, and by using equations Equation 1.5, Equation 1.6 and Equation 1.4 in Equation 1.3, the impedance can be expressed as:

$$Z = \frac{V_t}{I_t} = Z_0 \exp(j\varphi) = Z_0(cos\varphi + jsin\varphi) = Z' + jZ''$$

Equation 1.7

Where, the real part of impedance (Z') is typically an outcome of the resistance to the flow of current by the circuit (also associated with resistive part), whereas the

electrical energy storage ability of the circuit forms the imaginary part (also referred to the capacitive part) of the impedance (*Z''*).

Furthermore, for a specific system, the impedance of the electrochemical interface can be interpreted using a specific equivalent electrical circuit. Among many types of circuits available, Randles equivalent circuit (Figure 1.3) is the most common circuit used. A Randles circuit typically includes the resistance of the solution (R_s), the resistance for electron transfer (also called charge transfer resistance, R_{ct}), the double layer capacitance (C_{dl}) and a Warburg impedance element (W). Although the Warburg element only provides information about the diffusion of the redox couple, the R_s values depend only on the solution together with the distance between the working electrode (WE) and the counter electrode (CE). In a biosensor employing a biological element, the ideal capacitor element (n=1) is replaced by a Constant Phase Element (CPE) which models the capacitive behaviour of the double layer; however, the deviations from an ideal capacitance are reasonably small.

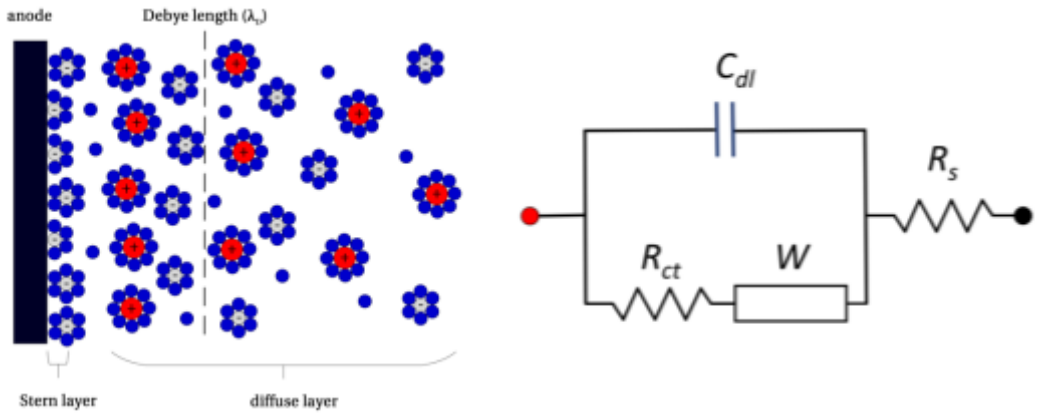

Figure 1.3: representation of the electric double layer (Hammond 2017) and the Randles equivalent circuit, where R_s is the solution resistance, R_{ct} is the charge transfer resistance (impedance), C_{dl} is the double layer capacitance and W is the Warburg impedance element

Furthermore, the impedance of the CPE can be expressed by Equation 1.8:

$$Z_{CPE} = Y_0(j\omega)^{-\alpha}$$

Equation 1.8

Where Y_0 is the magnitude of admittance, α is an exponent with a value between 0 and 1 (For a CPE, $\alpha < 1$). Using Z_{CPE}, an estimation of the C_{dl} can be obtained by using the following relationship (Hsu and Mansfeld 2001):

$$C_{DL} = \frac{(Y_O R_{ct})^{1/\alpha}}{R_{ct}}$$

Equation 1.9

As mentioned earlier, the Warburg impedance element (*W*) represents the pseudo-impedance which is due to the mass transfer effect (the diffusion of ions from the bulk solution to the electrode surface). Since Faradaic currents are affected by diffusion effects, the value of *W* at lower frequencies becomes predominant with a phase angle of 45˚ for a diffusion-controlled Faradaic process.

The results of an EIS measurement are typically represented in a Nyquist plot (Figure 1.4) showing both real and imaginary part of the impedance. Such a plot enables a direct comparison of the charge transfer resistance value given by the diameter of the semicircle along the *Z'* axes.

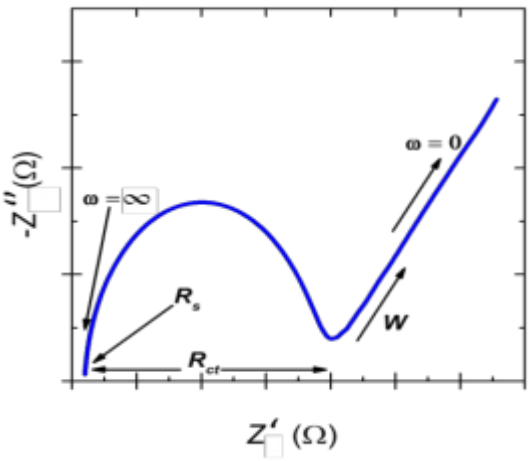

Figure 1.4 Typical Nyquist Plot

1.2.1.1 Faradaic EIS

A redox couple utilised in a typical Faradaic EIS experiment contains both the reduced and oxidised forms (e.g., $[Fe(CN)_6]^{3-/4-}$ which was used in this study). The redox probes are employed to facilitate the charge transfer (the Faradaic current) that can flow through the working electrode and easily detected by the potentiostat. It is worth mentioning that the equilibrium potential (also termed the formal potential) across the working electrode (WE) and the reference electrode (RE) is not only dependent upon the ratio between the concentrations of the oxidised and reduced forms of the redox couple, but also on the type of reference electrode employed. In the current studies presented in this thesis, a (Ag/AgCl) RE was used.

Typical Faradaic EIS experiments consist of recording the variations caused due to a binding event that can either produce a higher or lower blocking effect. As a result, there are changes to the accessibility of the redox markers from the electrolyte solution (bulk electrolyte) to the electrode surface. For instance, the impedance of a probed system can increase because of the blocking effect generated due to the binding of a bulky target that can result in an increased electrostatic barrier that obstructs the redox probes from approaching the electrode surface. On the other hand, a reduction in the impedance can be due to a decrease in the electrostatic barrier from other target molecules (e.g., if molecules having opposite sign with respect to the redox probes are bound on the surface). However, due to the complexity of the biological probes and their respective binding events, more complicated situations can arise due to a combination of different effects (for instance, binding of bulky target and screening of charges near the electrode surface can occur at the same time).

1.2.1.2 Non-Faradaic EIS

Unlike Faradaic EIS, non-Faradaic EIS is performed in the absence of redox markers. It is important to outline that in the case of non-Faradaic processes, the focus is given to the analysis of the double layer C_{dl} rather than R_{ct}. Indeed, in non-Faradaic experiments the charge transfer can be neglected as there are no redox markers in the solution and the main contribution to the impedance is given by the capacitive

component which is due to the charging and discharging effects (Tsouti et al., 2011). In such cases, a generic EIS experiment will have an impedance described as:

$$Z = Z' + jZ''$$

Equation 1.10

a complex capacitance can be defined and is represented by the following relationship:

$$C^* = \frac{1}{j\omega Z}$$

Equation 1.11

Such a relationship defines the changes in capacitance at the single frequency. As a result, a lot of information is lost. To address this, research groups have reported an alternative approach for calculating the capacitance of the electrochemical cell (Formisano et al., 2015; Jolly et al., 2015) termed a complex capacitance and can be expressed by using Equation 1.10 in Equation 1.11 to produce:

$$C^* = -\frac{z''}{\omega|Z|^2} - j\frac{z'}{\omega|Z|^2} = C' + jC''$$

Equation 1.12

Calculating C' and C'' from the respective measured values of Z' and Z'', the complex capacitance can be plotted (Figure 1.5). As a result, the diameter of the semicircle provides the estimate of the capacitance of the system.

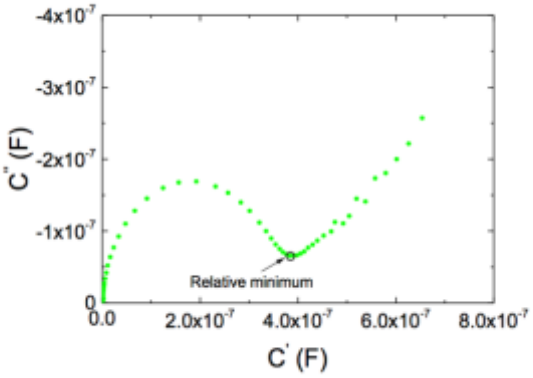

Figure 1.5 Example of complex capacitance plot. The circled point indicates the relative minimum of the imaginary part of capacitance at which the real part of the capacitance can be sampled

Another approach that has been reported in the literature for the C_{dl} calculation in the non-Faradaic experiment is often based on the assumption where the R_{ct} and the diffusion effects can be neglected (Couniot et al., 2015). Therefore, the equivalent electrical circuit of the system under study is simplified (a resistor in series with a capacitor) as shown in Figure 1.6:

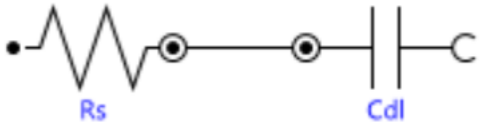

Figure 1.6 Electrical equivalent circuit for non-Faradaic measurements based on the assumption that charge transfer processes and diffusion contributions can be neglected

As a result of the simplification, the total impedance is given by:

$$Z = Z' + jZ'' \cong R_s^* - j\frac{1}{\omega C_{DL}^*}$$

Equation 1.13

There is a handful of studies that are based on the use of non-Faradaic EIS experiments to monitor the changes in capacitance of the system (Tsouti et al., 2011; Berggren et al., 2001, Daniels and Pourmand, 2007). These studies were stimulated by the first

capacitive biosensor to be reported in 1986 by Newman and co-workers. The biosensor was based on interdigitated electrodes (IDEs). At present, most capacitive sensors are based on a combination of IDEs and electrode-electrolyte interfaces. Sensors based on electrode-solution interfaces (as those reported in the present dissertation), instead, exploit the changes in the distance between the separation planes of the pseudo-capacitor and the displacement of ions and solvated molecules from the sensing surface (Tsouti et al., 2011; Daniels and Pourmand, 2007).

One key aspect of capacitive sensors based on electrode-electrolyte interfaces is to provide a homogeneous and compact layer on the surface of the electrode providing an enhanced insulation effect. Such a layer can be achieved by fabricating a compact and defect-free self-assembled monolayer (SAM) that massively prevents leakage current. The reason behind minimising leakage currents is to avoid short-circuiting the metal and solution phases resulting into a loss of sensitivity (Berggren et al., 2001).

Literature has reported multiple reasons that attribute the signal changes obtained to various factors such as changes in the dielectric properties, the displacement of water molecules, electrostatic repulsions between immobilised samples and ions in solution, the change of the molecular conformation onto the surface electrodes and so on. It is worth highlighting that there has been no self-contained explanation to the changes in the capacitance and therefore, different research groups have also reported contradicting results which are supported by their own explanations and references.

1.2.2 Square Wave Voltammetry

This thesis will also present square wave voltammetry (SWV) as a detection technique. Together with EIS, an amperometric technique like SWV has been used to provide a dual-mode detection platform. SWV is a technique that can circumvent the capacitive currents and monitors only Faradaic current, thus increasing the sensitivity of the system (Bard and Faulkner 1980) Figure 1.7:

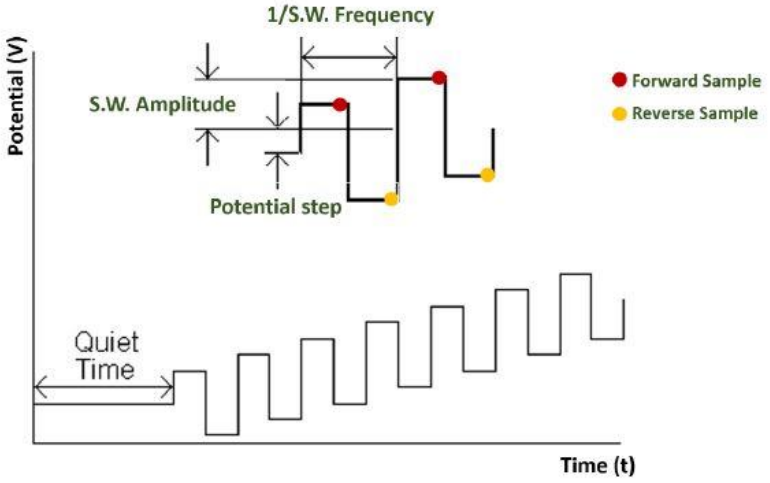

Figure 1.7 Square Wave voltammetry potential variation waveform

In a typical SWV experiment, The excitation signal consists of repetitive symmetrical square wave pulses of a fixed amplitude V_{sw}. Such pulses are superimposed on a staircase wave of step height of a fixed potential (ΔV) and with a defined pulse period (t). As a result, the forward pulse of the square wave coincides with the staircase step in a SWV experiment. Using such a system, the net current, i_{net}, is calculated by the system by taking into consideration, the difference between the forward and reverse current ($i_{total} - i_{reverse}$). This net current is calculated at the end of each half cycle respectively. Using a subtraction process, the background current is suppressed. As a result, the peak current height obtained can be considered to be a result of the redox reaction (Faradaic process) which is directly proportional to the concentration of the electroactive species.

1.2.3 Cyclic voltammetry

Another technique that has been presented in this thesis is Cyclic voltammetry (CV). It is worth mentioning that CV is widely adopted as a characterization technique. Such a measurement is performed by imposing a varying electrode potential at the WE (potential sweep) between two set potential limits as shown in Figure 1.8 (Bard and Faulkner 1980).

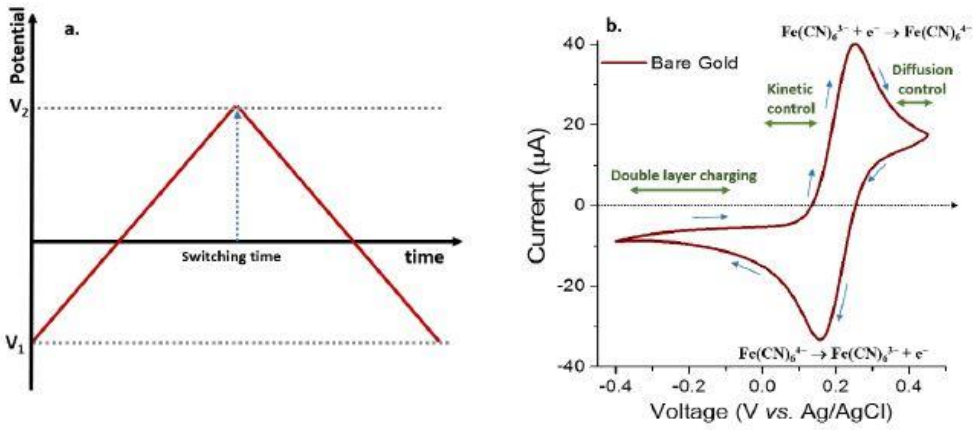

Figure 1.8 Potential plot of a redox reaction diffusing in solution (a); Cyclic voltammetry of a fully reversible redox reaction at the gold working electrode in 10 mM PBS, pH 7.4 containing 10 mM ferro/ferricyanide [Fe(CN)6]3-/4- vs. Ag/AgCl reference electrode

By sweeping the potentials, the electroactive molecules in the solution can lose electrons (oxidation) or gain electrons (reduction) at their respective potential and peaks can be realised in a CV scan. This technique often allows recognition along with quantification (Faradaic peak) of a large number of compounds under study. For instance, in Figure 1.8 when there is an increase in the applied potential across the working electrode (WE) and reaches closer to the reduction potential of the redox marker ($[Fe(CN)_6]^{3-/4-}$), WE loses an electron which is picked up by the redox marker ($[Fe(CN)_6]^{3-/4-}$) and therein, is reduced. Such a reaction causes a flow of electrons from the electrode to the bulk electrolyte solution resulting in the appearance of a reduction peak in the cyclic voltammogram. The opposite reaction occurs when the electrode potential is decreased. Moreover, such a process in the presence of the redox couple where both oxidation and reduction peaks are observed are often associated to a reversible process. A reversible system can be further described by the Randles-Sevčik law:

$$i_p = 0.4436An^{\frac{3}{2}}\left(\frac{F^3DS}{RT}\right)^{\frac{1}{2}}c$$

Equation 1.14

Where A is the active area of the working electrode, n is the number of electrons involved in the redox process, F is the Faraday's constant, D is the diffusion coefficient of the redox species, S is the scan rate, T is temperature and c is the bulk concentration of the redox species. In a CV, certain parameters such as the scan rate, can account for the reversibility of some reactions. In other words, the potential scan can produce a peak current for all analytes that can be reduced in the range of the potential sweep. The current (I) of the system which is measured either continuously or at specific times, is mainly the sum of Faradaic current, I_f, and non-Faradaic current, I_c.

In fact, the current (I) is a function of both potential (E) and time (t). On the other hand, I_c is due to the C_{dl} (charging and discharging of the layer) represented by the interface between the surface layer of the electrode and the adjacent layer of the electrolyte solution given by:

$$I_c = C_{DL}\frac{dv}{dt}$$

Equation 1.15

Where v is the potential applied to the electrode surface. Unlike Faradaic current, the capacitive current depends on the surface of the electrode, scan rate and the composition of the medium. Therefore, it is suggested to have a reasonable low scan rate to avoid non-Faradaic signals. In this dissertation, CV has been employed as a characterisation technique as well as a fabrication technique for the development of the biosensor.

1.3 Other characterisation techniques

For the development of biosensors mentioned in this thesis, techniques like Surface Plasmon Resonance (SPR), atomic force microscopy (AFM), Scanning Electron Microscopy (SEM) and contact angle measurements were also used for characterisation studies.

1.3.1 SPR

In order to understand the efficiency of the probe (molecular interactions) coupled with the surface chemistry employed on a solid surface, Surface Plasmon Resonance (SPR)

offers a powerful tool. SPR comes with an added advantage of not only being a label-free detection but also provides a real-time quantitative data for the molecular interactions under investigation. Typically, an SPR measurement consists of specific probes which are immobilised on the SPR chip (for instance DNA aptamers specific to PSA, Figure 1.9) and the analyte in the buffer solution which is flowed over the SPR chip surface (e.g., PSA). Lastly, the molecular binding events are measured by in real-time by monitoring the changes in the refractive index (RI) near the sensor surface using optical methods.

SPR is an optical phenomenon that takes place when a polarised light hits a thin metal film (in SPR, it is a thin layer of Au on SPR chips) at the interface of media with different RI. At a particular wavelength of light, all the energy is absorbed by the metal and results in the generation of plasmons through proper coupling of incident light to free electrons of the gold metal. Such a phenomenon is established by using an attenuated total reflection technique (ATR). In principle, ATR is a phenomenon where the plasmons are generated by an induced evanescent wave under a specific condition of total internal reflection. This evanescent wave penetrates into the gold metal and decays exponentially, perpendicular to the metal surface into the medium. Usually, the evanescent wave is observed within 300 nm from the sensor surface depending on the Au thickness and RI of the medium over the metal surface. SPR uses this evanescent field to monitor the changes due to the binding event and registers it as a change in RI (Van Der Merwe 2001). SPR technique, in theory, excite and detect oscillations of free electrons which are also known as surface plasmons, using the Kretschmann configuration. Such a configuration employs an incident light which is focused onto a thin metal film through a glass prism and the subsequent reflection is detected by a detector as shown in Figure 1.9.

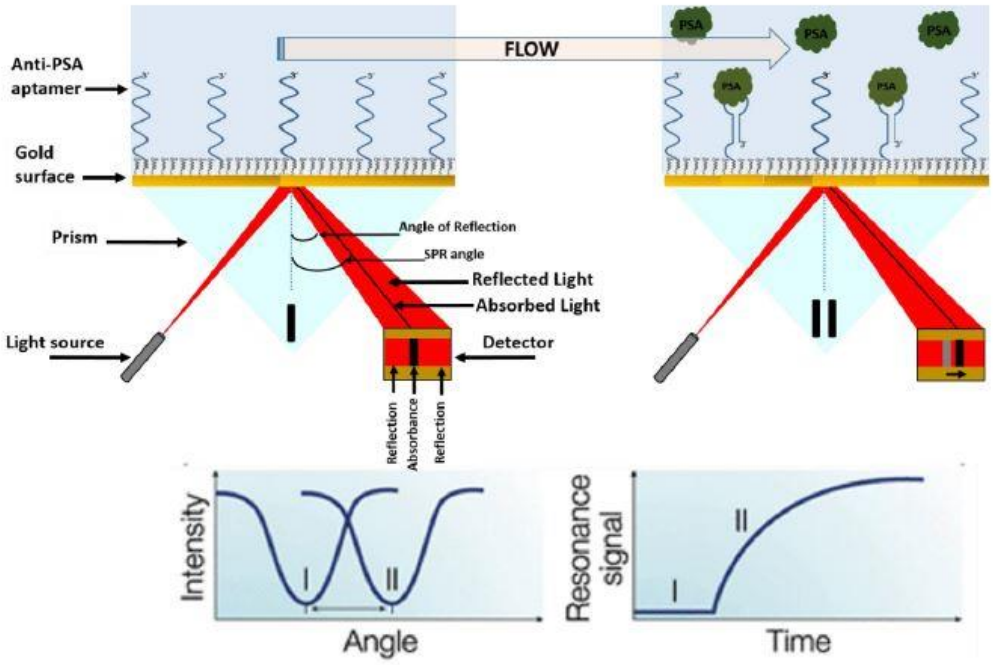

Figure 1.9 Surface Plasmon Resonance schematics (SPR) (Jolly 2016).

As mentioned earlier, at a certain incident angle (total internal reflection), the plasmons resonate with light which is as a result of the absorption of light at that particular angle. This creates a dark band line in the reflected beam (Figure 1.9). This respective dark band line detected can be observed as a dip in SPR reflection intensity. A shift in the reflectivity curve Figure 1.9 represents a binding event taking place either or a conformational change in the molecules bound to the film (like in the case of DNA aptamers). By monitoring this shift *vs.* time, researchers can study molecular binding events and draw conclusions on affinity constants of the probe.

In this dissertation, SPR is used mostly as a characterisation technique to investigate the binding characteristics of probes when restricted to the electrode surface especially for the affimers for Her4 described in Chapter 5.

1.3.2 AFM

The atomic force microscope (AFM) is one kind of scanning probe microscopes (SPM). SPMs are designed to measure local properties, such as height, friction,

magnetism, with a probe. To acquire an image, the SPM raster-scans the probe over a small area of the sample, measuring the local property simultaneously.

AFMs operate by measuring the force between a probe and the sample. Normally, the probe is a sharp tip, which is a 3-6 μm tall pyramid with 15-40 nm end radius, meanwhile, the used one loses its sharpness (Figure 1.10). Though the lateral resolution of AFM is low (~30 nm) due to the convolution, the vertical resolution can be up to 0.1 nm.

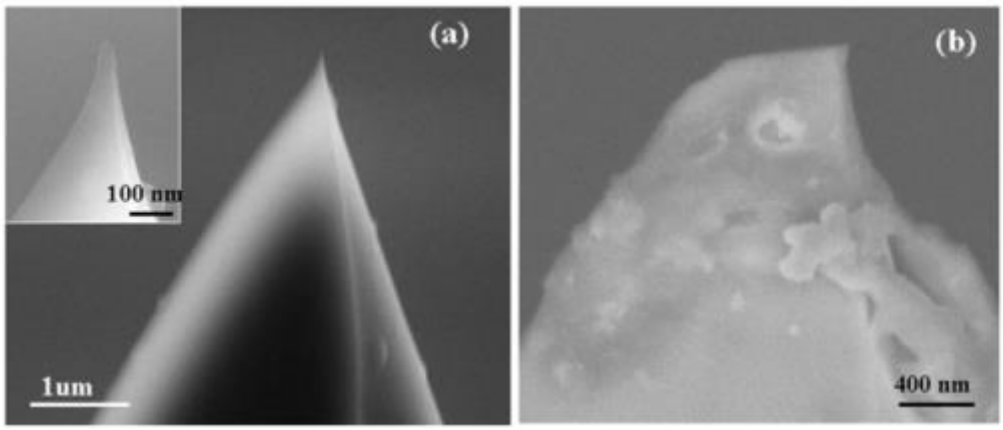

Figure 1.10 New AFM tip (a); Used AFM tip (b)

In the case of an AFM, the vertical and lateral deflections can be measured by the cantilever using the optical lever in order to acquire a good image resolution. The optical lever is operated by reflecting a laser beam on the cantilever. The reflected laser beam later strikes a position-sensitive photodetector consisting of four-segments. Finally, the differences are recorded and presented between the segments of photo-detector of signals. As a result, the signal obtained indicates the position of the laser spot on the detector and thus the angular deflections of the cantilever (Figure 1.11).

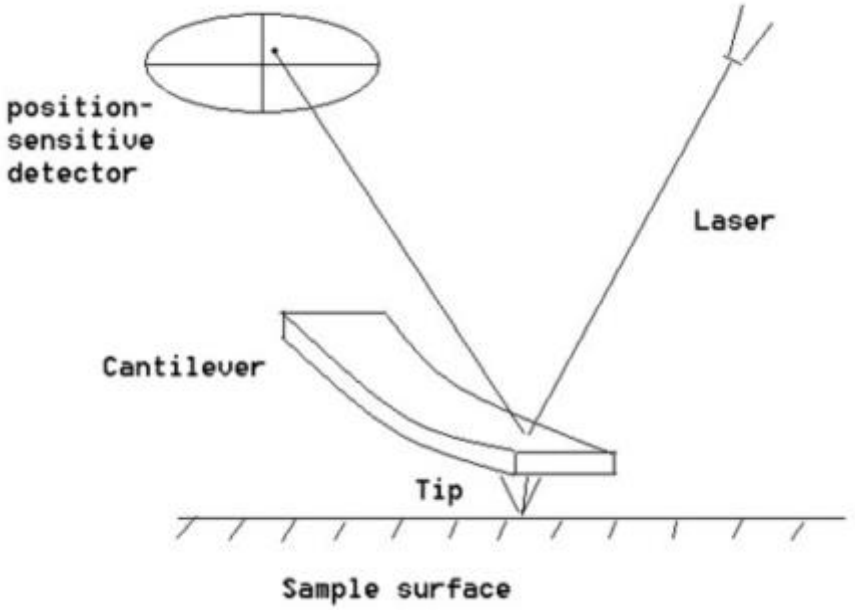

Figure 1.11 AFM is working with an optical lever

When a contact mode AFM is used, a feedback is generated which is used to regulate the force on the sample. As a result, the AFM not only measures the force on the sample under study but also regulates it, allowing acquisition of images at very low forces. The feedback loop consists of the tube scanner that controls the height of the tip; the cantilever and optical lever, which measures the local height of the sample; and a feedback circuit that attempts to keep the cantilever deflection constant by adjusting the voltage applied to the scanner.

1.3.3 SEM

Another surface characterisation technique is the use of a scanning electron microscope (SEM) which uses a focused beam of high-energy electrons. Such a beam is used to generate a variety of signals at the surface of solid specimens under study. The signals that are generated from the electron-sample interactions provides detailed information on external morphology (texture), chemical composition, and crystalline structure and orientation of materials of the sample specimen. Again, data is collected over a selected area of the surface of the sample under study, and a 2-dimensional

image is generated. Typically, areas ranging from 1 cm to 5 μm in width can be imaged in using conventional SEM techniques.

With SEM, a significant amount of kinetic energy is carried by accelerated electrons. Such a huge amount of energy is dissipated as a variety of signals as a result of the electron-sample interaction due to deceleration of the incident electrons in the solid sample. The secondary electrons generated because of the interaction constitutes the signals and also include backscattered electrons (BSE), diffracted backscattered electrons (EBSD that are used to determine crystal structures and orientations of minerals), photons (characteristic X-rays that are used for elemental analysis and continuum X-rays), visible light (cathodoluminescence–CL), and heat. Typically, for imaging samples, secondary electrons and backscattered electrons are used. Briefly, secondary electrons are important for showing morphology and topography on specimen samples and backscattered electrons are important for illustrating contrasts in the composition in the multiphase sample. Furthermore, generation of X-rays is mainly due to the inelastic collisions of the incident electrons with electrons in discrete orbitals (shells) of atoms in the specimen sample. Since the electrons which have been raised to the excited levels have to return to lower energy states, such a process yields X-rays that are of a fixed wavelength (difference in energy levels of electrons in different shells for a given element). As a result, characteristic X-rays are produced for each element in a mineral. It is worth mentioning that the SEM analysis is considered to be ‘non-destructive’; because the X-rays generated by electron interactions do not lead loss of volume in the sample, so it is possible to analyse the same materials repeatedly without any degradation of the sample.

In SEM analysis, sample preparation is often minimal, depending on the nature of the specimen and the output data required. By minimal preparation, it may include the acquisition of a sample that will fit into the SEM chamber and some surface modification to prevent charge build-up on insulating samples. In general, most insulating samples for SEM analysis are coated with a thin layer of conducting material, commonly carbon, gold, or some other metal or alloy to avoid charging of the sample. On the other hand, an electrically insulating sample can be examined without any coating in a SEM instrument capable of ‘low vacuum’ operation.

1.3.4 Contact angle

Finally, the thesis will also present contact angle measurements, this technique has been used to understand the characteristic of the sensor surface, Contact angle measurements provide the wetting properties of the surface under study. It is worth mentioning that every surface has a specific characteristic surface tension. The surface tension of the substrate makes it either hydrophobic or hydrophilic in nature. Upon modification of sensor surfaces, or upon binding of biomolecules to a sensor surface, there are changes in the surface tension of the sensor surface material that can be monitored by observing the spread of a water droplet on it. The angle that the water droplet makes with the sensor surface while it spreads is known as contact angle. Typically, contact angle measurements are simple and employ only simple instrumentation as it requires just a camera, optical lens and a light source to provide the correct contrast. Although information can be attained after surface modification or binding, contact angle measurements do not provide any information on the number of the molecules present on the sensor surface. Therefore, in order to understand whether the changes are due to the specific or non-specific interactions of the molecules on the sensor surface needs to be determined by other detection mechanisms.

1.4 Oligonucleotide and protein-based recognition layer

This section will cover the two different types of probes that were used to develop biosensors that are presented in the following chapters. This thesis will present the use of DNA aptamers (oligonucleotide-based) specific to PSA and Her2 protein biomarker and Affimer (protein-based) specific to Her4 protein biomarker.

1.4.1 DNA aptamers (Oligonucleotide-based probe)

DNA aptamers are simply short single-strand DNA strands (oligonucleotides) that can bind to their target with both high specificity and affinity. In the last two decades, DNA aptamers have gained huge interest as bioreceptors in the development of novel biosensors (aptasensors) or for medical therapeutic applications (Hianik and Wang 2009; Iliuk et al. 2011). DNA aptamers have specificity which is akin or higher than

those of their biological counterpart (antibodies) with dissociation constants (K_d) in the range from micromolar (μM) to picomolar (pM) levels. One of the most important advantages of DNA aptamers in the development of biosensor devices is their high affinity to not only proteins but also to other molecules with very low molecular weight, for example, toxins and drugs (Castillo et al. 2012; Evtugyn et al. 2009). There are a number of advantages of aptamers over antibodies, for example, higher stability. High stability helps aptamers to be suitable for applications in special conditions such as high temperature or extreme pH.

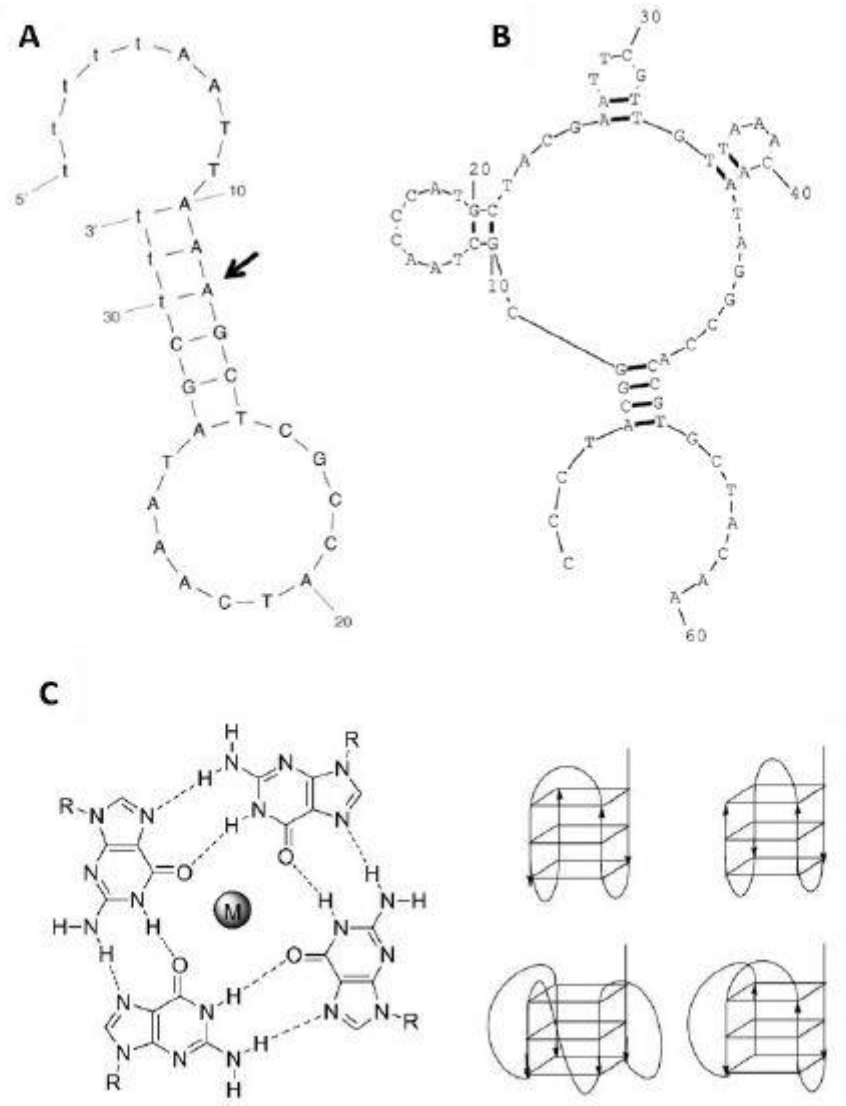

Figure 1.12 Example of aptamer structures: (A) Two-dimensional stem-loop structure of anti-PSA DNA aptamer (Savory et al. 2010); (B) multiple stem-loop structure of anti-AMACR DNA aptamer (Yang et al. 2014); (C) quadruplex structure of anti-thrombin DNA aptamer

Another advantage is that DNA aptamer-based biosensors can be regenerated without loss of integrity and selectivity (Mairal et al. 2008; Tombelli et al. 2005). What is very interesting is that an aptamer can undergo conformational changes upon recognition of its specific target, this property has been widely utilised in the development of novel biosensing applications (Jolly et al. 2015; Radi et al. 2006). Until now, DNA aptamers are known to form loops, stems, hairpins, triplexes or quadruplex structures. Figure

1.12A and Figure 1.12B shows a DNA aptamer specific to PSA in its stable loop configuration and a DNA aptamer raised for AMACR with multiple loop structures, respectively (Savory et al. 2010; Yang et al. 2014). The stem loops' formation is due to the specific interactions between nucleotides which are adenine, and thymine or guanine and cytosine present in DNA aptamer sequence chains. Quadruplexes are formed in DNA aptamer sequences that are rich in guanine and are able to form a four-stranded structure (Figure 1.12C). The quadruplex structure is further stabilised by the presence of a cation, especially potassium, which sits in a central channel between each pair of tetrads.

Furthermore, DNA aptamers can be easily chemically modified by various functional groups, such as thiols, amines or azides as well as biotin groups leading to flexibility in the type of immobilisation to various solid supports. For example, modification of DNA aptamers with thiols allows their attachment onto the Au surface using Au-S (thiol chemistry) interactions (Jolly *et al*. 2015). In another case, there could be more than one modification. For instance, one end of DNA aptamers can be modified with biotin molecule and binding of these biotin modified DNA aptamers could be easily realised on a solid support *via* avidin, streptavidin or neutravidin bridges while, the other end can be modified with ferrocene for electrochemical detection (where ferrocene can be used as a redox marker) (Cavic and Thompson 2002; Centi et al. 2007; Liss et al. 2002; Ostatná et al. 2008).

Since aptamers can be raised with high specificity against different binding sites of the target analyte, it can therefore provide high variability in the development of assay configuration (Figure 1.13) (Hianik and Wang 2009; Song et al. 2008). For example, a simple aptamer-based assay consists of the attachment of aptamers onto a support (in our case it will be the metal surface of the biosensor) and the interactions of aptamer/analyte can be directly monitored (Figure 1.13) (Formisano et al. 2015). With the development in the field of novel assay configuration, classical antibody ELISA has been replaced with aptamer-based ELISA. For instance, sandwich assays could be developed using aptamers which consist of capturing the target analyte by its specific aptamer followed by interactions with another aptamer or antibody as a reporter probe (Figure 1.B, Figure 1.C, and Figure 1.D). Similar to antibody-based (immune sensing)

assays, aptamers can also be modified with nanoparticles (Pavlov et al. 2004) or electrochemical markers (Kang et al. 2008) which enhance the electric signal or allow amplification of the signal.

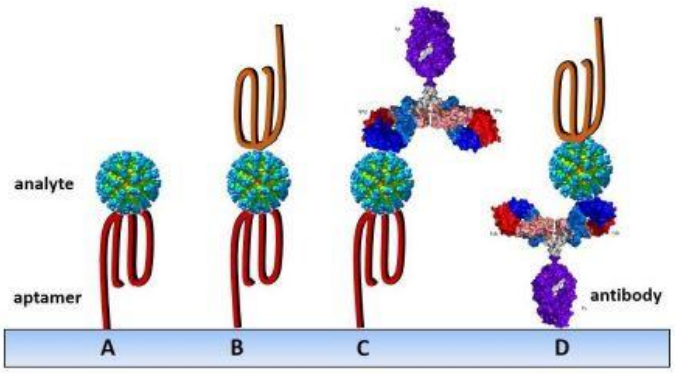

Figure 1.13 Examples of different assays based on aptamers. (A) Capture of analyte by immobilised aptamers. (B) Sandwich type assay with aptamers using two aptamers specific to two different sites of the analyte. (C) Capture of the analyte by the immobilised aptamer while a secondary antibody is used to detect in a modified ELISA format. (D) Capture of analyte by an immobilised antibody while aptamer is used as a secondary probe in a modified ELISA format.

1.4.2 Affimers (protein-based probes)

Affimer molecules typically small, highly stable recombinant proteins that are raised to bind to their respective target molecules (analyte) with similar or higher specificity and affinity to that of antibodies (Figure 1.14). These proteins are engineered non-antibody binding proteins that are basically designed to mimic the role of molecular recognition similar to monoclonal antibodies in multiple applications (Woodman et al. 2005). With the technology developed by protein engineers, it is an attempt to improve the experimental properties of affinity reagents, in order to increase their stability, making them more robust across a range stringent conditions (temperatures and pH), and offer small volumes of the reagent. Moreover, they can be easily expressed to produce high yields in *E.coli* and mammalian cells.

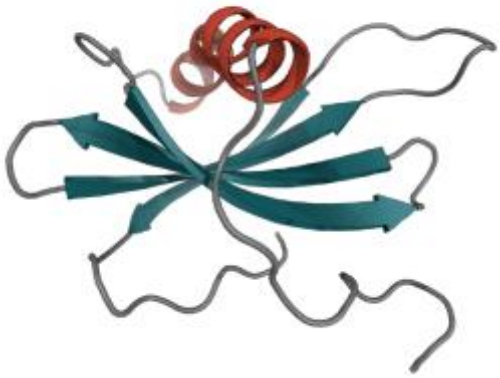

Figure 1.13 The Affimer protein scaffold – showing the two loops and the amino terminus where designer or random peptides can be inserted to create a target-specific binding surface

Affimer proteins typically displays two peptide loops on the protein surface and an N-terminal peptide sequence which is all present in a randomised fashion to bind to the desired target proteins with high affinity and specificity. A protein scaffold is employed to constrain the two peptide sequences in its possible conformation so that there is an increase in the binding affinity and specificity when compared to libraries of free peptides.

To date, a large number of affimer binders have been produced to a number of targets including ubiquitin chains, immunoglobulins, C-reactive protein, interleukin-8, complement C3 and magnetite nanoparticles for their use in molecular recognition applications.

Furthermore, affimers can also be modified to provide different tags and fusion proteins, such as fluorophores, histamine-tag and c-Myc for their use in various research applications including biosensing. Specific cysteine residues have also been introduced to the scaffold protein of the affimer which allows the use of thiol chemistry to bind the affimers to the gold surfaces in the development of biosensors (Sharma et al. 2016).

Affimer technology has been commercialised and developed by Avacta Life Sciences, who are developing these affinity reagents as tools for research and diagnostics and as

biotherapeutics. Chapter 4 will describe the use of affimers on interdigitated Au electrodes for the development of a novel biosensor for the detection of the stromal tumour.

References

Bard, A.J., Faulkner, L.R., 1980. Electrochemical methods: fundamentals and applications. Wiley New York.

Berggren, C., Bjarnason, B., Johansson, G., 2001. Capacitive biosensors. Electroanalysis 13(3), 173-180.

Bond, A.A.M., Scholz, F., 2010. Electroanalytical methods: guide to experiments and applications. Springer

Castillo, G., Trnkova, L., Hrdy, R., Hianik, T., 2012. Impedimetric aptasensor for thrombin recognition based on CD support. Electroanalysis 24(5), 1079-1087.

Cavic, B.A., Thompson, M., 2002. Interfacial nucleic acid chemistry studied by acoustic shear wave propagation. Analytica Chimica Acta 469(1), 101-113.

Centi, S., Tombelli, S., Minunni, M., Mascini, M., 2007. Aptamer-based detection of plasma proteins by an electrochemical assay coupled to magnetic beads. Analytical chemistry 79(4), 1466-1473.

Couniot, N., Afzalian, A., Van Overstraeten-Schlögel, N., Francis, L., Flandre, D., 2015. Capacitive biosensing of bacterial cells: Analytical model and numerical simulations. Sensors and Actuators B: Chemical, 211, 428-438

Daniels, J.S., Pourmand, N., 2007. Label-free impedance biosensors: Opportunities and challenges. Electroanalysis 19(12), 1239-1257.

Evtugyn, G., Porfireva, A., Ivanov, A., Konovalova, O., Hianik, T., 2009. Molecularly imprinted polymerized Methylene Green as a platform for electrochemical sensing of aptamer–thrombin interactions. Electroanalysis 21(11), 1272-1277.

Formisano N. (2015). A study on the optimisation of electrochemical impedance spectroscopy biosensors (Doctoral dissertation, University of Bath).

Hammond, J. L., Formisao, N., Estrela, P., Carrara, S., Tkac, J. 2016. Electrochemical biosensors and nanobiosensors. Essays in Biochemistry 60(1), 69-80.

Hammond, J. L., (2017) Micro- and nanogap based biosensors. (Doctoral dissertation, University of Bath).

Hianik, T., Wang, J., 2009. Electrochemical aptasensors–recent achievements and perspectives. Electroanalysis 21(11), 1223-1235.

Hsu, C. H., & Mansfeld, F. (2001). Technical note: concerning the conversion of the constant phase element parameter Y0 into a capacitance. Corrosion, 57(09), 1-2

Iliuk, A.B., Hu, L., Tao, W.A., 2011. Aptamer in bioanalytical applications. Analytical chemistry 83(12), 4440-4452.

Jolly, P., Formisano, N., Tkáč, J., Kasák, P., Frost, C.G., Estrela, P., 2015. Label-free impedimetric aptasensor with antifouling surface chemistry: A prostate specific antigen case study. Sensors and Actuators B: Chemical, 209, 306-312

Jolly, P., (2016) Oligonucleotide-based biosensors for the detection of prostate cancer biomarkers. (Doctoral dissertation, University of Bath).

J. Wang, Electrochemical biosensors: Towards point-of-care cancer diagnostics Biosensors and Bioelectronics 21 (2006) 1887–1892

Lasia, A., 2002. Electrochemical impedance spectroscopy and its applications. In Modern aspects of electrochemistry, pp. 143-248. Springer US

Liss, M., Petersen, B., Wolf, H., Prohaska, E., 2002. An aptamer-based quartz crystal protein biosensor. Analytical Chemistry 74(17), 4488-4495.

Kang, Y., Feng, K.-J., Chen, J.-W., Jiang, J.-H., Shen, G.-L., Yu, R.-Q., 2008. Electrochemical detection of thrombin by sandwich approach using antibody and aptamer. Bioelectrochemistry 73(1), 76-81.

Mairal, T., Özalp, V.C., Sánchez, P.L., Mir, M., Katakis, I., O'Sullivan, C.K., 2008. Aptamers: molecular tools for analytical applications. Analytical and bioanalytical chemistry 390(4), 989-1007.

Niina J. Ronkainen,*a H. Brian Halsallb and William R. Heinemanb, Electrochemical biosensors Chem. Soc. Rev., 2010,39, 1747-1763

Özen, H., Sözen, S., 2006. PSA isoforms in prostate cancer detection. European urology supplements 5(6), 495-499.

Pavlov, V., Xiao, Y., Shlyahovsky, B., Willner, I., 2004. Aptamer-functionalised Au nanoparticles for the amplified optical detection of thrombin. Journal of the American Chemical Society 126(38), 11768-11769.

Radi, A.-E., Acero Sánchez, J.L., Baldrich, E., O'Sullivan, C.K., 2006. Reagentless, reusable, ultrasensitive electrochemical molecular beacon aptasensor. Journal of the American Chemical Society 128(1), 117-124.

Sharma, R., Deacon, S. E., Nowak, D., George, S. E., Szymonik, M. P., Tang, A. A. S., ... & Wälti, C. (2016). Label-free electrochemical impedance biosensor to detect human interleukin-8 in serum with sub-pg/ml sensitivity. Biosensors and Bioelectronics, 80, 607-613

Song, S., Wang, L., Li, J., Fan, C., Zhao, J., 2008. Aptamer-based biosensors. TrAC Trends in Analytical Chemistry 27(2), 108-117.

Tombelli, S., Minunni, M., Mascini, M., 2005. Analytical applications of aptamers. Biosensors and Bioelectronics 20(12), 2424-2434.

Tsouti, V., Boutopoulos, C., Zergioti, I., Chatzandroulis, S., 2011. Capacitive microsystems for biological sensing. Biosensors and Bioelectronics, 27(1), 1-11

Turner, A.P., Karube, I., Wilson, G., 1986. Biosensors: fundamentals and applications. Oxford Science Publications, Oxford

Van Der Merwe, P.A., 2001. Surface plasmon resonance. Protein-Ligand Interactions: Hydrodynamics and Calorimetry, Oxford University Press: New York, NY, USA, pp.137-170

Wang, J. Glucose biosensors: 40 years of advances and challenges. Electroanalysis 2001, 13(12), 983–988

Wang J, Kawde A. Pencil-based renewable biosensor for label-free electrochemical detection of DNA hybridization. Anal Chim Acta 2000; 431:219–25

Woodman, R., Yeh, J. T. H., Laurenson, S., & Ferrigno, P. K. (2005). Design and validation of a neutral protein scaffold for the presentation of peptide aptamers. Journal of molecular biology, 352(5), 1118-1133.

Chapter 2. Cancer

The aim of the work in this thesis is to develop the electrochemical biosensors able to detect different cancer biomarkers. For the fabrication of these kind of sensors, it is important to understand the physiology of cancer in patients. In this chapter, I will describe prostate, breast and gastrointestinal cancer, their current diagnosis status, and their potential biomarkers.

The main cause of the cancer is the uncontrolled proliferation of cells in certain tissues of the human body. The reasons for this proliferation can be different: long-term exposure to certain types of viruses, various chemical carcinogens or simply age. The result of this abnormal behaviour is a disruption of the life balance in the cells of the involved tissue. Cancer can be considered as an infection which is transmittable from the foreign invader, but it arises from the cells within our own body.

The tumours are very complex tissues with different cell types which allow the possibility to grow and to develop as a normal tissue. The cell behaviour depends on the internal and external signals that the cell receives from the nervous system and it can be compared to an electronic circuit, where there are different switches that affect the behaviour of the entire connection network. The malfunction of the circuit can affect the entire organism bringing in the worst of cases, death.

2.1 Prostate cancer

As mentioned previously, cancer is a disease caused by the abnormal proliferation of the cells in the human body. This uncontrolled phenomenon could be caused by different carcinogens, genetic and environmental factors. It is these mutations within the cell that are responsible for prostate cancer (PCa) (Lilja et al. 1987).

Prostate cancer is related to the prostate gland, which is a male reproductive organ that weighs between 7-16 g depending on the person (Leissner and Tisell 1979). The gland is located below the bladder and surrounds the urethra which carries urine from the bladder to the penis Figure 2.1.

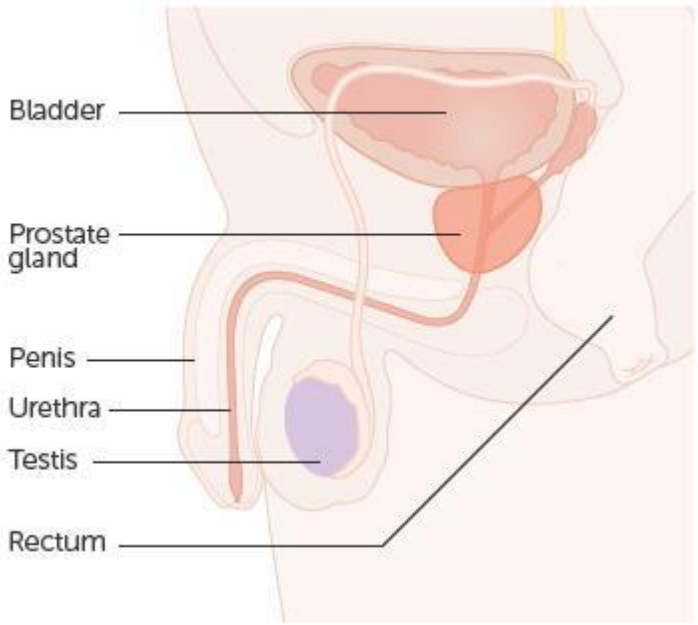

Figure 2.1 Prostate gland. Source internet: Cancer Research UK

2.1.1 Current status and detection techniques

The problem associated with prostate cancer is that it develops very slowly and that symptoms are not always evident during the first disease stages. Another crucial point of PCa diagnosis is the presence of the false readings in the test results of the principal detection techniques used in the laboratories and hospitals.

Currently, there are three commonly used techniques which are practised worldwide. The first is a digital rectal examination (DRE), where the irregularities in terms of bumps of the prostate gland are examined by a doctor by inserting a sterilised gloved finger through the rectum (Carvalhal et al. 1999). The second technique is the transrectal ultrasound (TRUS) which involves an ultrasound probe that is inserted into the rectum of the patient to image the prostate gland which is used to examine the pathology of the tumour. TRUS is also used for biopsy applications by guiding a needle together with the ultrasound probe for sampling tissues (Hara et al. 2008). Nevertheless, the most common technique used for PCa screening is a blood test where the altered levels of prostate specific antigen (PSA) are measured (Walter et al. 2006). The clinical cutoff level of PSA in blood is 4 ng/ml (Catalona et al. 1991). Prostate

specific antigen (PSA) was discovered in 1971, and soon became the foundation and gold standard of PCa detection and monitoring (Balk et al. 2003; Hara et al. 1971). PSA is a protein that belongs to the family of kallikrein proteins which are also called serine proteases. There are about 15 kallikrein proteins present in the human body where PSA (hK3) is the only kallikrein protein specific to the prostate (Balk et al. 2003).

The active PSA is a 30 kDa protein and is found in both semen and serum of men.

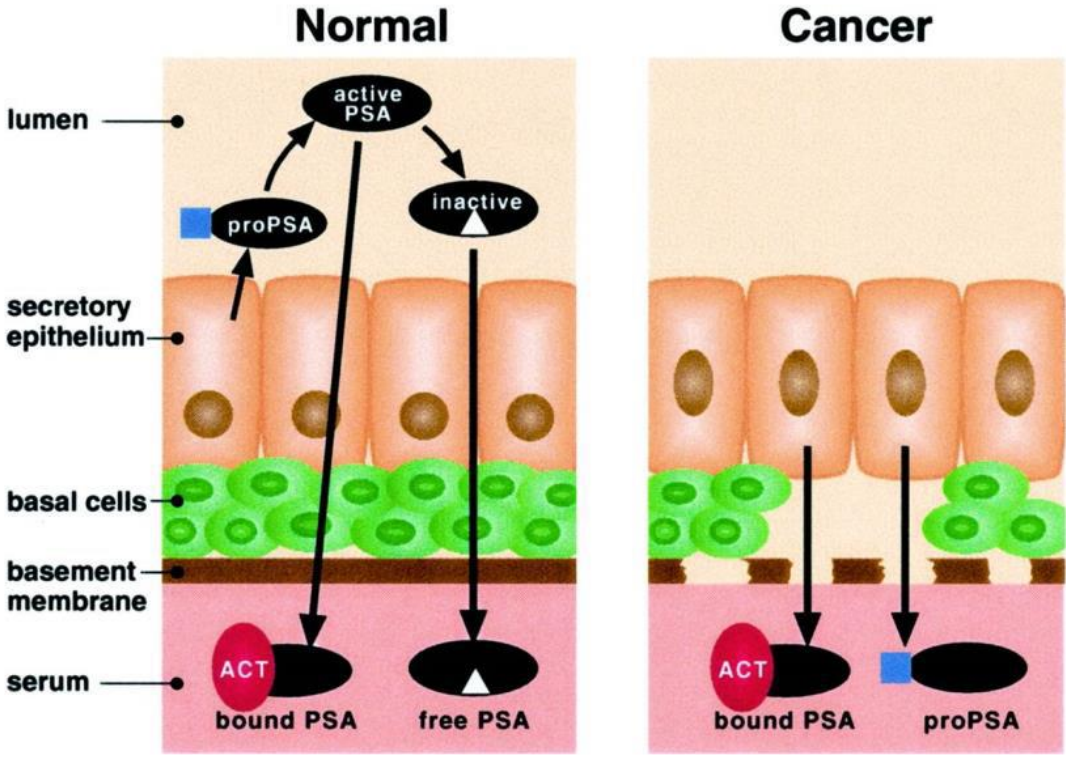

Figure 2.2 Model of PSA biosynthesis in normal and cancer prostate gland (Balk et al. 2003)

The physiological role of PSAin semen is to de-coagulate semen (range 0.5-2 mg/ml) by breaking down the proteins semenogelin I and II (Lilja et al. 1987; Lövgren et al. 1999).

It is worth mentioning that in semen, about 30% of PSA is enzymatically active, while only 5% of PSA is complexed to protein inhibitors. Furthermore, the remaining PSA often becomes inactive by internal cleavages catalysed by hK proteases. Some of the active PSA also escapes into the blood stream of the human body where it is rapidly bound to inhibitors and becomes such as alpha chymotrypsin (ACT) and α2-

microglobulin (A2M) (Hara et al. 1971). However, in PCa patients, both active PSA and pro-PSA leaks into the blood stream due to rupture of the basal membrane of the prostate gland leading to fluctuations of blood PSA levels. Moreover, internally cleaved forms of PSA also enter the blood stream and remain uncomplexed and are taken into free PSA (fPSA) count. fPSA together with complexed PSA is termed as total PSA (tPSA) (Takayama et al. 1997).

It is worth mentioning that with the introduction of PSA testing, there has been an increase in the early detection of PCa (Balducci et al. 1997).

2.2 Breast cancer

Cancer that develops in the breasts of the female is called breast cancer (Siegel et al. 2013). Like any other cancer, there are specific markers in the body fluids that are released. The fluctuation of these markers could be potentially used for the prognosis and diagnosis of breast cancer. One of the most important biomarkers for breast cancer is the human Epidermal growth factor receptor 2 (Her2). Her2 is typically a transmembrane receptor tyrosine kinase (protein-based) and is a member of the Epidermal growth factor receptor (EGFR) family, which also includes EGFR (Her1), Her3, and Her4 (Patris et al. 2014).

Her2 acts as an oncogene in breast cancer. The regulation of Her2 is often a signal for the clinicians to proceed with a further investigation to confirm cancer. Her2 overexpression results in the ligand-independent dimerization which often leads to the constitutive activation of its cytoplasmic kinase domain. This constitutive activation of Her2 further leads to unregulated activation of the PI3K/AKT/mTOR and MAPK pathways, which promotes uncontrolled cell proliferation, leading to tumour growth and progression.

2.2.1 Her2 Expression in Breast Cancer

From the expression level, 15-20% of overexpression is commonly observed in patients with primary breast cancers and in approximately 10% of oestrogen-receptor-

positive (ER+) breast cancers. As a result of the high-level expression, it drives the basal level of Her2 activity above a threshold that can stimulate tumour growth.

Her2 is often reported as a potential prognostic biomarker for breast cancer which was first reported in 1987. It has been reported that its amplification is usually associated with reduced time to progression and reduced overall survival. Thereafter, many subsequent research studies that have confirmed this link. With poor prognosis Her2 is also considered as an important predictive biomarker to the response to Her2-targeted therapies (Chun et al. 2013; Hung et al. 1995).

In central laboratories, Her2 testing is performed by either immunohistochemistry (IHC), or in situ hybridization (ISH) using either fluorescent (FISH), chromogenic (CISH) or silver (SISH) detection methods. Such tests often involve core biopsy or resected tumour tissue samples that are fixed in buffered formalin and embedded in paraffin wax. Since is an invasive technique, it leads to patients suffering and is also time-consuming and can only be performed by well-trained specialists.

IHC detects Her2 protein expression which employs antibodies which are easily available commercially for this type of assay. On the other hand, ISH can detect the addition or deletion of specific DNA sequences on chromosomes by using complementary probes that are able to hybridise to the particular region of interest. As mentioned earlier, not only are these tests are done in centralised laboratories, these tests are time-consuming, costly and require trained professionals. Therefore, by developing a point-of-care device using biosensors, the costs and time could be greatly reduced and also help the physicians take necessarily mode of action.

This thesis is a step towards the development of a sensitive and selective aptamer-based biosensor for the detection of Her2. Chapter 4 will detail such an approach and demonstrate the detection of Her2 in undiluted human serum samples.

2.3 Gastrointestinal stromal tumour

Another type of cancer under study in this thesis is a gastrointestinal stromal tumour (GIST) which is the most common (80%) form of cancer among mesenchymal tumours. GIST represents an extensive spectrum of tumours with different clinical,

locations, histology and prognosis. GIST can also occur throughout the gastrointestinal tract and may also have involvement in extragastrointestinal. With the discovery of molecular biology, the clinical relevance of GIST was generated. (Mucciarini et al. 2007; Nilsson et al. 2005; Sandvik et al. 2011; Steigen and Eide 2009)

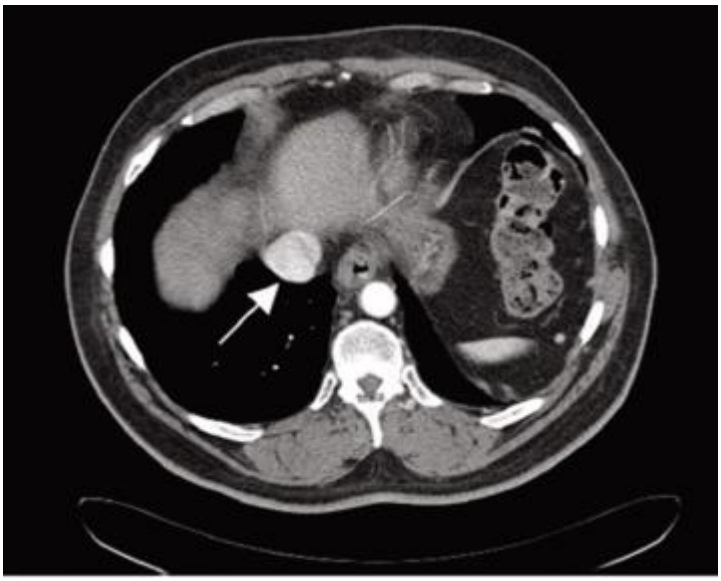

Figure 2.3 Computed tomography scan revealed a partially exophytic, dumbbell shaped solid mass (arrow) arising from the posterior aspect of the gastric fundus along the greater curvature, measuring approximately 6.7 cm × 4.5 cm

To date, there are no blood tests to detect GIST. This thesis is also a step towards the development of a biosensor that could detect Her4 marker which is associated with GIST. Chapter 5 will present an Affimer-based electrochemical sensor targeting Her4.

It is worth mentioning that most GIST remains 'silent' until reaching a large size which often leads to the late diagnosis. Moreover, the symptoms associated with GIST vary depending on the location and size. Some of the symptoms include abdominal pain, fatigue, dyspepsia, nausea, anorexia, weight loss, fever and obstruction. Patients with chronic GIST can show over bleeding due to mucosal ulceration which can lead to life-threatening intraperitoneal haemorrhage. Also, some GIST patients may have externally palpable masses (Zhao et al. 2012).

The current diagnostic tests for GIST is based on imaging techniques (Figure 2.3), with involves a special role of well trained endoscopic examiner because it is usually

accessible when tumours are in the stomach, oesophagus and large intestine. In addition, endoscopic ultrasonography (EUS) also plays an important role in the diagnosis of GISTs.

References

Balducci, L., Pow-Sang, J., Friedland, J., Diaz, J.I., 1997. Prostate cancer. Clinics in geriatric medicine 13(2), 283-306.

Balk, S.P., Ko, Y.-J., Bubley, G.J., 2003. Biology of prostate-specific antigen. Journal of Clinical Oncology 21(2), 383-391.

Catalona, W.J., Smith, D.S., Ratliff, T.L., Dodds, K.M., Coplen, D.E., Yuan, J.J., Petros, J.A., Andriole, G.L., 1991. Measurement of prostate-specific antigen in serum as a screening test for prostate cancer. New England Journal of Medicine 324(17), 1156-1161.

Carvalhal, G.F., Smith, D.S., Mager, D.E., Ramos, C., Catalona, W.J., 1999. Digital rectal examination for detecting prostate cancer at prostate specific antigen levels of 4 ng./ml. or less. The Journal of urology 161(3), 835-839.

Chun, L., Kim, S.-E., Cho, M., Choe, W.-s., Nam, J., Lee, D.W., Lee, Y., 2013. Sensors and Actuators B: Chemical 186, 446-450.

Hara, M., Koyanagi, Y., Inoue, T., Fukuyama, T., 1971. Some physico-chemical characteristics of"-seminoprotein", an antigenic component specific for human seminal plasma. Forensic immunological study of body fluids and secretion. VII. Nihon hōigaku zasshi= The Japanese journal of legal medicine 25(4), 322.

Hung, M.-C., Matin, A., Zhang, Y., Xing, X., Sorgi, F., Huang, L., Yu, D., 1995. Gene 159(1), 65-71.

Leissner, K.-H., Tisell, L.-E., 1979. The weight of the human prostate. Scandinavian journal of urology and nephrology 13(2), 137-142.

Lilja, H., Oldbring, J., Rannevik, G., Laurell, C., 1987. Seminal vesicle-secreted proteins and their reactions during gelation and liquefaction of human semen. Journal of Clinical Investigation 80(2), 281.

Lövgren, J., VALTONEN-ANDRÉ, C., Marsal, K., LIUA, H., Lundwall, Å., 1999. Measurement of Prostate-Specific Antigen and Human Glandular Kallikrein 2 in Different Body Fluids. Journal of andrology 20(3), 348-355.

Mucciarini, C., Rossi, G., Bertolini, F., Valli, R., Cirilli, C., Rashid, I., Marcheselli, L., Luppi, G., Federico, M., 2007. BMC Cancer 7:230(1), 1-7.

Nilsson, B., Bümming, P., Meis-Kindblom, J.M., Odén, A., Dortok, A., Gustavsson, B., Sablinska, K., Kindblom, L.-G., 2005. Cancer 103(4), 821-829.

Patris, S., De Pauw, P., Vandeput, M., Huet, J., Van Antwerpen, P., Muyldermans, S., Kauffmann, J.-M., 2014. Talanta 130, 164-170.

Sandvik, O.M., Søreide, K., Kvaløy, J.T., Gudlaugsson, E., Søreide, J.A., 2011. Cancer Epidemiology 35(6), 515-520.

Steigen, S.E., Eide, T.J., 2009. APMIS 117(2), 73-86.

Siegel, R., Naishadham, D., Jemal, A., 2013. CA: A Cancer Journal for Clinicians 63(1), 11-30.

Takayama, T.K., Fujikawa, K., Davie, E.W., 1997. Characterization of the precursor of prostate-specific antigen Activation by trypsin and by human glandular kallikrein. Journal of Biological Chemistry 272(34), 21582-21588.

Walter, L.C., Bertenthal, D., Lindquist, K., Konety, B.R., 2006. PSA screening among elderly men with limited life expectancies. Jama 296(19), 2336-2342.

Zhao, X., & Yue, C. (2012). Gastrointestinal stromal tumor. J Gastrointest Oncol, 3(3), 189-208.

Chapter 3. Self-assembled gold nanoparticles for impedimetric and amperometric detection of a prostate cancer biomarker

This declaration concerns the article entitled:								
Self-assembled gold nanoparticles for impedimetric and amperometric detection of a prostate cancer biomarker								
Publication status (tick one)								
draft manuscript	**Submitted**		**In review**		**Accepted**		**Published**	X
Publication details (reference)	Sensors and Actuators B: Chemical https://doi.org/10.1016/j.snb.2017.05.040							
Candidate's contribution to the paper (detailed, and also given as a percentage).	The candidate contributed predominantly to: Formulation of ideas: The idea was formulated together with Dr Pawan Jolly. My contribution was more on the impedimetric part. In total my contribution was 30% Design of methodology: The methodology was a combined effort from Bath University and Slovak Academy of Sciences where my contribution was on the optimisation of surface modification and detection. In percentage my contribution was 25% Experimental work: The experimental work and analysis was majorly performed by myself with the help of Dr Pawan Jolly. My contribution was 80%. Presentation of data in journal format: I was involved in reporting the experimental data and also in the writing of the paper together with Dr Pawan Jolly. We had equal contribution in writing and presenting the data. (50%). I have also presented the work on international conferences in both oral and poster format.							
Statement from Candidate	This paper reports on original research I conducted during the period of my Higher Degree by Research candidature.							
Signed					**Date**	30/05/2017		

Pawan Jolly [1,†], Pavel Zhurauski [1,†], Jules L. Hammond[1], Anna Miodek[1,‡], Susana Liébana [2,‖], Tomas Bertok [3], Jan Tkáč [3], Pedro Estrela[1,*]

[1] *Department of Electronic and Electrical Engineering, University of Bath, Bath BA2 7AY, UK*

[2] *Applied Enzyme Technology Ltd., Gwent Group Ltd., Pontypool NP4 0HZ, UK*

[3] *Department of Glycobiotechnology, Institute of Chemistry, Slovak Academy of Sciences, Dubravska Cesta 9, 845 38 Bratislava, Slovak Republic*

‡ Current address: *Alternative Energies and Atomic Energy Commission (CEA), Institute of Biomedical Imaging (I^{2}BM), Molecular Imaging Research Center (MIRCen), 18 Route du Panorama, 92265 Fontenay-aux-Roses, France; Neurodegenerative Diseases Laboratory, Centre National de la Recherche Scientifique (CNRS), Université Paris-Saclay, Université Paris-Sud, UMR 9199, Fontenay-aux-Roses, France*

‖ Current address: *Pragmatic Diagnostics S.L., Mòdul de Recerca B- Campus de la UAB, 08193 Bellaterra (Cerdanyola del Vallès) - Barcelona, Spain*

‡ Authors equal contribution

*Corresponding author: Department of Electronic & Electrical Engineering,
University of Bath,
Claverton Down, Bath, BA2 7AY, United Kingdom
E-mail: P.Estrela@bath.ac.uk
Phone: +44-1225-386324

The work is this chapter has been published in the journal Sensors and Actuators in Jolly et al. (https://doi.org/10.1016/j.snb.2017.05.040) which included an equal contribution from Pavel Zhurauski and Dr Pawan Jolly. The contribution includes experimental design, performing experiments, analysis of data and preparation of the manuscript.

Abstract

A label-free dual-mode impedimetric and amperometric aptasensor platform was developed using a simple surface chemistry step to attach gold nanoparticles (AuNPs) to a gold planar surface. As a case study, the strategy was employed to detect prostate specific antigen (PSA), a biomarker for prostate cancer. An anti-PSA DNA aptamer was co-immobilised with either 6-mercapto-1-hexanol (MCH) or 6-(ferrocenyl)hexanethiol (FcSH) for both impedimetric or amperometric detection, respectively. We show that the use of AuNPs enables a significant improvement in the limit of impedimetric detection as compared to a standard binary self-assembled monolayer aptasensor. A PSA detection of as low as 10 pg/mL was achieved with a dynamic range from 10 pg/mL to 10 ng/mL, well within the clinically relevant values, whilst retaining the high specificity of analysis. The reported approach can be easily generalised to various other bioreceptors and redox markers in order to perform multiplexing.

Keywords: aptamer, aptasensor, gold nanoparticles, prostate cancer, PSA

3.1 Introduction

There is an increasing demand for the simple, low-cost, reliable and rapid screening of biomarkers for the early detection of diseases such as cancer and this has led to a scurry of activity towards label-free biosensors. Removing the labelling step can provide significant savings in cost and time, making point-of-care sensing more viable than labelled alternatives. However, the removal of the label can lead to a more difficult determination of the analyte due to non-specific interactions in complex

media, resulting in decreased sensitivity and sometimes a system incapable of meeting the clinical requirements.

Given that a biosensor's signal is generally proportional to the surface coverage, most methods for increasing the sensitivity of label-free biosensors revolve around surface modifications to increase probe loading. Forming meso- and micro-porous surfaces with methods such as electrodeposition can provide increased surface area whilst still maintaining detection with low sample volumes. However, it is often easier and more controllable to increase surface area by anchoring nanoparticles to the surface. Nanoparticles may be formed from metals, oxides, semiconductors and conducting polymers, but it is the use of gold nanoparticles (AuNPs) which has attracted most attention for biosensing applications, in particular for biosensors based on optical and electrochemical transduction [1, 2].

The wide adoption of AuNPs has in part been down to their excellent biocompatibility, conductivity, and catalytic properties. AuNPs offer an important structural surface, amplifying the resulting electrical response. They can act as electroactive intermediates between electrodes and solution and hence increase the sensitivity of biosensors. AuNPs offer also a suitable platform for multi-functionalization with a wide range of organic or biological ligands for the selective detection of small molecules and biological targets [3-5]. Whilst antibodies remain the molecular recognition workhorse of choice for many biosensing devices, their use can impose limitations on both technology adoption and resulting applications [6]. One long-championed alternative to antibodies has been DNA aptamers. DNA aptamers are short, stable oligonucleotide sequences possessing high affinity and specificity for particular targets. DNA aptamers have many advantageous properties compared to their biological antibody counterparts such as long-term stability, affordability and ease of development compared to antibodies [7, 8]. They can also be regenerated without loss of integrity or selectivity [9] providing a platform to develop multi-use sensors. Aptamers are however prone to protein fouling in serum due to DNA binding proteins [10] which mean that the surface chemistry should be considered to provide optimal performance.

The use of both AuNPs and aptamers for improved specificity and signal amplification have been previously demonstrated for electrochemical [11-13], optical [14, 15] and mass-based [16] biosensors. In this work, we show how a simple step to attach AuNPs to a planar gold surface results in a significant amplification of the biosensor response. The key focus of this work is to keep the number of fabrication steps to a minimum with low complexity. By doing this, we ensure a robust surface chemistry is achieved. Such an approach has been demonstrated by using a prostate cancer (PCa) biomarker as a case study. PCa is the most commonly diagnosed cancer amongst men worldwide. One of the key issues surrounding PCa diagnosis is that it develops very gradually over time and the absence of symptoms often results in a late diagnosis of the tumour which puts pressing needs on the development of reliable and sensitive diagnostic platforms. Currently, changes in levels of prostate specific antigen (PSA), a biomarker for PCa, in the blood can be used for PCa screening; levels higher than the cut-off level of 4 ng/mL prompt biopsy procedures to be considered [17-20]. PSA is a 30–33 kDa serine protease secreted by the prostate gland. Despite well-documented controversies linked with PSA testing [21-23], PSA still remains the most commonly used biomarker for PCa screening, monitoring the effectiveness of treatment and post-treatment [22, 24].

Taking a previous system based on an impedimetric aptasensor which used a planar gold surface with co-immobilised DNA aptamer / 6-mercapto-1-hexanol (MCH) probe layer [25], we show how sensitivity can be significantly improved by the addition of a single fabrication step to attach AuNPs to the planar gold electrode. As a result, we shift the limit of quantification from 60 ng/mL to 10 pg/mL, i.e. nearly 4 orders of magnitude improvement, so that it aligns with the clinically relevant range of 1 to 10 ng/mL. The fabricated aptasensor was successfully tested with spiked human serum samples and a detection of PSA as low as 10 pg/mL was achieved. Furthermore, simply by replacing MCH with 6-(ferrocenyl)hexanethiol (FcSH), a thiolated redox marker, during the co-immobilisation of the aptamer, the aptasensor could be similarly used for sensitive amperometric detection of PCa at clinically relevant concentrations. Such a dual-detection approach could potentially reduce false positives, providing additional validation of the signals.

3.2 Experimental

3.2.1 Reagents

Thiolated anti-PSA aptamer, 5'-HS-$(CH_2)_6$-TTT TTA ATT AAA GCT CGC CAT CAA ATA GCT TT-3' and a random DNA sequence non-specific to PSA (5'- HS -$(CH_2)_6$-AAA AAT TAA TTT CGA GCG GTA GTT TAT CGA AA-3') used as control DNA probe were obtained from Sigma-Aldrich (UK). Prostate specific antigen (PSA) from human semen was obtained from Fitzgerald (MA, USA). Human serum albumin (HSA), human serum, 11-aminoundecanethiol hydrochloride, 6-mercapto-1-hexanol (MCH), 6-(ferrocenyl)hexanethiol (FcSH), potassium buffer saline tablets (pH 7.4), potassium hexacyanoferrate (III), potassium hexacyanoferrate(II), gold nanoparticles (20 nm, stabilized suspension in 0.1 mM PBS, reactant free) were all purchased from Sigma-Aldrich (UK). All other reagents were of analytical grade. All aqueous solutions were prepared using 18.2 MΩ cm ultrapure Milli-Q water with a Pyrogard® filter (Millipore, MA, USA). For binding studies, different concentrations of PSA were prepared in 10 mM PBS, pH 7.4. The specificity of the aptamer was evaluated by studying its interaction with 10 ng/mL HSA as a control protein dissolved in 10 mM PBS, pH 7.4. For experiments with serum, different concentrations of PSA were prepared in 1:10 diluted human serum (diluted in 10 mM PBS, pH 7.4). 10 times diluted human serum solution was further filtrated through a 0.22 µm pore filter.

3.2.2 Apparatus

The electrochemical measurements were performed using a µAUTOLAB III / FRA2 potentiostat (Metrohm Autolab, Netherlands) using a three-electrode cell setup with an Ag/AgCl reference electrode (BASi, USA) and a Pt counter electrode (ALS, Japan). The impedance spectrum was measured in 10 mM PBS (pH7.4) containing 4 mM ferro/ferricyanide $[Fe(CN)_6]^{3-/4-}$ in a frequency range from 100 kHz to 100 mHz, with a 10 mV AC voltage superimposed on a bias DC voltage of 0.2 V *vs.* Ag/AgCl. Cyclic voltammetry was performed in 10 mM PBS (pH 7.4) containing 10 mM ferro/ferricyanide $[Fe(CN)_6]^{3-/4-}$ and scanning the potential between -0.3 V to 0.5 V *vs.* Ag/AgCl. Square wave voltammetry was performed in 10 mM PBS (pH 7.4) in the potential range from -0.4 V to 0.65 V *vs.* Ag/AgCl with a conditioning time of 120 s, modulation amplitude of 20 mV and frequency of 50 Hz.

Surface characterisation of gold electrodes modified with gold nanoparticles was performed using a scanning electron microscopy (JSM-6480 Jeol, Japan) on gold evaporated chips at 100,000× magnification with an acceleration voltage of 5 kV. Ambient contact mode (tapping mode) atomic force microscopy (AFM) imaging was carried out with a MultiMode NanoScope with IIIa controller in conjunction with version 6 control software (Bruker, Germany). Gold evaporated chips modified as described in the fabrication section for gold electrodes were imaged with a 10 nm diameter AFM ContAl-G tip (BudgetSensors®, Bulgaria), images were then processed by the NanoScope Analysis software, version 1.5.

3.2.3 Electrode preparation

Prior to functionalisation, gold disc working electrodes with a radius of 1.0 mm (ALS, Japan) were cleaned by mechanical polishing for 5 minutes with 50 nm alumina slurry (Buehler, UK) on a polishing pad (Buehler, UK) followed by 5 minutes sonication in ethanol and then in water. The electrodes were then subjected to chemical cleaning with piranha solution (3 parts of concentrated H_2SO_4 with 1 part of H_2O_2 for 5 minutes). The electrodes were then rinsed with Milli-Q water. Thereafter, electrodes were electrochemically cleaned in 0.5 M H_2SO_4 by scanning the potential between 0 V and +1.5 V *vs.* Ag/AgCl for 50 cycles until no further changes in the voltammogram were observed. After electrochemical cleaning, electrodes were extensively washed with MilliQ water to remove any acid residues. Finally, electrodes were cleaned with ethanol and were left to dry in an air-filtered environment for several minutes.

3.2.4 Sensor fabrication

An overview of the aptasensor fabrication for both impedimetric and amperometric determination is illustrated in Figure 3.1. The protocol for the modification of planar gold electrodes with gold nanoparticles was adapted from Bertok *et al.* [26]. Briefly, clean gold electrodes were immersed in 150 µL of 1 mM solutions of 11-amino alkanethiol dissolved in pure ethanol for 16 hours at ~4°C. This step was performed to provide a high-density monolayer. After incubation, electrodes were washed with pure ethanol followed by MilliQ water to remove any unattached thiols. To ensure complete thiol coverage of the gold surface, the electrodes were backfilled with 1 mM

MCH for 1 hour at room temperature. Thereafter, the electrodes were incubated with 100 µL of 20 nm gold nanoparticle (AuNP) solution (undiluted stock solution) in an inverted position overnight.

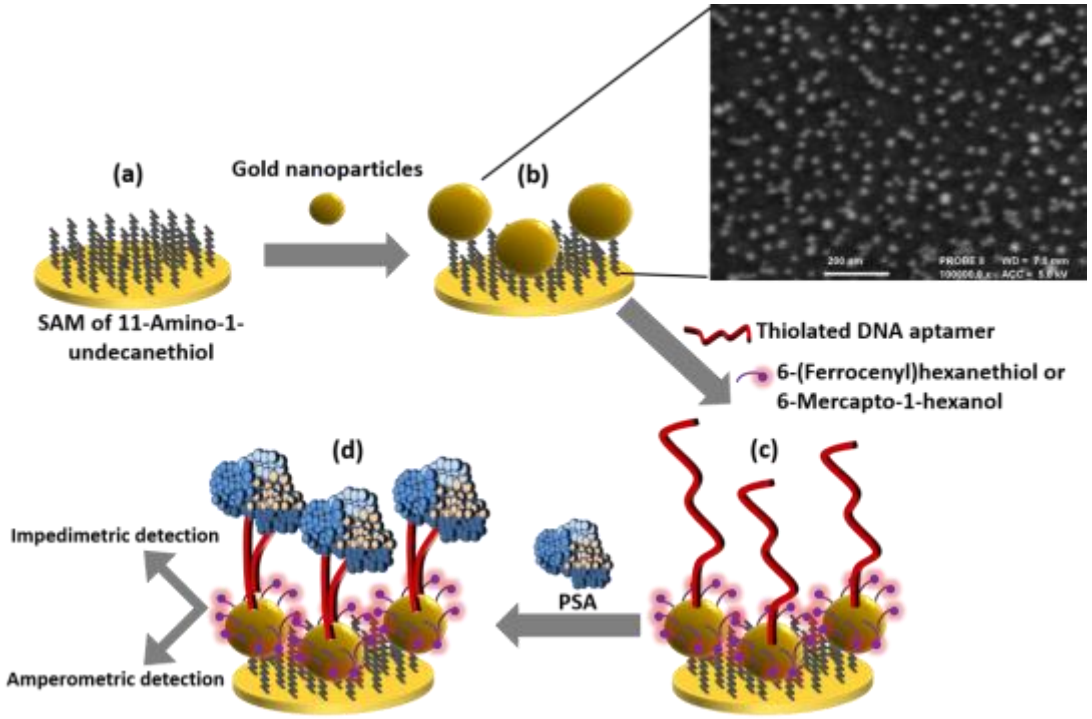

Figure 3.1 Schematic of the AuNP-modified aptasensor showing how either impedimetric or amperometric detection can be used depending on whether the DNA aptamer is co-immobilised with MCH or FcSH

A second mixed SAM layer was deposited on the AuNP-modified electrodes with different ratios of thiolated DNA aptamer to MCH (1:10, 1:50, 1:75 and 1:100) in 10 mM PBS (pH 7.4) for 2 hours at room temperature. High concentrations of MCH were prepared in ethanol and then diluted to working concentrations in buffer solutions. Prior to the addition of MCH, DNA aptamers were activated by heating to 95°C for 10 minutes and allowed to cool gradually to room temperature over 30 minutes [4]. MCH was included in order to alter the lateral density of thiolated DNA on the surface; this was to passivate the gold surface and reduce non-specific binding as well as minimise steric hindrance and facilitate the charge transfer during the EIS measurements [25]. After immobilisation, the electrodes were rinsed with ultra-pure water to remove any unbound DNA aptamers. Finally, the electrodes were placed in the measurement buffer for 1 hour to stabilise the SAM prior to measurements. For

amperometric detection, the same fabrication protocol was adapted but MCH was replaced with FcSH.

3.3 Results and discussion

3.3.1 Characterisation of the AuNP-modified surface fabrication

The morphology of the AuNP-modified surface was characterised using both scanning electron microscopy (SEM) and atomic force microscopy (AFM). Figure 3.1 shows an SEM image showing a homogeneous distribution of AuNPs on the electrode surface. Moreover, Figure 3.2 shows AFM images of the planar gold surface before (a) and after (b) the attachment of 20 nm AuNPs. The modified surface is shown to have a well-ordered assembly of AuNPs on the surface. Analysis of the AFM images of a gold electrode before AuNP attachment showed a mean roughness (R_a) value of 0.64, root means square roughness (R_q) value of 0.87 with a maximum roughness depth (R_{max}) value of 8.32. On the other hand, gold electrodes modified with AuNPs showed a high mean roughness (R_a) value of 5.56, root means square roughness (R_q) value of 6.71 with a maximum roughness depth (R_{max}) value of 35.8.

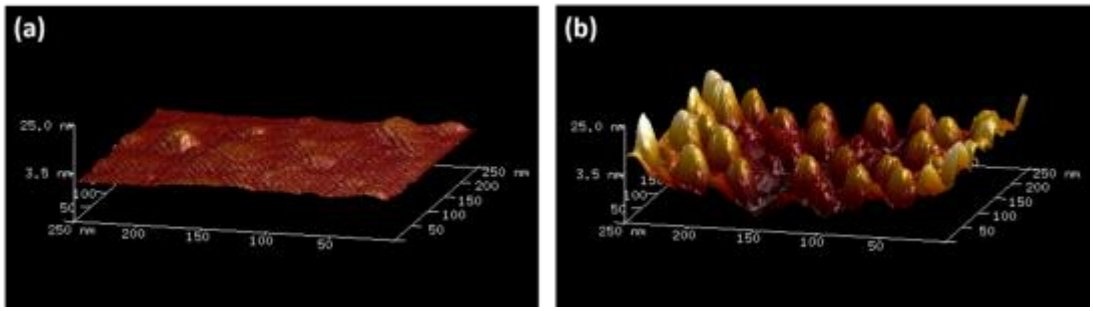

Figure 3.2 Images created from AFM data showing the difference in surface morphology for the original planar gold surface (a) and the AuNP-modified surface (b)

3.3.2 Optimisation of probe surface using electrochemical impedance spectroscopy

The probe density can play an important role in biosensor performance, providing a trade-off between surface coverage and analyte capture efficiency. Notably, the conformation change occurring as a result of the aptamer to PSA binding can lead to significant steric hindrance for high-density coverage [25]. As surface coverage and

spacing of the probe molecules are dependent on the concentrations of co-immobilised molecules, a range of ratios was tested to see whether the sensor response was affected. The AuNP-modified gold substrates were co-immobilised with the thiolated DNA aptamer and MCH in ratios of 1:20, 1:50, 1:75 and 1:100 and their impedimetric response to increasing PSA concentration in 10 mM PBS (pH 7.4) were characterised using electrochemical impedance spectroscopy (EIS).

Typical Nyquist plots for the system are presented in Figure 3 (a), where the charge transfer resistance (R_{ct}) of the prepared SAM (co-immobilized DNA aptamer and MCH) was determined by fitting the data to a Randles equivalent circuit, with a constant phase element (non-ideal capacitance), in parallel with R_{ct} and a Warburg element that models diffusion [25]. The Nyquist plots in Figure 3 (a) show the effect of increasing PSA concentration on the charge transfer resistance for a 1:50 ratio of thiolated probe to MCH. By comparing the responses for the 1:10, 1:50, 1:75 and 1:100 ratios, it can be seen in Figure 3 (b) that the response is not hugely affected by the density of surface-bound probe on AuNPs. To further highlight this, the response to the lowest (10 pg/mL) and highest (10 ng/mL) concentrations of PSA were compared with the response to a 10 ng/mL HSA control. The aptasensor demonstrated excellent selectivity response with less than 2% of signal variation upon incubation with HSA, which is present in abundance in human blood. A full dose response for different ratios has also been examined for a range of PSA concentrations from 0.01 ng/mL until 10 ng/mL and has been presented in supplementary information, Figure S-1. From all the ratios tested, the 1:50 ratio provided a slight improvement in reproducibility along with better discrimination against the HSA control compared to the higher probe density 1:20 ratio. This demonstrates the trade-off between surface coverage and efficacy of analyte capture.

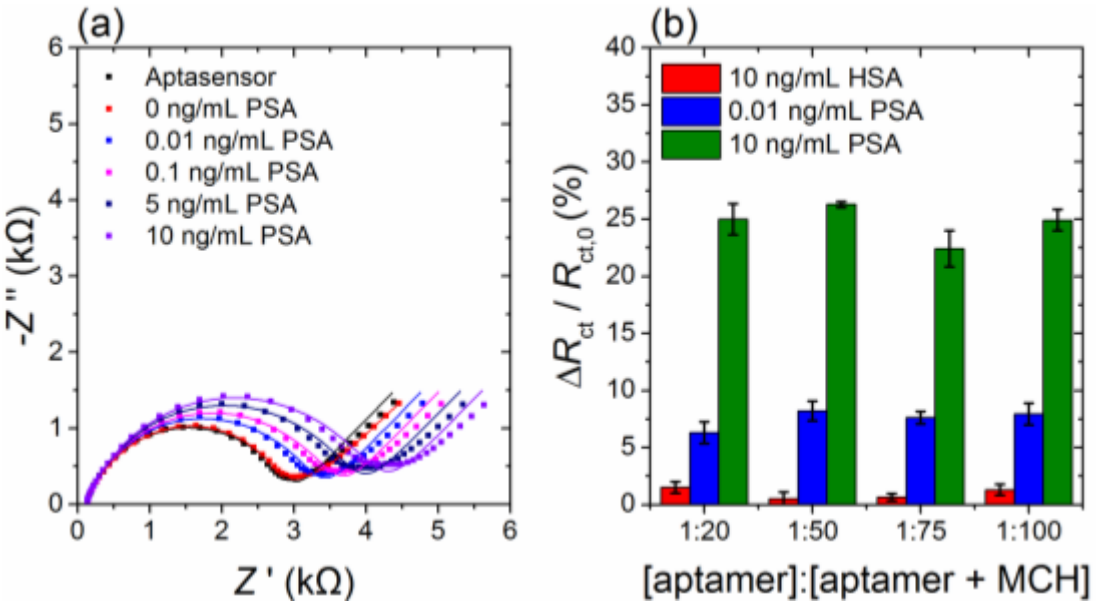

Figure 3.3 (a) EIS response for 0.01 ng/mL to 10 ng/mL PSA in 10 mM PBS (pH 7.4) for a surface density of 1:50. (b) Percentage increase of Rct for a range of aptamer: MCH concentrations for the detection of 0.01 ng/mL and 10 ng/mL PSA compared to the response for the 10 ng/ml HSA control (all in 10 mM PBS, pH 7.4) with standard mean errors from 4 independent samples.

3.3.3 Analytical performance

3.3.3.1 Amperometric performance

To verify that the aptasensor's electrochemical response was specific to PSA target binding to the aptamer probe rather than non-specific interactions caused by the presence of the surface-bound FcSH molecules, we replaced the PSA probe with a random DNA sequence and tested the response using square-wave voltammetry (see Supplementary Information, Figure S-2). With the random sequence a mean shift of 1.03 $\pm$ 0.37% was observed, attributed to non-specific interactions, compared to a mean shift of nearly 28.00 $\pm$ 2.10% for the correct anti-PSA probe. The difference in the response indicates that the specificity of the surface chemistry developed for PSA detection is good.

With the probe surface ratio optimised and the selectivity of the probe confirmed, an amperometric dose response to PSA was carried out for concentrations increasing from 10 pg/mL to 500 ng/mL. The square wave voltammograms are shown in the inset of Figure 5 with the FcSH redox marker's characteristic oxidative peak at 0.27 V. On incubation with different concentrations of PSA, a reduction in peak current was observed. Such a response could be attributed to the change in the electrochemical

environment around the redox marker on the binding of the target and the change in the conformation of the DNA aptamer [27]. The current was measured at a constant peak potential of 0.27 V after incubation with different concentrations of PSA. The percentage change in peak current was plotted against logarithmic concentration and shown in Figure 4. A logarithmical response between 1 ng/mL and 100 ng/mL was achieved, which aligns with the clinically relevant range of 1– 10 ng/mL.

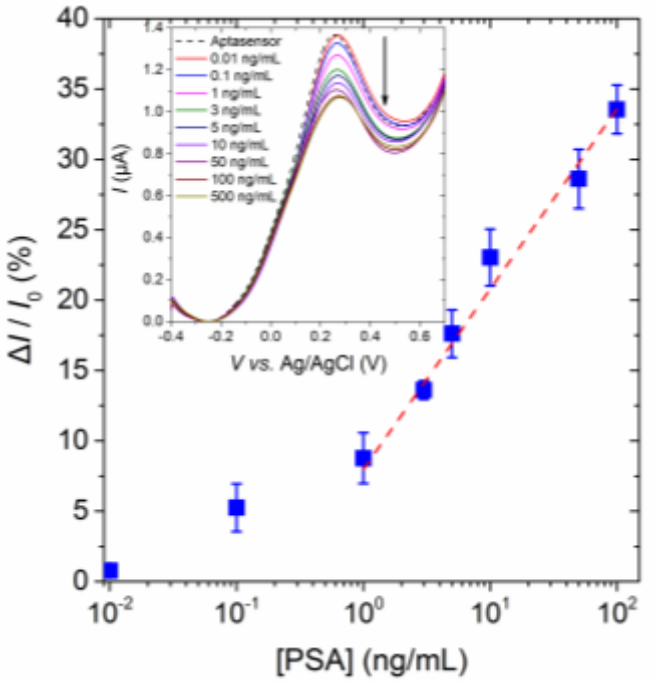

Figure 3.4 Electrochemical dose response of the aptasensor for increasing concentrations of PSA in 10 mM PBS (pH 7.4) with standard mean errors from 3 independent samples. Inset: Square wave voltammograms for increasing concentrations of PSA showing the decrease i in the oxidative peak current of FcSH.

3.3.3.2 Impedimetric performance

Reverting from the redox-modified FcSH co-immobilised probe layer to the MCH co-immobilised probe layer, the impedimetric performance was assessed in both 10 mM PBS (pH 7.4) and 1:10 diluted human serum against the original planar gold platform on which this work is based on [25]. The performance in human serum provides a good indicator for the aptasensor's feasibility for practical application. In order to negate any non-specific interactions, the aptasensor was incubated in serum sample without any PSA. The response of the sensor measured in the form of R_{ct} was used as a reference signal.

Figure 3.5 shows the aptasensor's percentage shift in R_{ct} plotted against a logarithmic scale of PSA concentration. The results illustrate how the detection range is shifted from 60 ng/mL – 1 µg/mL in the case of the planar gold surface to 10 pg/mL – 10 ng/mL for the AuNP-modified surface. The efficiency in terms of signal output has also been drastically improved from a signal change of 2.59 $\pm$ 1.19% for 60 ng/mL PSA using a planar gold surface to 8.22 $\pm$ 0.88% for 10 pg/mL PSA using the AuNP-modified surface. Improved sensitivity of the AuNP-modified surface is evident as the aptasensor performs well in human serum to concentrations well below the lower point of clinical interest. The fabricated sensor demonstrated an excellent improvement in the sensitivity, which is better or comparable to the existing state of art PSA biosensors reported to date. With this new method, we have been able to shift the detection range from outside the clinical grey zone (1 ng/mL to 10 ng/mL), indicated in Figure 6, to below and across this grey zone in both buffer and human serum spiked samples.

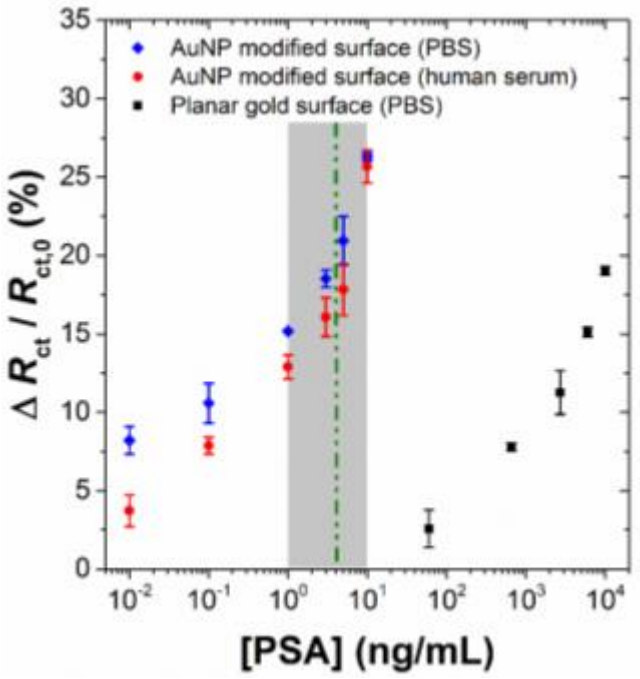

Figure 3.5 Comparison of the performance originally achieved with a planar gold surface as per previous work [25] with that of the AuNP-modified surface in both 10 mM PBS (pH 7.4) and 1:10 diluted human serum. The simple addition of AuNPs shifts the detection into the clinically relevant 1-10 ng/mL range (shaded area). The data for planar gold surface has been taken from Formisano et al. [25].

In order to further demonstrate the practical application of the developed aptasensor, the signal changes obtained from serum samples were used to calculate the recovery of the system from below the clinical range of PSA (0.1 ng/mL) to its upper limit (10

ng/mL). The recovery was calculated as the ratio of the sensor performance in spiked human serum samples to that obtained in the buffer for the same concentrations of PSA. The results are presented in Table 1, where it can be seen that the sensor performance in serum samples is in good accordance with the response in a buffer. The sensor demonstrated a minimum recovery of 74.46% at 0.1 ng/mL PSA and a maximum of 97.64% at 10 ng/mL PSA. It is probable that protein-protein interactions within the sample matrix are causing a small loss in sensitivity, with similar behaviour reported for aptamer ELISA assays [20]. Specifically, this assay used free PSA derived from seminal fluid, which may interact with complementary anti-chymotrypsin and albumin proteins present in plasma, thus preventing the desired interactions with the aptasensor. In comparison, the free PSA in patient blood is internally cleaved and therefore avoids interactions with anti-chymotrypsin [28] and this could result in an improved limit of detection for clinical samples.

PSA added (ng/mL)	**PSA found (ng/mL)**	**R.S.D. (%)**	**R.E. (%)**	**Recovery (%)**
0.1	0.07	6.99	0.74	74.46
1	0.85	5.96	0.90	85.01
3	2.60	7.7	1.43	86.71
5	4.26	9.27	1.94	85.11
10	9.76	4.10	1.08	97.64

Table 3.1Detection of PSA in human serum. The amount of PSA found in spiked plasma corresponds to the percentage signal calculated on basis of PSA detection in PBS buffer. Results represent mean ± SD (standard deviation) obtained from three independent experiments s; R.S.D. (relative standard deviation) = standard deviation/mean × 100; R.E. (relative error) = [(true value-measured value)/true value] × 100; n = 3

An overview of existing electrochemical PSA aptasensors is presented in Table 2. It is important to distinguish between results obtained in human serum with those obtained in buffers. Whilst Kavosi *et al.* [29] produced an aptasensor with very low detection limits (10 fg/mL for DPV) with a wide dynamic range (0.1 pg/mL - 90 ng/mL), the mechanism is enzymatic and utilises a complex composite. Most recently Rahi *et al.* [30] have reported a relatively simple system based on electrodeposited gold nanospheres using an arginine template to achieve a 50 pg/mL detection limit.

However, the surface morphology and control is more complex due to the mechanism of electrodepositing of gold nanospheres using an arginine template.

Regardless of achieving a slightly lower detected concentration of PSA, we feel the real strength of our approach is the simplicity and flexibility of the fabrication process. Simply switching the MCH for FcSH during co-immobilisation of the aptamer probe allows for amperometric detection. Most importantly modifying the planar gold surface with AuNPs can be extended to many other metallic substrates and the simple process of controlling surface coverage of the aptamer probe through co-immobilisation provides mechanisms to achieve robust anti-fouling properties for improved surface chemistry.

Scheme	Electrode	Immobilisation strategy	LOD	Detection range	in serum	Reference
DPV	GCE	biotinylated aptamers on AuNPs encapsulated in graphitised mesoporous carbon via affinity method	0.25 ng/mL	0.25 - 200 ng/mL	yes	Liu *et al.* 2012 [31]
EIS	Au	amine-terminated DNA aptamers on a SAM of mercaptoundecanoic acid and thiol terminated sulfobetaine	0.5 ng/mL	0.5 - 1000 ng/mL	no	Jolly *et al.* 2015 [32]
EIS	Au	co-immobilised SAM of DNA-aptamer and MCH	60 ng/mL	60 ng/mL - 10 mg/mL	no	Formisano *et al.* 2015 [25]
EIS	Au	DNA-directed immobilisation aptamer sensors with pre incubation of aptamer and PSA	0.5 pg/mL	0.05 - 50 ng/mL	no	Yang *et al.* 2015 [33]
DPV/EIS	GCE	graphene chitosan composite deposited on GCE followed by immobilisation of capture antibodies. AuNPs–PAMAM functionalised with PSA aptamer to complete the sandwich	DPV: 10 fg/mL EIS: 5 pg/mL	DPV: 100 fg/mL - 90 ng/mL EIS: 5 pg/mL - 35 ng/mL	yes	Kavosi *et al.* 2015 [29]
SWV	GCE	covalent grafting of amine-terminated DNA aptamers on quinone-based conducting polymer	> 1 ng/mL	> 1 ng/mL - 10 µg/mL	no	Souada *et al.* 2015 [34]
DPV	GCE	carboxylated carbon nanotubes mixed with chitosan physisorped to electrode. Amine terminated DNA aptamers covalently attached to carboxylic groups with glutaraldehyde linker	0.75 ng/mL	0.85 - 12.5 ng/mL and 12.5 - 500 ng/mL	yes	Tahmasebi & Noobakhsh 2016 [35]
DPV	Au	electrodeposited gold nanospheres with arginine template on gold electrode for further immobilisation of aptamer	0.05 ng/mL	0.125 - 200 ng/mL	yes	Rahi *et al.* 2016 [30]
EIS	Au	Amalgamation of DNA aptamers and molecularly imprinted polymers	1 pg/mL	1 pg/mL – 10 ug/mL	No	Jolly *et al.* [36]
EIS/SWV	Au	DNA aptamer immobilised on self-assembled AuNP-modified surface	EIS: 0.01 ng/mL SWV: 0.1 ng/mL	EIS: 0.01 - 10 ng/mL SWV: 1 - 100 ng/mL	yes	This work

Notes: DPV: Differential Pulse Voltammetry; SWV: Square Wave Voltammetry; EIS: Electrochemical Impedance Spectroscopy; GCE: Glassy Carbon Electrode

Table 3.2 Comparison of existing electrochemical PSA aptasensors performance

3.4 Conclusions

We have shown how the detection limit of a previously reported methodology using a planar gold surface can be significantly improved with the addition of a simple step to attach AuNPs. Co-immobilising the anti-PSA aptamer with either FcSH or MCH provides a platform for the amperometric or impedimetric detection of PSA, respectively within the clinically relevant 1-10 ng/mL range. The aptasensor performed markedly better in its impedimetric guise, with PSA concentrations down to 10 pg/mL detected in diluted human serum with a dynamic range up to 10 ng/mL. The sensitivity and specificity of the aptasensor make it applicable for clinical analysis of PCa. We believe the simplicity of the fabricated aptasensor offers several advantages compared to other current PCa detection techniques.

Acknowledgements

This work was funded by the European Commission FP7 Programme through the Marie Curie Initial Training Network PROSENSE (grant no. 317420, 2012-2016). J.L.H. is supported by an UK Engineering and Physical Sciences Research Council (EPSRC) Doctoral Training Award.

References

[1] M-C. Daniel & D. Astruc, Gold Nanoparticles: Assembly, Supramolecular Chemistry, Quantum-Size-Related Properties, and Applications toward Biology, Catalysis, and Nanotechnology, *Chem. Rev.* 104 (2004), 293–346.

[2] J.M. Pingarrón, P. Yáñez-Sedaño, A. González-Cortés, Gold nanoparticle-based electrochemical biosensors, *Electrochim. Acta* 53 (2008) 5848-5866. [3] S. Zeng, K.T. Yong, I. Roy, X.Q. Dinh, X. Yu, F. Luan, A Review on Functionalized Gold Nanoparticles for Biosensing Applications, *Plasmonics* 6 (2011) 491-506.

[4] K. Saha, S.S. Agasti, C. Kim, X. Li, X. V.M. Rotello, Gold Nanoparticles in Chemical and Biological Sensing, Chem. Rev. 112 (2012) 2739-2779.

[5] W. Zhou, X. Gao, D. Liu, X. Chen, Gold Nanoparticles for *In Vitro* Diagnostics, *Chem. Rev.* 115 (2015) 10575-10636.

[6] A.D. Keefe, S. Pai, A. Ellington, Aptamers as therapeutics, *Nat. Rev. Drug Discov.* 9 (2010) 537-550.

[7] J.G. Bruno, Predicting the Uncertain Future of Aptamer-Based Diagnostics and Therapeutics. *Molecules* 20 (2015) 6866-6887.

[8] J.W. Lee, H.J. Kim, K. Heo, Therapeutic aptamers: developmental potential as anticancer drugs, *BMB Rep.* 48 (2015) 234-237.

[9] T. Mairal, V.C. Özalp, P.L. Sánchez, M. Mir, I. Katakis, C.K. O'Sullivan, Aptamers: molecular tools for analytical applications, *Anal. Bioanal. Chem.* 390 (2008) 989-1007.

[10] J.W. Keum, H. Bermudez, Enhanced resistance of DNA nanostructures to enzymatic digestion, *Chem. Commun.* 45 (2009) 7036-7038.

[11] L.D. Li, Z.B. Chen, H.T. Zhao, L. Guo, X. Mu, An aptamer-based biosensor for the detection of lysozyme with gold nanoparticles amplification, *Sens. Actuators B* 149 (2010). 110-115.

[12] S.M. Taghdisi, N.M. Danesh, P. Lavaee, M. Ramezani, K. Abnous, An electrochemical aptasensor based on gold nanoparticles, thionine and hairpin structure of complementary strand of aptamer for ultrasensitive detection of lead, *Sens. Actuators B* 234 (2016) 462-469.

[13] S. Karash, R. Wang, L. Kelso, H. Lu, T.J. Huang, Y. Li, Rapid detection of avian influenza virus H5N1 in chicken tracheal samples using an impedance aptasensor with gold nanoparticles for signal amplification, *J. Virol. Methods* 236 (2016) 147-156.

[14] N.H. Kim, S.J. Lee, M. Moskovits, Aptamer-Mediated Surface-Enhanced Raman Spectroscopy Intensity Amplification, *Nano Lett.* 10 (2010) 4181-4185.

[15] Y.M. Liu, J.J. Zhang, G.F. Shi, M. Zhou, Y.Y. Liu, K.J. Huang, Y.H. Chen, Label-free electrochemiluminescence aptasensor using $Ru(bpy)_3^{2+}$ functionalized dopamine-melanin colloidal nanospheres and gold nanoparticles as signal-amplifying tags, *Electrochim. Acta* 129 (2014) 222-228.

[16] Z.M. Dong, G.C. Zhao, Quartz Crystal Microbalance Aptasensor for Sensitive Detection of Mercury(II) Based on Signal Amplification with Gold Nanoparticles, *Sensors* 12 (2012) 7080-7094.

[17] S. Jeong, S.R. Han, Y.J. Lee, S.W. Lee, Selection of RNA aptamers specific to active prostrate-specific antigen, *Biotechnol. Lett.* 32 (2010) 379-385.

[18] W.J. Catalona, D.S. Smith, T.L. Ratliff, K.M. Dodds, D.E. Coplen, J.J. Yuan, J.A. Petros, G.L. Andriole, Measurement of prostate-specific antigen in serum as a screening test for prostate cancer, *N. Engl. J. Med.* 324 (1991) 1156-1161.

[19] D.A. Healey C.J. Hayes, P. Leonard, L. McKenna, R. O'Kennedy, Biosensor developments: application to prostate-specific antigen detection, *Trends Biotechnol.* 25 (2007) 125-131.

[20] N. Savory, K. Abe, K. Sode, K. Ikebukuro, Selection of DNA aptamer against prostate specific antigen using a genetic algorithm and application to sensing. *Biosens. Bioelectron.* 26 (2010) 1386-1391.

[21] V.A. Moyer, Screening for prostate cancer: U.S. Preventative Services Task Force recommendation statement, *Ann. Intern. Med.* 157 (2012) 120-134..

[22] J. H. Hayes, M. J. Barry, Screening for Prostate Cancer With the Prostate-Specific Antigen Test A Review of Current Evidence, *JAMA – J. Am. Med. Assoc.* 311 (2014) 1143-1149,

[23] J. Sutton, J. Melia, M. Kirby, J. Graffy, S. Moss, GPs views and understanding of PSA testing, screening and early detection; survey, *Int. J. Clin. Pract.* 70 (2016) 389-395.

[24] A. Heidenreich, P.J. Bastian, J. Bellmunt, M. Bolla, S. Joniau, T. van der Kwast, M. Mason, V. Mateev, T. Wiegel, F. Zattoni, N. Motten, EAU guidelines on prostate cancer. Part II: Treatment of advanced, relapsing, and castration-resistant prostate cancer. *Eur. Urol.* 65 (2014) 467-479,

[25] N. Formisano, P. Jolly, N. Bhalla, M. Cromhout, S.P. Flanagan, R. Fogel, J.L. Limson, P. Estrela, Optimisation of an electrochemical impedance spectroscopy aptasensor by exploiting quartz crystal microbalance with dissipation signals, *Sens. Actuators B* 220 (2015) 369-375.

[26] T. Bertok, A. Sediva, J. Katrlik, P. Gemeiner, M. Mikula, M. Nosko, J. Tkáč, Label-free detection of glycoproteins by the lectin biosensor down to attomolar level using gold nanoparticles. *Talanta* 108 (2013) 11-18.

[27] W. Argoubi, M. Saadaoui, S.B. Aoun, N. Raouafi, Optimized design of a nanostructured SPCE-based multipurpose biosensing platform formed by ferrocene-tethered electrochemically-deposited cauliflower-shaped gold nanoparticles. *Beilstein J. Nanotechnol.* 6 (2015) 1840-1852.

[28] S.P. Balk, Y.J. Ko, G.J. Bubley, Biology of prostate-specific antigen. *J. Clin. Oncol.* 21 (2003) 383-391.

[29] B. Kavosi, A. Salimi, R. Hallaj, F. Moradi, Ultrasensitive electrochemical immunosensor for PSA biomarker detection in prostate cancer cells using gold nanoparticles/PAMAM dendrimer loaded with enzyme linked aptamer as integrated triple signal amplification strategy, *Biosens. Bioelectron.* 74 (2015) 915-923.

[30] A. Rahi, N. Sattarahmady, H. Heli, Label-free electrochemical aptasensing of the human prostate-specific antigen using gold nanospears. *Talanta* 156-157 (2016) 218-224.

[31] B. Liu, L. Lu, E. Hua, S. Jiang, G. Xie, Detection of the human prostate-specific antigen using an aptasensor with gold nanoparticles encapsulated by graphitizes mesoporous carbon. *Microchim. Acta* 178, (2012) 163-170.

[32] P. Jolly, N. Formisano, J. Tkáč, P. Kasák, C.G. Frost, P. Estrela, Label-free impedimetric aptasensor with antifouling surface chemistry: A prostate specific antigen case study, *Sens. Actuators B* 209 (2015) 306-312.

[33] Z. Yang, B. Kasprzyk-Hordern, S. Goggins, C.G. Frost, P. Estrela, A novel immobilization strategy for electrochemical detection of cancer biomarkers: DNA-directed immobilization of aptamer sensors for sensitive detection of prostate specific antigens, *Analyst* 140 (2015) 2628-2633.

[34] M. Souada, B. Piro, S. Reisberg G. Anquetin, V. Noël, M.C. Pharm, Label-free electrochemical detection of prostate-specific antigen based on nucleic acid aptamer, *Biosens. Bioelectron.* 68 (2015) 49-54.

[35] F. Tahmasebi, A. Noorbakhsh, Sensitive Electrochemical Prostate Specific Antigen Aptasensor: Effect of Carboxylic Acid Functionalized Carbon Nanotube and Glutaraldehyde Linker, *Electroanalysis* 28 (2016) 1134-1145.

[36] P. Jolly, V. Tamboli, R. L. Harniman, P. Estrela, C. J. Allender, J. L. Bowen. Aptamer–MIP hybrid receptor for highly sensitive electrochemical detection of prostate specific antigen. *Biosensors and Bioelectronics* 75 (2016) 188-195.

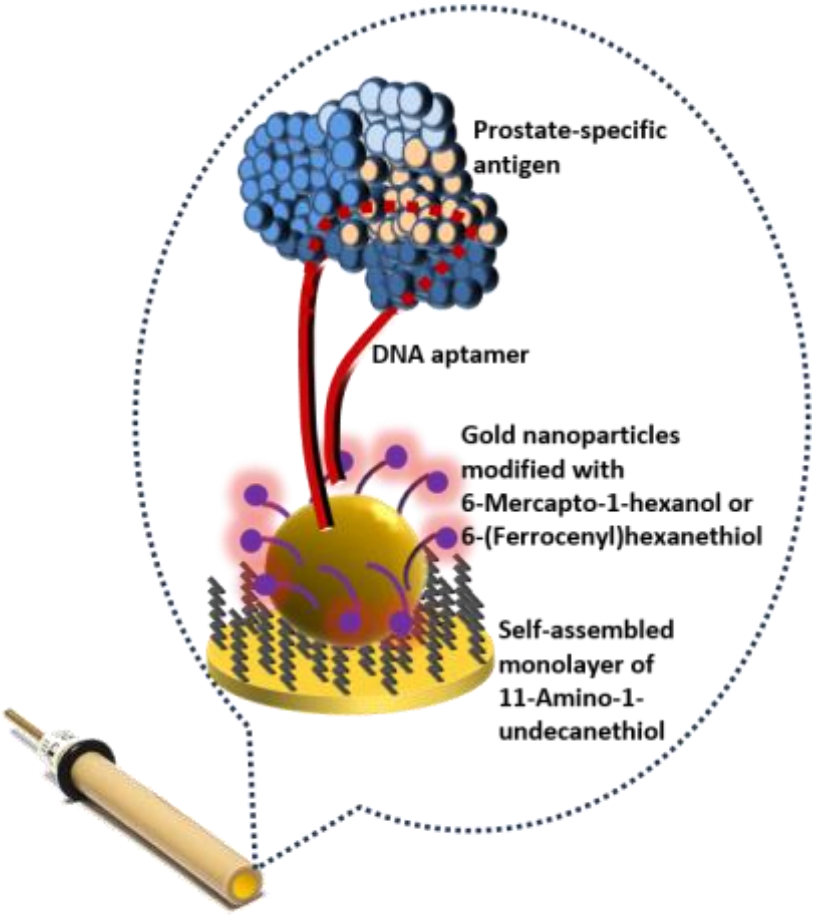

Table 3.3 Graphical abstract

Supplementary Information

S-1: Selectivity study with control protein using electrochemical impedance spectroscopy

By overlaying the dose responses for the 1:10, 1:50, 1:75 and 1:100 ratios, it can be seen in Figure S-1 that the response is not hugely affected by the density of surface-bound probe on AuNPs. An attempt to fit the dose responses data from different ratios was performed. The ΔR_{ct} versus [PSA] curves roughly follow a Hill dose-response equation of the type $y = y_0 + (y_{max}-y_0)\, c^n/(k^n + c^n)$ where c is the concentration. Fitting

demonstrated good root mean square (RMS) values of 0.94, 0.99, 0.99, 0.91 for 1:10, 1:50, 1:75 and 1:100 respectively. However, without having demonstrated the saturation phase, no accurate values of the parameters can be extracted from the fits. From all the ratios tested, the 1:50 ratio provided a slight improvement in reproducibility along with better discrimination against the HSA control compared to the higher probe density 1:20 ratio. This demonstrates the trade-off between surface coverage and efficacy of analyte capture.

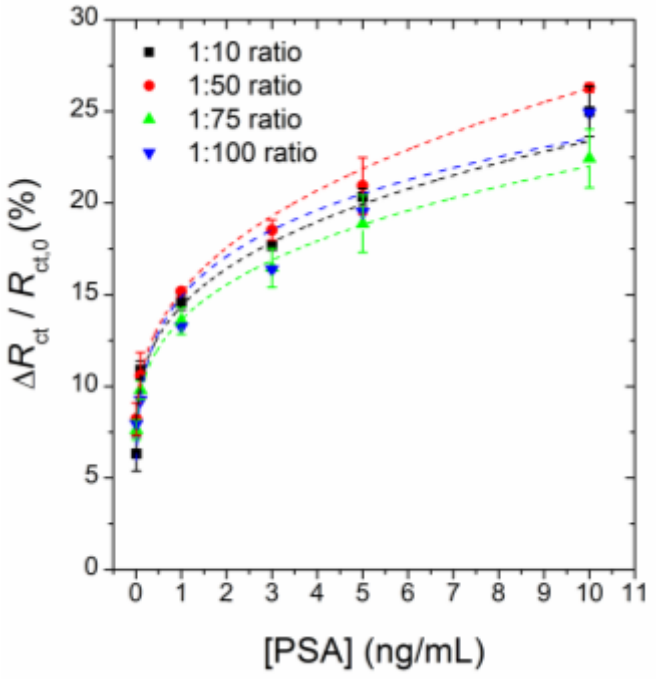

Figure 3.6 Dose response for 0.01 ng/mL to 10 ng/mL PSA in 10 mM PBS (pH 7.4) for the aptasensor with different MCH to probe ratios with standard mean errors from 4 independent samples

S-2: Electrochemical surface selectivity test using a random probe sequence

To verify that the aptasensor electrochemical response was caused by the PSA target binding to the aptamer probe rather than non-specific interactions caused by the presence of the surface-bound FcSH molecules, we replaced the PSA probe with a random DNA sequence and tested the response using square-wave voltammetry.

Figure 3.7 (a) shows the voltammogram for the blank response of the random DNA sequence attached to the AuNP-modified planar gold surface and with the addition of 50 ng/mL PSA target. Changes in peak current for both the random and anti-PSA systems were calculated and shown in Figure 3.7 (b). With the random sequence a

mean shift of ~1% was observed, attributed to non-specific interactions, compared to a mean shift of ~28% for the correct anti-PSA probe. The difference in the response indicates the specificity of the surface chemistry developed for PSA detection is acceptable.

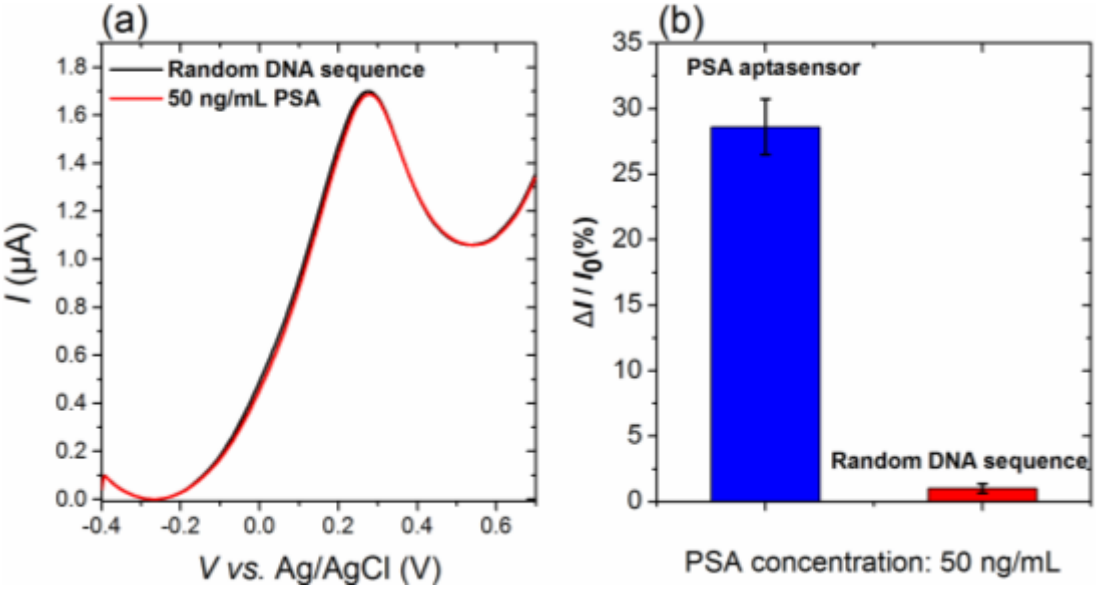

Figure 3.7 (a) Forward sweep of the square-wave voltammograms (in 10 mM PBS, pH 7.4) showing the blank response of the random DNA sequence (blue) and the response after the addition of 50 ng/mL PSA (red). (b) Comparison of the PSA aptasensor (blue) and the control surface (red) with an addition of 50 ng/mL PSA (n=3)

Chapter 4. Capacitive aptasensor based on interdigitated electrode for breast cancer detection in undiluted human serum

<table>
<tr><td colspan="9">This declaration concerns the article entitled:</td></tr>
<tr><td colspan="9">Capacitive aptasensor based on interdigitated electrode for breast cancer detection in undiluted human serum</td></tr>
<tr><td colspan="9">Publication status (tick one)</td></tr>
<tr><td>draft manuscript</td><td>Submitted</td><td></td><td>In review</td><td>X</td><td>Accepted</td><td></td><td>Published</td><td></td></tr>
<tr><td>Publication details (reference)</td><td colspan="8"></td></tr>
<tr><td>Candidate's contribution to the paper (detailed, and also given as a percentage).</td><td colspan="8">The candidate contributed predominantly to:

Formulation of ideas: The idea was formulated together with Dr Sunil Arya. My contribution was more on the experimental part. In total my contribution was 35%

Design of methodology: The methodology was elaborated much more by Dr Sunil Arya. In percentage my contribution was 20%

Experimental work: The experimental work and analysis was majorly performed equally with Dr Sunil Arya. My contribution was 50%.

Presentation of data in journal format: The paper about this work was written in collaboration with Dr. Sunil Arya and Dr Pawan Jolly. My contribution was of 40%</td></tr>
<tr><td>Statement from Candidate</td><td colspan="8">This paper reports on original research I conducted during the period of my Higher Degree by Research candidature.</td></tr>
<tr><td>Signed</td><td colspan="5">  </td><td>Date</td><td colspan="2">30/05/2017</td></tr>
</table>

Sunil Arya[1*], Pavel Zhurauski[1], Pawan Jolly[1], Marina Batistuti[2], Marcelo Mulato[2], Pedro Estrela[1*]

[1]*Department of Electronic & Electrical Engineering, University of Bath, Bath BA2 7AY, United Kingdom*

[2]*Department of Physics, University of São Paulo, 14040-901, Ribeirão Preto, SP, Brazil*

[*]*Corresponding Author:* Phone: +44 7405106621, Email: *sunilarya333@gmail.com* (Sunil K Arya), *P.Estrela@bath.ac.uk* (Pedro Estrela)

The work in this chapter is submitted to Biosensors and Bioelectronics journal. The work included as a project leader Dr Sunil Arya and Pavel Zhurauski as his first collaborator. The contribution included the suggestions for the development of the experimental design, experimental performing, analysis of data and preparation of the manuscript.

Abstract

We report the development of a simple and powerful capacitive aptasensor for the detection and estimation of Her2, a biomarker for breast cancer, in undiluted serum. The study involves the incorporation of interdigitated gold electrodes, which were used to prepare the electrochemical platform. A thiol terminated DNA aptamer with affinity for Her2 was used to prepare the bio-recognition layer via self-assembly on interdigitated gold surfaces. Non-specific binding was prevented by blocking free spaces on surface via starting block phosphate buffer saline-tween20 blocker. The sensor was characterized using cyclic voltammetry, electrochemical impedance spectroscopy (EIS), atomic force microscopy and contact angle studies. Non-Faradic

EIS measurements were utilised to investigate the sensor performance via monitoring the changes in capacitance. The aptasensor exhibited logarithmically detection for HER2 from 1 pM to 100 nM in the buffer and undiluted serum with limits of detection lower than 1 pM in both buffer and serum, respectively. The results pave the way to develop other aptamer-based biosensors for protein biomarkers detection in undiluted serum.

Keywords: Aptamer; impedimetric; capacitance; biosensor; HER2; breast cancer

4.1 Introduction

Breast cancer is one of the most common cancers and the second major cause of deaths in women worldwide (Diaconu et al. 2013; Siegel et al. 2013). More than 90% of these deaths are related to metastatic growth (Siegel et al. 2013). Therefore, early stage detection of cancer is crucial to increase the chances of survival. Human epidermal growth factor receptors (Her/erbB) are involved in normal growth and cell differentiation, however, a malignant growth can be related with Her2 overexpression and it is present in some cases of breast, ovarian, lung, gastric, oral, prostate and other cancers (Patris et al. 2014). Her2 has also been shown to be overexpressed in around 20–30% of aggressive breast cancers and associated with poor prognosis (Diaconu et al. 2013). Breast cancer patients possess high Her2 concentrations in their blood (15–75 ng/ml) compared to normal individuals (2–15 ng/ml) and can be utilised for diagnosis (Chun et al. 2013; Hung et al. 1995). To evaluate these concentrations, various Her2 detection techniques have been reported, including fluorescence in situ hybridization (FISH) assays and immunohistochemical (IHC) assays (Press et al. 2002). However, these techniques require sophisticated instrumentation, special training, are labour-intensive and time-consuming.

To satisfy these unmet clinical needs, several biosensors that recognise enzymes, receptors and antibodies have been reported (Camacho et al. 2009; Wang et al. 2009b). One of the disadvantages of using antibodies is their instability due to irreversible denaturation. Therefore, alternative bio-recognition elements are desirable to develop stable biosensors. Synthetic molecules such as oligonucleotide aptamers have shown

great promise to fulfil these gaps associated with biomarkers. Aptamers, single strand oligonucleotides (DNA or RNA), that are designed and develop synthetically in the laboratory have been shown to bind to specific targets, such as proteins (Qureshi et al. 2015). Aptamers are known to be more stable, cheaper, are easily modified chemically and can be easily produced in bulk. Furthermore, the unique binding properties of aptamers have shown great potential for biosensors using optical, electrochemical, and mass-sensitive approaches (Cho et al. 2009; Qureshi et al. 2015).

Among various types, electrochemical biosensors have gained much interest due to their simplicity, miniaturizeability, faster and more sensitive response (Arya and Bhansali 2012; Bollella et al. 2017; Wang et al. 2017). Among electrochemical biosensors, electrochemical impedance spectroscopy (EIS)-based biosensors are recently gaining much attention (Arya et al. 2014; Gong et al. 2017). EIS based biosensors allow the label-free detection of an analyte binding to a bio-recognition layer at the electrode surface and can be measured in form of changes in capacitance and/or resistance (Ramón-Azcón et al. 2008). It has been shown in the literature that the use of interdigitated microelectrodes (IDμEs) to develop EIS-based biosensors present additional advantages of faster reaction kinetics, enhanced sensitivity and improved signal-to-noise ratio (Arya and Bhansali 2012; Ramón-Azcón et al. 2008; Wang et al. 2009a). Moreover, due to faster mass transport with a lower iR drop and double layer charging effects, IDμEs attain steady state faster, resulting in easier measurement than with conventional macroelectrodes (Arya and Bhansali 2012; Varshney and Li 2009).

In impedimetric biosensors, the use of Faradaic impedance, where transduction happens via changes in the hindrance presented by surface interface to a solution phase probe is very common (Arya et al. 2014; Santos et al. 2014); however, the use of non-Faradaic approaches, where capacitive changes are monitored (Berggren et al. 2001; Luo and Davis 2013), do not require the pre-addition of redox probes to the analytical solution and can be applied for highly sensitive detection of analytes (Berggren et al. 2001; Qureshi et al. 2010). Furthermore, for practical applications, where the measurement in real samples is required, non-Faradaic measurements are desirable. In non-Faradaic impedance, where redox active probes are absent in the solution,

transduction occurs via changes in the hindrance presented by a surface dielectric, charge distribution or local conductance, and can be monitored through capacitance measurement (Berggren et al. 2001). Such capacitance change may arise when a target protein binds to the receptor immobilised onto the electrode surface, displacing water molecules and ions away from the surface (Tkac and Davis 2009), or due to varying protein conformation (Berggren et al. 2001).

In this study, the combination of interdigitated microelectrodes (IDμE), aptamer and capacitive measurement has been utilised to develop a simple and sensitive biosensor for Her2 protein biomarker estimation. For biosensor development, gold IDμE chips were functionalized with DNA aptamers via self-assembly and used for specific capture of Her2 protein. The surface was further blocked using phosphate buffer saline-tween 20 based starting block (SB) to prevent non-specific binding and fouling of the surface. The non-Faradaic electrochemical impedance spectroscopy was utilised to quantify Her2 binding events in buffer and serum samples by monitoring the changes in capacitance.

4.2 Experimental

4.2.1 Materials

Thiol-terminated Her2 specific DNA aptamer (5'-SH-(CH2)6-AAC CGC CCA AAT CCC TAA GAG TCT GCA CTT GTC ATT TTG TAT ATG TAT TTG GTT TTT GGC TCT CAC AGA CAC ACT ACA CAC GCA CA-3') was procured from Sigma (UK). For binding studies, different concentrations of Her2 and other targets were prepared in 10 mM PBS, pH 7.4 or in undiluted serum. StartingBlock phosphate buffer saline-Tween 20; (SB) was procured from Fisher Scientific (UK); Dulbecco's phosphate buffered saline and phosphate buffered saline with 0.05% Tween20 were procured from Sigma (UK). All other chemicals were of analytical grade and were used without further purification. All aqueous solutions were prepared using 18.2 MΩ cm ultra-pure water (milli-Q water) with a Pyrogard® filter (Millipore, MA, USA).

4.2.2 Measurement and apparatus

Blank and aptamer modified IDμE chips were characterised via atomic force microscopy (AFM) imaging in ambient tapping mode using a MultiMode NanoScope

with IIIa controller (Bruker, Germany) in conjunction with version 6 control software. AFM images were recorded using 10 nm diameter AFM ContAl-G tip (BudgetSensors®, Bulgaria), and then processed by the NanoScope Analysis software, version 1.5. Aptamer binding was also characterised via contact angle measurements using an in-house built optical angle measurement system (Miodek et al. 2015). For measurement, chips were placed on the stage and a 10 µl of water drop was dispensed on the electrode with the dispensing system. The wetting of surface was then captured using a Nikon p520 camera. The contact angle was measured using a screen protractor version 4.0 procured from Iconico.

Biosensor fabrication was also characterised electrochemically via electrochemical impedance spectroscopy (EIS) and cyclic voltammetry (CV) in a three-electrode configuration with on-chip gold (2 µm thick) as a counter and a pseudo reference electrode. EIS measurements were performed at open circuit potential (equilibrium potential), without external biasing in the frequency range of 105-0.1 Hz with a 25 mV amplitude using a µAutolab III / FRA2 potentiostat/galvanostat (Metrohm, Netherlands). EIS and CV measurements were carried out using 50 µl of PBS solution (10 mM, pH 7.4) containing a mixture of 5 mM $Fe(CN)_6^{4-}$ (ferrocyanide) and 5 mM of $Fe(CN)_6^{3-}$ (ferricyanide) as a redox probe. Non-Faradaic EIS measurements on IDµEs (in the absence of redox couple) using a two-electrode configuration were utilised for HER2 detection and estimation in 10 mM PBS (pH 7.4) in a frequency range from 0.1-105 Hz with a 200 mV amplitude.

4.2.3 Electrode preparation and functionalization

4.2.3.1 Gold electrode fabrication

The deposition of interdigitated gold microelectrode arrays on Silicon/Silicon oxide wafer was performed using standard lithographic and micro-fabrication techniques as previously described (Pui et al. 2013) The 3200 µm long interdigitated fingers of 5 µm, spaced at 10 µm and attached to single base of 5500 µm length were deposited and utilized for biosensor development. Prepared IDµEs were cleaned thoroughly with isopropyl alcohol, acetone and with excess amounts of milli-Q water followed by 30 min UV-ozone treatment (ProCleaner, BioForce Nanosciences, USA) before aptamer functionalization.

4.3.3.2 Aptamer assembly and blocking

For thiolated aptamer assembly and immobilisation on IDµEs, stock aptamer immobilisation solution (100 µM in tris buffer) was heated to 95°C for 5 min followed by ice-cooling to room temperature and thereafter, diluted to 2 µM solution in PBS 1x pH 7.4. Pre-cleaned IDµEs were then incubated with 2 µM aptamer solution for 120 min at room temperature. Later, the chips were washed with PBST-20 (pH 7.4) and PBS (10 mM. pH 7.4) to remove any unbound Aptamers. The free spaces on the chip were blocked using SB incubation for 30 min, after which extra solution was removed and developed sensor electrodes were stored at 4 ˚C until further use. Figure 4.1 shows the schematic for aptasensor electrode preparation.

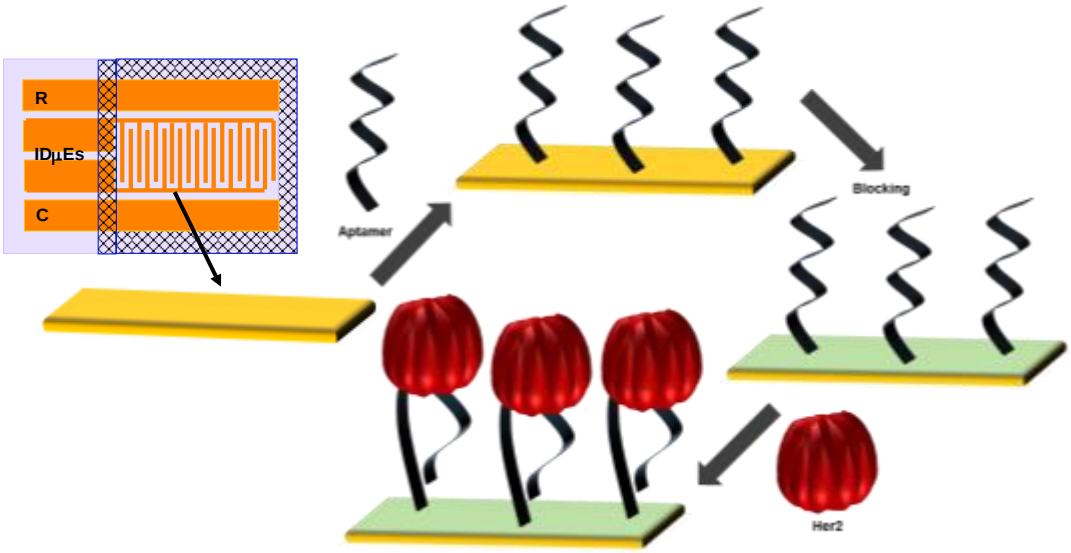

Figure 4.1 Schematic for aptasensor electrode preparation

4.3 Results and Discussion

4.3.1 Characterisation of the biosensor fabrication

4.3.1.1 Contact angle and AFM measurements

Figures 4.2a and 4.2b show the variation of contact angle of blank gold and after aptamer immobilization. The clear decrease in contact angle value from 23º for blank gold (Au) to 10º for aptamer/IDµE suggests the successful formation of aptamer self-assembled monolayer (SAM). Further, Fig. 2c and 2d shows the AFM images of blank gold and aptamer modified surface taken in tapping mode using a 10 nm AFM tip. The observed change in non-uniform morphology for blank gold (Fig 4.2c) surface to

uniformly distributed structure (Fig. 4.2d) for aptamer modified IDμE confirms the successful SAM formation by thiolated aptamer.

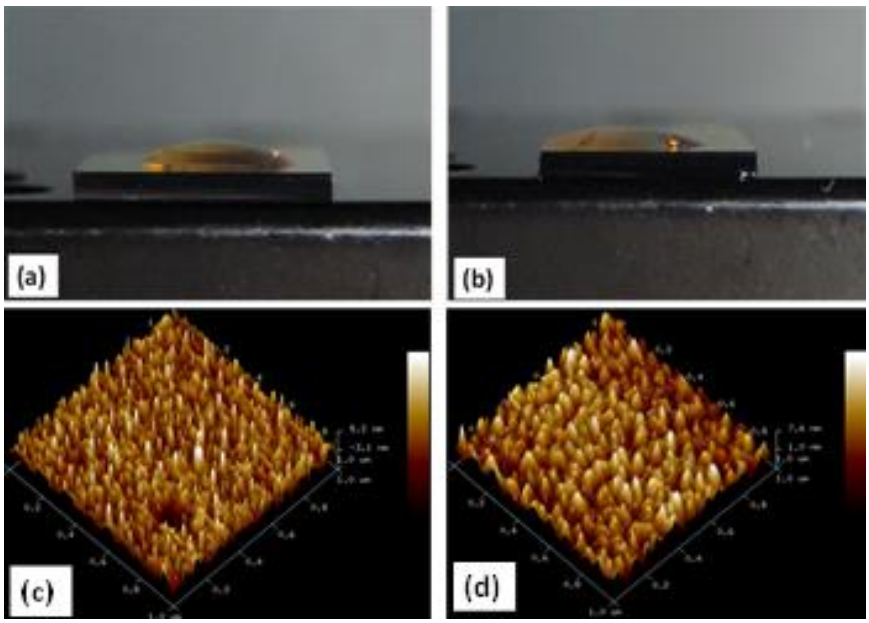

Figure 4.2 Contact angle image for (a) blank cleaned gold surface, (b) after aptamer SAM formation and AFM image for (c) blank cleaned gold surface, (d) after aptamer SAM formation

4.3.2 CV and EIS characterization for biosensor development

Biosensor fabrication was characterised using cyclic voltammetry (CV) in PBS (1x) containing 5 mM potassium ferrocyanide 5mM potassium ferricyanide ($FeCN_6^{3-/4-}$). Fig 3a decrease in peak current from 156 μA for blank IDμE to 132 μA for aptamer SAM indicate successful SAM formation. Further, reduction in peak current to 96 μA after blocking confirms the filling of free surface on IDμEs with blocker proteins. Inset in Fig 3a shows the Nyquist plots for each step, where an increase in charge transfer resistance (R_{ct}) from 217 Ω for the blank chip to 661 Ω after aptamer SAM formation reveals successful immobilisation. Further, increase in R_{ct} to 1021 Ω after blocking can be attributed to adsorption of non-conducting blocker proteins in free areas on gold.

Blank, aptamer modified and after blocking, electrodes were further investigated under different scan rates (30-100 mV/s), where observed oxidation and reduction peaks even after aptamer SAM formation and blocking suggested good redox activity of electrode. Moreover, the observed linear variation in oxidation peak currents with

the square root of scan rate (Fig. 4.3c) obey Equations 4.1 to 4.3 and suggest a diffusion-controlled process on sensor surface (Vasudev et al. 2013).

$$I_{oxi}\ (Blank\ ID\mu E)\ (\mu A) = -21.62\ \mu A + 796.85\ (Scan\ rate)^{1/2}\ \mu A;\ r^2 = 0.999 \quad (4.1)$$

$$I_{oxi}\ (Aptamer/ID\mu E)\ (\mu A) = 18.99\ \mu A + 504.33\ (Scan\ rate)^{1/2}\ \mu A;\ r^2 = 0.999 \quad (4.2)$$

$$I_{oxi}\ (SB\text{-}Aptamer/ID\mu E)\ (\mu A) = 20.69\ \mu A + 340.81\ (Scan\ rate)^{1/2}\ \mu A;\ r^2 = 0.991 \quad (4.3)$$

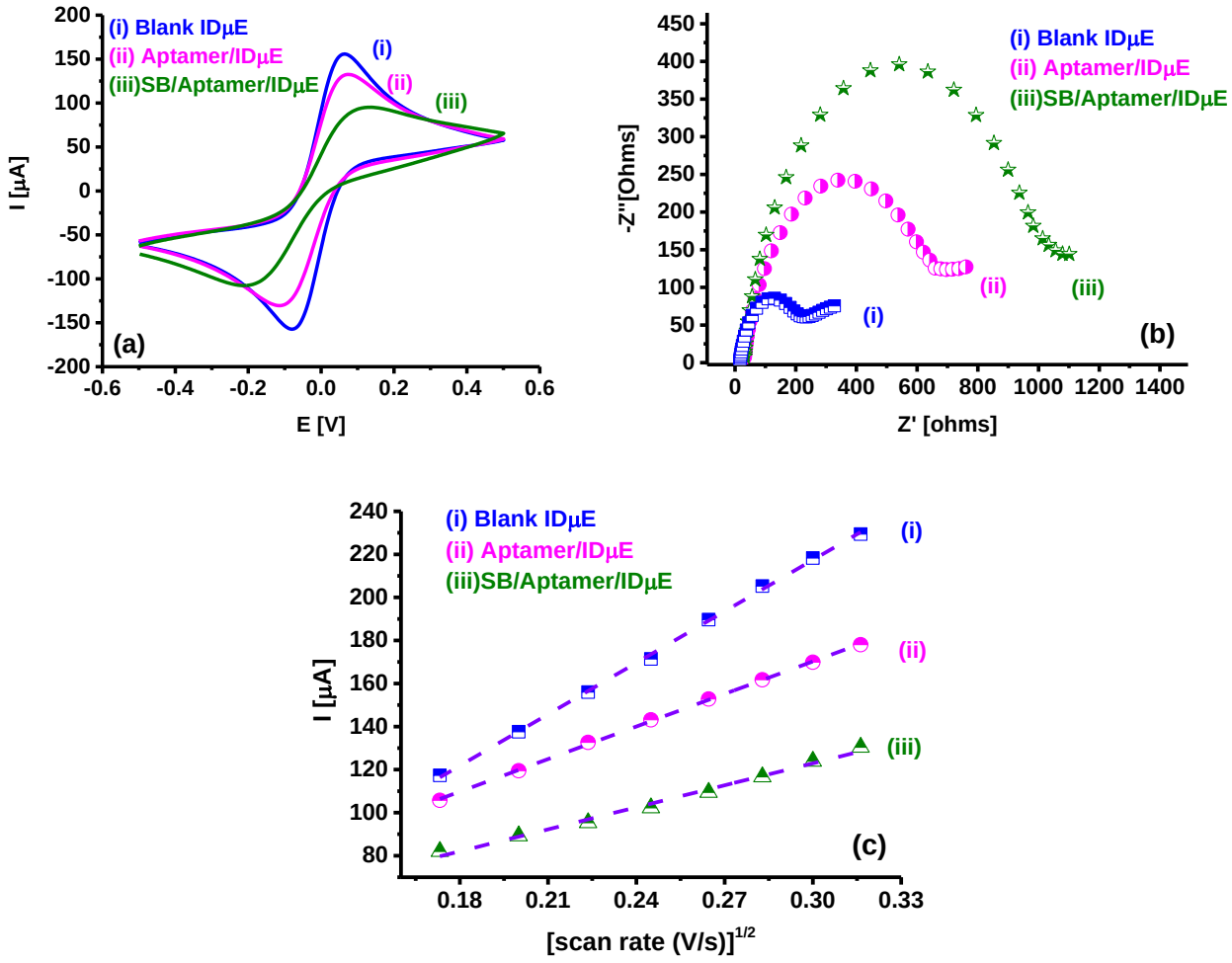

Figure 4.3 Characterization of biosensor electrode fabrication at each step via (a) CV, (b) EIS and (c) scan rates study showing oxidation peak current response as a function of square root of scan rate.

4.3.3 HeR 2 studies

4.3.3.1 Capacitive measurement via electrochemical impedance for Her2 in PBS

The SB-Aptamer/IDμE bio-electrodes were utilized to study aptamer-Her2 binding on the surface in 1 pM to 100 nM concentration range (Fig. 4.4). For measurement, the desired concentration of Her2 (50 µl) was poured onto bio-electrode and incubated for 30 min, followed by washing with PBST20 and PBS to remove unbound HER2 molecules. Non-faradic EIS spectra were then recorded for washed electrodes in 10 mM PBS (pH 7.4) and then 1/(Freq)(imaginary part of impedance (-*Z''*)) was utilised to convert obtained data to capacitance data. From capacitance curves (Fig. 4.4b), capacitance values were recorded at 2 Hz, where maximum phase angle was observed (Fig. 4.4a), indicating maximum capacitive effect.

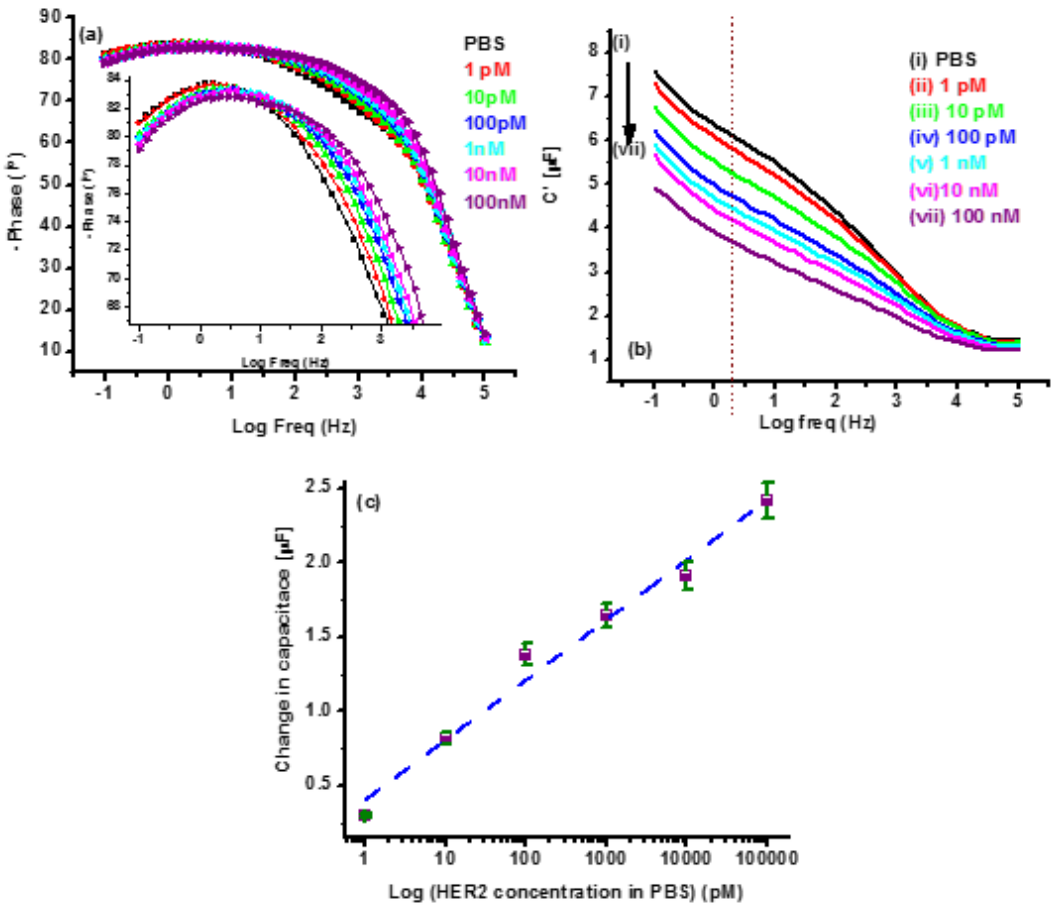

Figure 4.4 (a) phase data, (b) capacitance data for Aptamer-Her2 binding on biosensor surface in PBS and (c) calibration curve using capacitance data for different concentration at 2 Hz

Capacitive values at 2 Hz were then utilised to plot calibration curve for Her2 concentrations in PBS (Fig 4c). Decreasing capacitance value observed in Fig. 4.4b for increasing Her2 concentration may be attributed to the successful capture of Her2 proteins onto surface bound aptamer. Calibration graph generated using relative change in capacitance (Fig. 4.4c) suggested that bioelectrode can be used for linear detection of Her2 on a logarithmic scale at 1 pM to 100 nM range and can be characterised using Change in capacitance (µF) = 0.403 (µF) + 0.404 log CHER2 (pM). Further, the bio-electrode exhibited sensitivity of 0.404 µF/ log([Her2] pM a correlation coefficient of 0.981. Different electrodes were found to exhibit similar response within 5% as shown by error bars in Fig 4c.

4.3.3.2 Capacitive measurement via electrochemical impedance for Her2 in undiluted serum

For real world application, SB-Aptamer/IDµE bio-electrodes were tested with Her2 spiked in undiluted serum to study the effect of all types of serum proteins on the interaction between surface bound Aptamer and Her2 molecules (1 pM to 100 nM). (Fig. 4.5). Similar to Her2 in PBS, bioassay and measurements were carried out for Her2 in serum and obtained non-Faradaic EIS data was changed to capacitance for plotting capacitance graphs for different Her2 concentrations (Fig. 4.5b). Capacitance values at 1Hz, where maximum phase angle is observed (Fig. 4.5a), and indicating maximum capacitive effect was utilized for calibration curve (Fig. 4.5c). Observed maxima in phase angle at slightly lower frequency may be attributed to the presence of all different types of serum proteins and different conductivity and ionic strength of Her2 in serum sample compare to Her2 samples in PBS. The graph in Fig 4.5b, shows a decrease in capacitance for increasing Her2 concentrations in serum, clearly suggesting that the bio-electrode can successfully be utilized for Her2 estimation in serum. Calibration graph plotted using relative change in capacitance (Fig. 4.5c) indicated that bio-electrode can be used for linear detection of Her2 in 1 pM to 100 nM range at 1Hz and can be characterized using Change in capacitance (µF) = 0.414 (µF) + 0.201 log CHER2 (pM). Further, bioelectrode exhibited sensitivity of 0.201 µF/ log([Her2] pM with a correlation coefficient of 0.98. Different electrodes were

found to exhibit similar response within 5% as shown by error bars in Fig. 4.5c. As indicated by lower sensitivity, signal for Her2 in serum was found to be lower when compared to Her2 in PBS, which might be attributed to the presence of all serum proteins in sample causing hindrance in Aptamer-Her2 interaction. Further, other than serum proteins, bio-electrode was also tested for specificity against proteins like PSA (100ng/ml), thrombin (100 ng/ml) and Her4 (100ng/ml) spiked in serum (data not shown) and found to exhibit negligible signal when compared with signal for serum only sample, indicating good selectivity of developed electrode.

Obtained data in this work was compared with other sensor used for Her2 estimation (Table 4.1) and found that present system exhibits better response and can be utilised for the real sample application.

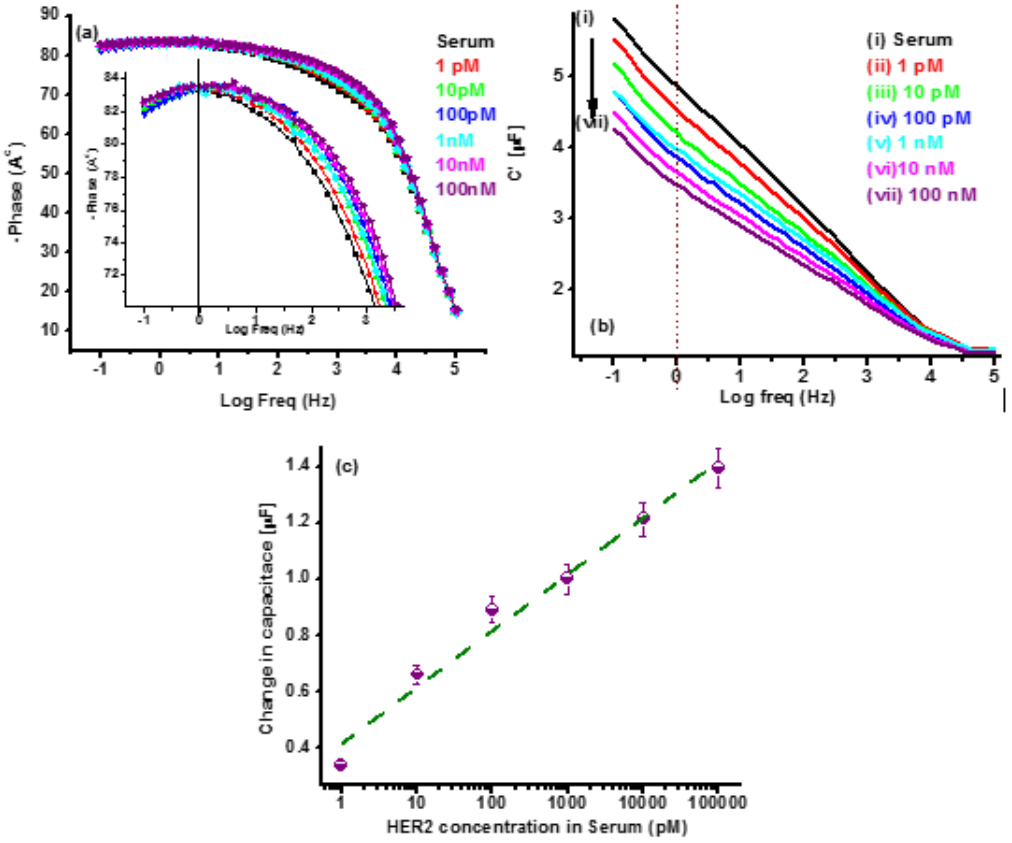

Figure 4.5 (a) phase data, (b) capacitance data for interaction between surface bound Aptamer with Her2 concentrations in undiluted serum and (c) calibration curve using capacitance data for different concentration at 1Hz

Technique	Electrode/Surface	Probe	LOD	Reference
EIS	Gold nanostructured screen-printed graphite	Affibody cysteine-modified affibody	6 ng/ml	(Ravalli et al. 2015)
Opto-fluidic ring resonator (OFRR)	Silica glass capillaries modified with cross-linkers to bind protein G	HER2 antibody	10 ng/ml	(Gohring et al. 2010)
Fluorescence	Carbon nanotube wrapped anti-HER2 ssDNA aptamers	Aptamer	38 nM (4.75 ng/ml)	(Niazi et al. 2015)
Capacitance	Interdigitated microelectrodes	Aptamer	0.2 ng/ml	(Qureshi et al. 2015)
Surface acoustic wave (SAW)	SAW resonator with gold transducer	Antibody	10 ng/ml	(Gruhl et al. 2010)
Microfluidic with fluorescence transduction	Quantum Dots (QD)	Immunoassay/ Antibody	0.27 ng/ml	(Jokerst et al. 2009)
Amperometric (CV)	Carbon screen printed electrodes	Immunoassay (nanoimmunoassay)/ Antibody	1 µg/ml	(Patris et al. 2014)
Surface acoustic wave (SAW)	SAW resonators based on 36° YX-Li-TaO3 substrates	Antibody	10 ng/ml	(Gruhl and Länge 2012)
Surface plasmon resonance (SPR) spectroscopy	Protein G based	Antibody	11 ng/ml	(Martin et al. 2006)
Capacitance	Interdigitated electrodes	Aptamer	1pM (0.1 ng/ml)	Present study

Table 4.1 Comparison between present approach with the state-of-art technologies

4.4 Conclusion

An aptamer-based capacitive biosensor strategy has been demonstrated for the detection of Her2 in undiluted serum. The biosensor showed excellent selectivity when challenged with other serum protein. The prepared biosensor exhibited linear detection for Her2 at 1 pM to 100 nM range with a high sensitivity of 0.201 µF/ log([Her2] pM

in undiluted serum. Furthermore, the fabrication method is simple and can be applied for detection of other biomarkers in a serum sample, paving the way to a new platform for alternative low-cost and rapid biosensors.

Acknowledgements

S.K.A. was funded by a Marie Skłodowska-Curie Individual Fellowship through the European Commission's Horizon 2020 Programme (grant no. 655176). P.Z and P.J. were funded by the European Commission FP7 Programme through the Marie Curie Initial Training Network PROSENSE (grant no. 317420, 2012-2016). M.R.B. is funded by FAPESP (process number 2015/14403-5). M.M. and P.E. acknowledge funding from FAPESP and the University of Bath through the SPRINT programme.

References

Arya, S.K., Bhansali, S., 2012. Biosensors Journal 1, H110601, 110607 pages.

Arya, S.K., Kongsuphol, P., Wong, C.C., Polla, L.J., Park, M.K., 2014. Sensors and Actuators B: Chemical 194, 127-133.

Berggren, C., Bjarnason, B., Johansson, G., 2001. Electroanalysis 13(3), 173-180.

Bollella, P., Fusco, G., Tortolini, C., Sanzò, G., Favero, G., Gorton, L., Antiochia, R., 2017. Biosensors and Bioelectronics 89, Part 1, 152-166.

Camacho, C., Chico, B., Cao, R., Matías, J.C., Hernández, J., Palchetti, I., Simpson, B.K., Mascini, M., Villalonga, R., 2009. Biosensors and Bioelectronics 24(7), 2028-2033.

Cho, E.J., Lee, J.-W., Ellington, A.D., 2009. Annual Review of Analytical Chemistry 2(1), 241-264.

Chun, L., Kim, S.-E., Cho, M., Choe, W.-s., Nam, J., Lee, D.W., Lee, Y., 2013. Sensors and Actuators B: Chemical 186, 446-450.

Diaconu, I., Cristea, C., Hârceagă, V., Marrazza, G., Berindan-Neagoe, I., Săndulescu, R., 2013. Clinica Chimica Acta 425, 128-138.

Gohring, J.T., Dale, P.S., Fan, X., 2010. Sensors and Actuators B: Chemical 146(1), 226-230.

Gong, Q., Wang, Y., Yang, H., 2017. Biosensors and Bioelectronics 89, Part 1, 565-569.

Gruhl, F.J., Länge, K., 2012. Analytical Biochemistry 420(2), 188-190.

Gruhl, F.J., Rapp, M., Länge, K., 2010. Procedia Engineering 5, 914-917.

Hung, M.-C., Matin, A., Zhang, Y., Xing, X., Sorgi, F., Huang, L., Yu, D., 1995. Gene 159(1), 65-71.

Jokerst, J.V., Raamanathan, A., Christodoulides, N., Floriano, P.N., Pollard, A.A., Simmons, G.W., Wong, J., Gage, C., Furmaga, W.B., Redding, S.W., McDevitt, J.T., 2009. Biosensors and Bioelectronics 24(12), 3622-3629.

Luo, X., Davis, J.J., 2013. Chemical Society Reviews 42(13), 5944-5962.

Martin, V.S., Sullivan, B.A., Walker, K., Hawk, H., Sullivan, B.P., Noe, L.J., 2006. Appl. Spectrosc. 60(9), 994-1003.

Miodek, A., Regan, E., Bhalla, N., Hopkins, N., Goodchild, S., Estrela, P., 2015. Sensors 15(10), 25015.

Niazi, J.H., Verma, S.K., Niazi, S., Qureshi, A., 2015. Analyst 140(1), 243-249.

Patris, S., De Pauw, P., Vandeput, M., Huet, J., Van Antwerpen, P., Muyldermans, S., Kauffmann, J.-M., 2014. Talanta 130, 164-170.

Press, M.F., Slamon, D.J., Flom, K.J., Park, J., Zhou, J.-Y., Bernstein, L., 2002. Journal of Clinical Oncology 20(14), 3095-3105.

Pui, T.S., Kongsuphol, P., Arya, S.K., Bansal, T., 2013. Sensors and Actuators B: Chemical 181, 494-500.

Qureshi, A., Gurbuz, Y., Niazi, J.H., 2010. Procedia Engineering 5, 828-830.

Qureshi, A., Gurbuz, Y., Niazi, J.H., 2015. Sensors and Actuators B: Chemical 220, 1145-1151.

Ramón-Azcón, J., Valera, E., Rodríguez, Á., Barranco, A., Alfaro, B., Sanchez-Baeza, F., Marco, M.P., 2008. Biosensors and Bioelectronics 23(9), 1367-1373.

Ravalli, A., da Rocha, C.G., Yamanaka, H., Marrazza, G., 2015. Bioelectrochemistry 106, Part B, 268-275.

Santos, A., Davis, J.J., Bueno, P.R., 2014. J Anal Bioanal Tech, S7:016.

Siegel, R., Naishadham, D., Jemal, A., 2013. CA: A Cancer Journal for Clinicians 63(1), 11-30.

Tkac, J., Davis, J.J., 2009. Chapter 7 Label-free Field Effect ProteinSensing. Engineering the Bioelectronic Interface: Applications to Analyte Biosensing and Protein Detection, pp. 193-224. The Royal Society of Chemistry.

Varshney, M., Li, Y., 2009. Biosensors and Bioelectronics 24(10), 2951-2960.

Vasudev, A., Kaushik, A., Bhansali, S., 2013. Biosensors and Bioelectronics 39(1), 300-305.

Wang, L., Xiong, Q., Xiao, F., Duan, H., 2017. Biosensors and Bioelectronics 89, Part 1, 136-151.

Wang, R., Wang, Y., Lassiter, K., Li, Y., Hargis, B., Tung, S., Berghman, L., Bottje, W., 2009a. Talanta 79(2), 159-164.

Wang, X., Zhao, M., Nolte, D.D., 2009b. Analytical and Bioanalytical Chemistry 393(4), 1151.

Chapter 5. Sensitive and selective Affimer-modified interdigitated electrode-based capacitive biosensor for tumour markers

This declaration concerns the article entitled:								
Sensitive and selelctive Affimer-modified interdigitated electrode-based capacitive biosensor for tumour markers								
Publication status (tick one)								
draft manuscript	**Submitted**		**In review**	X	**Accepted**		**Published**	
Publication details (reference)								
Candidate's contribution to the paper (detailed, and also given as a percentage).	The candidate contributed predominantly to: Formulation of ideas: The idea was formulated together with Dr Sunil Arya and Dr Pawan Jolly. My contribution was 40% Design of methodology: The methodology was a combined effort with Avacta Life Sciences which has furnished the biological probes and Dr. Pawan Jolly and Sunil Arya. My contribution is 35% Experimental work: The experimental work and analysis of data was majorly performed by myself with the help of Dr Pawan Jolly and Dr Sunil Arya. My Contributiom was of 70% Presentation of data in journal format: I was involved in reporting the experimental data and also in the writing of the paper together with Dr Pawan Jolly and Sunil Arya. We had equal contribution in writing the paper (30%). I have presented the work on international conferences in both oral and poster format.							
Statement from Candidate	This paper reports on original research I conducted during the period of my Higher Degree by Research candidature.							
Signed	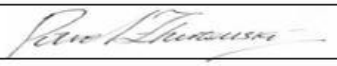				**Date**	30/05/2017		

Pavel Zhurauski[1], Sunil K. Arya[1,*], Pawan Jolly[1], Darren C. Tomlinson2, Paul Ko Ferrigno[2], Pedro Estrela[1,*]

[1] *Department of Electronic and Electrical Engineering, University of Bath, Bath BA2 7AY, UK*

[2] *Astbury Centre for Structural and Molecular Biology, University of Leeds, Leeds LS2 9JT, UK*

[2] *Avacta Life Sciences Ltd, Unit 20, Ash Way, Thorp Arch Estate, Wetherby, LS23 7FA, UK*

[*] *Corresponding authors:* Phone: +44 7405106621, Email: sunilarya333@gmail.com (Sunil K Arya), P.Estrela@bath.ac.uk (Pedro Estrela)

The work in this chapter is submitted to ACS Sensors. The work included as a project leader Pavel Zhurauski and Dr Sunil Arya and Dr Pawan Jolly as his collaborators. The contribution included the creation and development of the experimental design, experimental performing, analysis of data and preparation of the manuscript.

Abstract

A novel Affimer-modified interdigitated electrode-based capacitive biosensor platform has been developed for detection and estimation of Her4, a tumour biomarker, in undiluted serum. A pre-modified cysteine-terminated Affimer with an affinity for Her4 was utilised to prepare the bio-recognition layer via self-assembly on gold interdigitated electrodes for the sensor fabrication. Electrochemical impedance spectroscopy (EIS) in the absence of redox markers was used to evaluate the sensor performance by monitoring the changes in capacitance. The Affimer sensor in the buffer and in undiluted serum demonstrated high sensitivity with a broad dynamic range from 1 pM to 100 nM and a limit of detection lower than 1 pM both in the buffer and in serum. Furthermore, the Affimer sensor demonstrated excellent specificity for

other serum protein, suggesting resilience to non-specific binding. The sensing ability of the present Affimer sensor in spiked undiluted serum suggest its potential for a new range of Affimer-based sensors. The fabricated Affimer sensor can thus be further adapted with other probes having affinities to other biomarkers for a new range of biosensors.

Keywords: Affimer; impedimetric; capacitance; biosensor; Her4

5.1 Introduction

In recent years, there has been a huge turnover in the development of novel bioreceptors, which is mainly due to the emergence of different molecular cloning techniques along with simultaneous accessibility of varied development methods. The primary motivations behind these developments for the biochemists / molecular biologists have been not only the huge biological potential but also an enormous demand for synthetic bio-receptors. Whilst antibodies remain the workhorse choice for the molecular recognition for many biosensing devices and laboratory assays, their usage can still impose limitations on technology adoption (Song et al. 2008). One long-championed alternative to antibodies has been DNA aptamers, which are single-stranded oligonucleotide sequences possessing high affinity and specificity for its desired target. DNA aptamers, in their own right, have been extensively used for biosensing applications (‘Aptasensors’), yet the approach has had little impact as a viable bioanalytical tool till date (Rimmele 2003; Xu et al. 2009). Despite many advantages over antibodies, they still possess a number of limitations, for example, degradation by nucleases (DNAse and RNAse) or protein fouling in serum due to DNA binding proteins (Keum and Bermudez 2009; Sylvia et al. 1975).

A new emerging class of bioreceptors inspired from the increasing understanding of antibodies are Affimers®, generically termed as peptide aptamers. Affimers are engineered from either human stefin A protein or a plant cystatin consensus that has been designed to mimic the molecular recognition characteristic of monoclonal antibodies for the detection of biomolecules. Affimers consist of a scaffold, which

works as a protein platform for the restriction of two variable recognition peptide region (Johnson et al. 2012; Straw et al. 2013; Tiede et al. 2014; Woodman et al. 2005). Unlike antibodies, Affimers display robust characteristics of low molecular weight, high thermostability, and resistance to extreme pH conditions (Tiede et al. 2014). Of key relevance, there is recent work demonstrating the application of Affimers for biosensing applications (Houseman et al. 2002; Klenkar et al. 2006; Seigel et al. 1997; Uchida et al. 2005; Woodman et al. 2005).

This study aims to develop for the first time an Affimer-based electrochemical sensor targeting Her4. Her 4 belongs to the Her (human epidermal growth factor receptor related) family, which includes four transmembrane tyrosine kinase receptors named EGFR: Her1, (ErbB1), Her2 (ErbB2), Her3 (ErbB3) and Her4 (ErbB4) (Tebbutt et al. 2013). The altered expression of the Her family have been implicated in many human diseases and has been proposed as a potential prognostic and diagnostic biomarker (Zhao et al. 2014). Her4, for example, is an emerging biomarker for the detection of gastrointestinal stromal tumours, which accounts for more than 80% of all gastrointestinal mesenchymal tumours and is the most common type of gastrointestinal tumours with increased incidence rate (Mucciarini et al. 2007; Nilsson et al. 2005; Sandvik et al. 2011; Steigen and Eide 2009).

In the current study, a cysteine-terminated Affimer having an affinity towards HER 4 has been used to form a self-assembled monolayer on gold interdigitated microelectrodes (IDμE). The surface was then blocked using phosphate buffer saline (PBS) based PBST20 starting block (SB) to prevent fouling of the surface. The fabricated SB/Affimer/IDμE based Affimer sensor was used to detect HER 4 both in the buffer and spiked human serum samples using non-Faradaic electrochemical impedance spectroscopy (EIS). The Affimer sensor was also characterised with Faradaic EIS, AFM and contact angle measurements. The fabricated Affimer sensor demonstrated excellent sensitivity and a wide dynamic range from 1 pM to 100 nM in both buffer and spiked undiluted human serum samples. When challenged with other serum proteins, the Affimer exhibited excellent specificity towards Her4.

5.2 Experimental

5.2.1 Reagents

Cysteine terminated Affimer binders to Her 4 were generated by Avacta Life Sciences Ltd (Wetherby, UK). For binding studies, different concentrations of HER4 and control molecules were prepared in 10 mM PBS, pH 7.4 or in undiluted serum. Phosphate buffer saline (PBS) based PBST20 starting block (SB) was procured from Fisher Scientific (UK); Dulbecco's Phosphate Buffered Saline and Phosphate Buffered Saline with 0.05% Tween20 was procured from Sigma (UK). All other chemicals were of analytical grade and were used without further purification. All aqueous solutions were prepared using 18.2 MΩ cm ultra-pure water with a Pyrogard® filter (Millipore, MA, USA)

5.2.2 Apparatus

Biosensor fabrication was characterized using electrochemical impedance spectroscopy (EIS) in a three-electrode configuration with gold as counter and pseudo reference electrode at equilibrium potential (open circuit potential generated between electrodes dipped in electrolyte), without external biasing in the frequency range of 100 kHz - 100 mHz, with a 25 mV amplitude using a CompactStat potentiostat/galvanostat (Ivium, The Netherlands). EIS measurements were carried out using 50 μL of PBS solution (10 mM, pH 7.4) containing a mixture of 5 mM $Fe(CN)_6^{4-}$ (ferrocyanide) and 5 mM of $Fe(CN)_6^{3-}$ (ferricyanide) as a redox probe. For HER4 detection and estimation, non-Faradaic EIS measurements (absence of redox couple) were performed in interdigitated two electrodes configuration in 10 mM PBS (pH7.4) in a frequency range 100 kHz - 100 mHz, with a 200 mV amplitude.

Surface characterisation of gold electrodes modified with Affimer was performed using ambient contact mode (tapping mode) atomic force microscopy (AFM) imaging using MultiMode NanoScope with IIIa controller (Bruker, Germany) in conjunction with version 6 control software. Gold chips modified as described in the fabrication section for gold electrodes were imaged with a 10 nm diameter AFM ContAl-G tip (BudgetSensors®, Bulgaria), images were then processed by the NanoScope Analysis software, version 1.5. Contact angle measurements were performed using an in-house

built optical angle measurement system (Miodek et al. 2015). The electrodes were placed on the stage and a 5 µL drop was dispensed on the electrode with the dispensing system. The wetting of surface was then captured using a Nikon p520 camera. Contact angle was measured using a screen protractor version 4.0 procured from Iconico.

5.2.3 Electrode preparation and functionalisation

5.2.3.1 Gold electrode fabrication

Gold interdigitated micro-electrode arrays (IDµE) on silicon/silicon oxide wafers were created using lithographic and micro-fabrication techniques as described in an earlier report (Pui et al. 2013). Interdigitated fingers of 5 µm thickness and 3200 µm length, spaced at 10 µm were deposited over a 5500 µm length. Prior to functionalisation, electrodes were pre-cleaned thoroughly with isopropyl alcohol, acetone and de-ionized milli-Q water (Millipore, UK), followed by treating for 30 min using UV-ozone (ProCleaner, BioForce Nanosciences, USA). For Affimer SAM formation, 100 µg/mL solution of cys-HER4 Affimer containing 5 mM Tris (2-carboxyehyl) phosphine hydrochloride (TCEP 75259 Sigma, UK) was prepared in 10 mM PBS buffer (pH 7.4). and incubated for 30 min at 37 ºC to reduce any di-sulphide bonds. After reduction, 50 µL of this mixture was poured onto the IDµE electrodes and incubated for 120 min at 37 °C. Thereafter, the chips were washed with PBST20 (10 mM, pH 7.4) and PBS (10 mM, pH 7.4) to remove any unbound Affimer. The chips were finally blocked with SB for 30 min and after removing extra solution, chips were stored at 4 ºC until further use. Figure 5.1 shows the schematic for Affimer sensor electrode preparation.

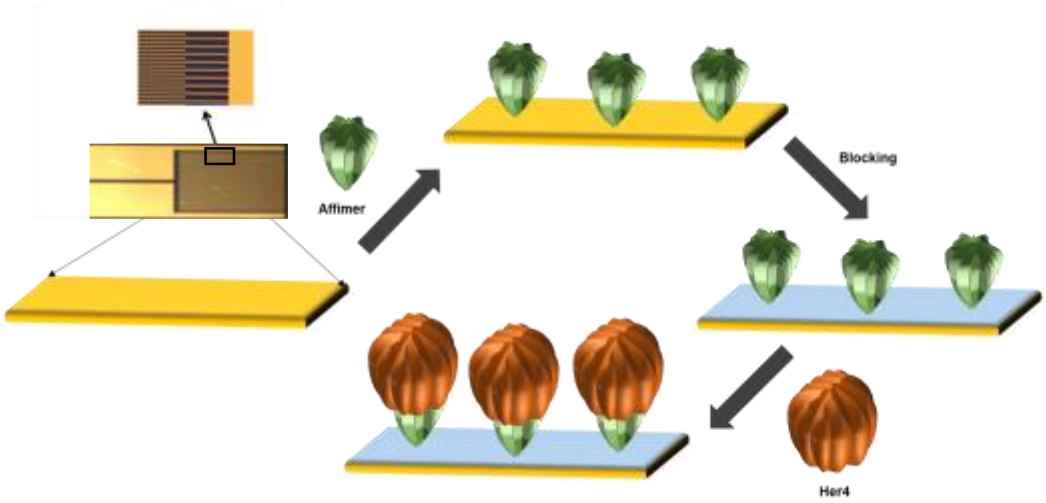

Figure 5.1 Schematic for Affimer sensor preparation and HER4 capture

5.3 Results and discussion

5.3.1 Characterisation of the Affimer sensor fabrication

5.3.1.1 Contact angle and Atomic force microscopic (AFM) characterization

Figure 5.2a and Figure 5.2b show the variation of contact angle of blank gold and after Affimer immobilization. The clear increase in contact angle value from 23º for blank gold to 44º for Affimer/IDµE indicates the formation of an Affimer SAM. Figures 5.2c and 5.2d show the AFM images of blank gold and Affimer-modified gold surface taken in tapping mode using a 10 nm AFM tip. The observed change in non-uniform morphology for blank gold surface to uniformly distributed globular structure for Affimer modified surface confirms the successful immobilization of cysteine modified Affimer onto the gold surface.

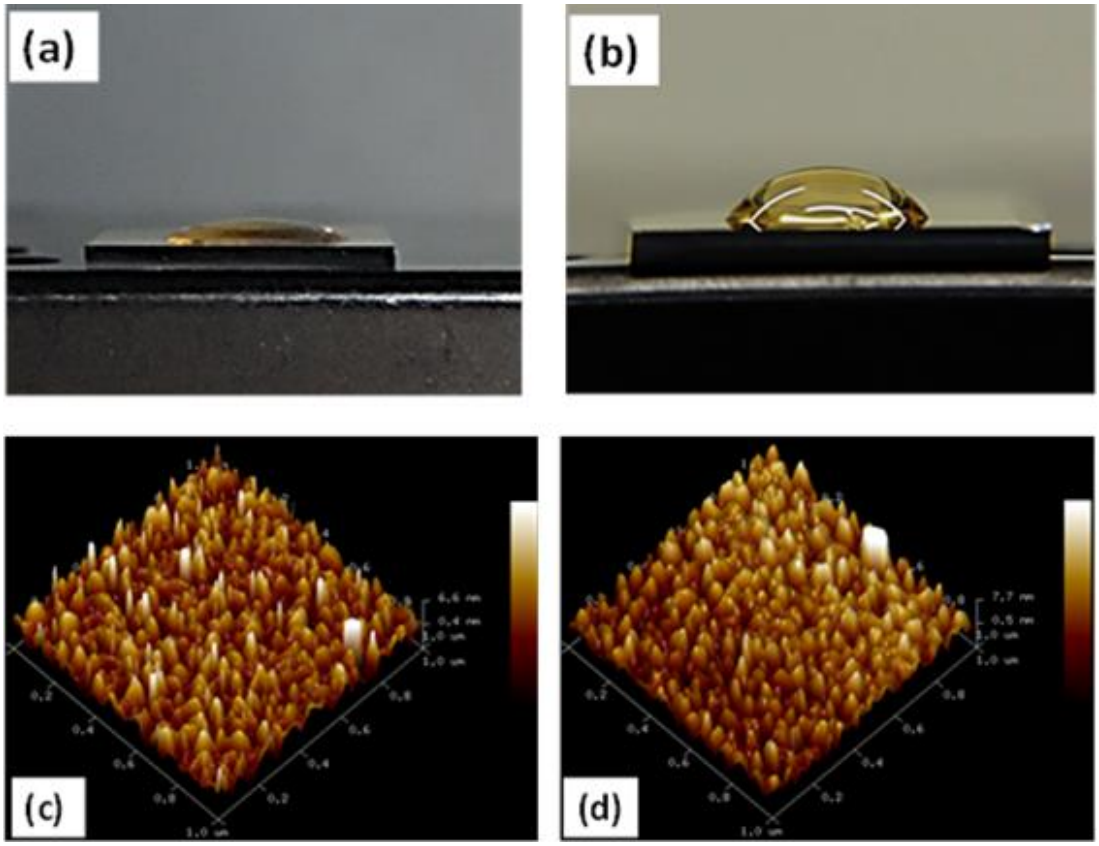

Figure 5.2 Contact angle images for (a) blank cleaned gold surface and (b) after Affimer SAM formation and AFM images for (c) blank cleaned gold surface and (d) after Affimer SAM formation

5.3.1.2 Electrochemical impedance spectroscopy (EIS) and surface plasmon resonance (SPR) characterization

Figure 3a shows the impedance vs. frequency plots for blank, Affimer SAM and blocker modified sensor surface. A change in impedance value from 680 Ω for blank to 50.7 kΩ shows the immobilization of Affimer in high density forming SAM. The large change in impedance can be attributed to the insulating nature and dense immobilization of pre-reduced Affimer solution onto the gold surface. A very small change in impedance is observed after the blocking step, further suggesting the dense coverage by Affimer, which leave very few free spaces on surface to be taken up by blocker protein molecules.

To characterize the ability of surface attached Affimer molecules to capture Her4 molecules, SPR gold chips were modified using the same procedure as that used for IDμE modification. The modified SPR chips were then utilized to investigate Her4 capture in PBST20. Figure 3b shows the SPR binding curves for buffer, 100 pM, 10

nM and 100 nM Her4 in PBST20. Increasing SPR signal for increasing Her4 concentration confirms the activity of Affimer molecules bound on surface.

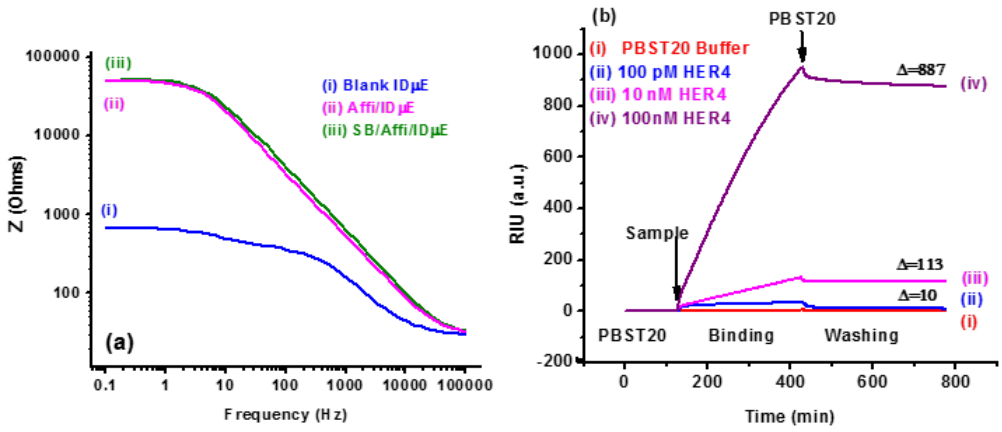

Figure 5.3 (a) Impedance vs. frequency plots for (i) blank IDμE, (ii) Affimer/IDμE and (iii) blocker/Affimer/IDμE. (b) SPR response for (i) PBST20, (ii) 100 pM HER4 in PBST20, (iii) 10 nM Her4 in PBST20 and (iv) 100 nM Her4 in PBST20 using Affimer sensor

5.3.2 Her4 studies

5.3.2.1 Capacitive measurement via electrochemical impedance for Her4 in PBS

The SB/Affimer/IDμE based sensors were utilized to investigate the interaction between surface bound Affimer and Her4 concentrations from 1 pM to 100 nM (Figure 5.4). For measurement of each concentration, the bio-electrode was incubated with a Her4 solution for 30 min, followed by PBST20 and PBS washing. Non-Faradaic EIS spectra was then recorded on washed electrode using PBS (10 mM, pH 7.4) and the obtained data was converted to capacitance values using $C = 1/\omega Z''$. From the capacitance curves (Figure 5.4b), values were noted at 3 Hz, where a maximum in phase angle is observed (Figure 5.4a), corresponding to a maximum capacitive effect. The values were then plotted for different concentrations of Her4 for calibration curve (Figure 5.4c). It is clear from Figure 0.4c that the capacitance decreases linearly with increasing Her4 concentration, which can be attributed to the binding of Her4 proteins onto surface bound Affimer. The electrodes can be used for Her4 sensing in the 1 pM to 100 nM range and can be characterized using the linear equation ΔC (μF) = 3.0949 + 0.2207 log cHer4 (cHer4 is the concentration of Her4 in M) Affimer sensor thus exhibit a sensitivity of 0.22 μF/log cHer4 with a correlation coefficient of 0.996 and a

limit of detection lower than 1 pM. For relative changes, results of different electrodes were found to fall within a 4% error range as indicated by error bars in Figure 5.4c.

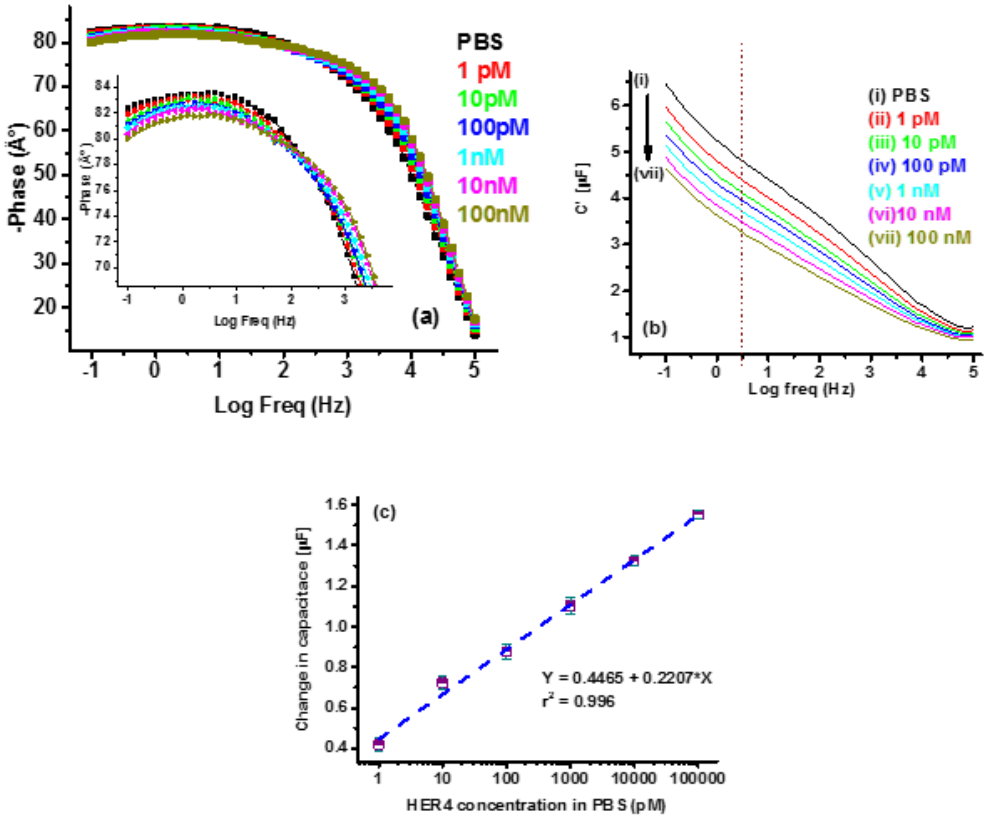

Figure 5.4 (a) EIS phase angle vs. frequency; (b) capacitance data for interaction between surface bound Affimer with HER4 concentrations in PBS; (c) calibration curve using capacitance data for different concentration at 3 Hz

5.3.2.2 Capacitive measurement via electrochemical impedance for Her4 in undiluted serum

To validate the electrode for real sample applications, Affimer sensor electrodes were tested with undiluted serum spiked with Her4 to investigate the interaction between surface bound Affimer and Her4 molecules (1 pM to 100 nM) in presence of all types of serum proteins (Figure 5.5). Bioassay and measurements were carried out in same manner as for PBS. Similarly, non-Faradaic EIS data was converted to capacitance and using capacitance curves (Figure 5.5b), capacitance values were noted at 1 Hz, where the maximum phase angle is observed (Figure 5.5a). The slight shift in the frequency for which a maximum phase occurs may be attributed to the presence of all different types of proteins in serum and to different conductivity and ionic strength of

the serum compared to PBS. The capacitance values were then plotted for different concentrations of Her4 for calibration curve (Figure 5.5c). It is clear from Figure 5b that undiluted serum in absence of Her4 shows negligible effects at 1 Hz and a linear decrease in capacitance was observed only in the presence of Her4 in serum indicating selective and successful interaction between Her4 proteins and surface bound Affimer. Again, for sensing application, the relative change in capacitance data was estimated and utilized for more significant information. Figure 5c shows that the electrodes can be used for Her4 sensing in the 1 pM to 100 nM range following linear equation ΔC (μF) = 4.074 + 0.284 log cHer4. Affimer sensor electrode thus exhibit sensitivity of 0.28 μF/log cHer4 with a correlation coefficient of 0.977 and a limit of detection below 1 pM. Results for different electrodes were found to fall within a 5% error range as indicated by the error bars in Figure 5.5c.

The signal for Her4 was found to be higher in serum, which might be attributed to the better interaction of Her4 molecules in their natural environment of serum proteins. However, a slightly lower detection limit and deviation from linearity might be attributed to hindrance in Her4 interaction with bound Affimer caused by other protein molecules present in serum. Affimer sensor electrodes were also tested for serum spiked with the control proteins prostate specific antigen and thrombin and found to result in an insignificant effect on the signal.

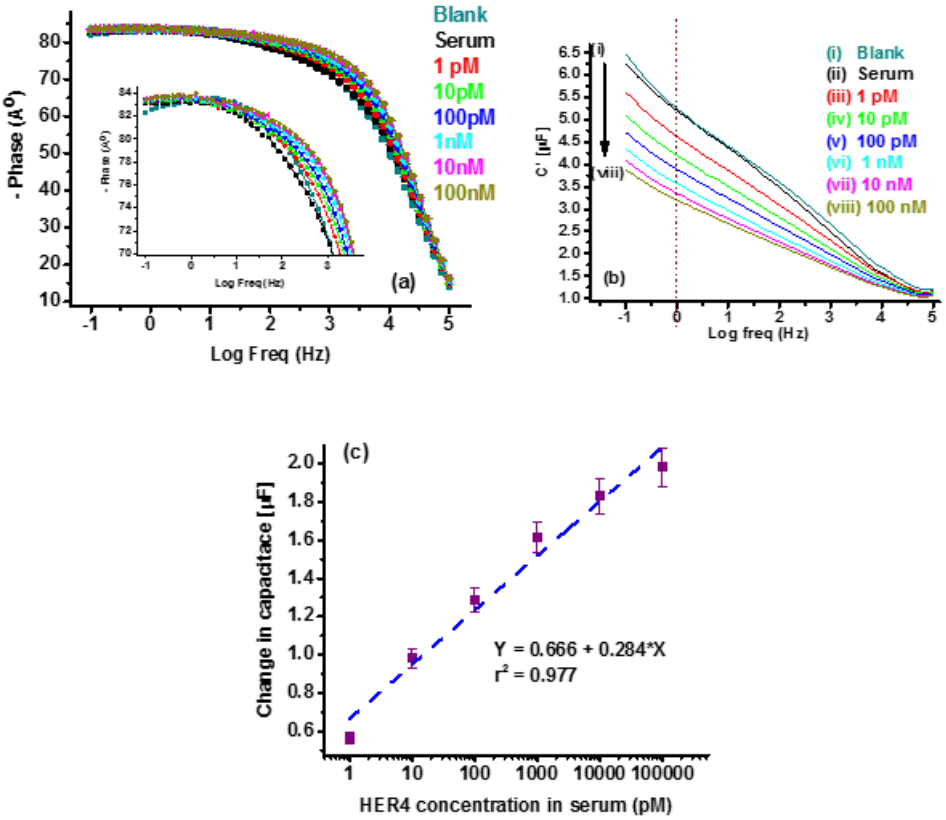

Figure 5.5 (a) EIS phase angle vs. frequency; (b) capacitance data for interaction between surface bound Affimer with HER4 concentrations in undiluted serum; (c) calibration curve using capacitance data for different concentration at 1 Hz

5.4 Conclusions

In conclusion, a new Affimer-based alternative strategy has been demonstrated for the detection of HER4. The Affimer-based sensor shows better sensitivity as compared to antibody-based assays available commercially (LifeSpan BioSciences). The Affimer sensor also showed excellent selectivity when challenged with other serum protein. The prepared electrodes showed the high sensitivity of 0.284 µF/ log cHER4 in undiluted serum with a detection limit lower than 1 pM. The biosensor shows good selective measurement of Her4 in undiluted serum in the concentration range of 1 pM – 100 nM, with very low non-specific response to serum proteins. Furthermore, the fabrication method is simple and can be applied for detection of other biomarkers in a serum sample, paving the way to new platforms for alternative low-cost and rapid biosensors.

Acknowledgements

P.Z and P.J were funded by the European Commission FP7 Programme through the Marie Curie Initial Training Network PROSENSE (grant no. 317420, 2012-2016). Sunil Kumar Arya was funded by the European Commission Horizon 2020 Programme through a Marie Skłodowska-Curie Individual Fellowship (grant no. 655176, 2015-2017).

References

Arya, S.K., Chornokur, G., Venugopal, M., Bhansali, S., 2010. Biosensors and Bioelectronics 25(10), 2296-2301.

Atkins, P., Paula, J.d., 2006. In: Atkins, P., Paula, J.d. (Eds.), ATKINS' PHYSICAL CHEMISTRY, pp. 909-958, 8th ed. W. H. Freeman and Company, New York.

Houseman, B.T., Huh, J.H., Kron, S.J., Mrksich, M., 2002. Nat Biotech 20(3), 270-274.

Huang, Y., Bell, M.C., Suni, I.I., 2008. Analytical Chemistry 80(23), 9157-9161.

Johnson, A., Song, Q., Ko Ferrigno, P., Bueno, P.R., Davis, J.J., 2012. Analytical Chemistry 84(15), 6553-6560.

Keum, J.-W., Bermudez, H., 2009. Chemical Communications(45), 7036-7038.

Klenkar, G., Valiokas, R., Lundström, I., Tinazli, A., Tampé, R., Piehler, J., Liedberg, B., 2006. Analytical Chemistry 78(11), 3643-3650.

Li, X., Shen, L., Zhang, D., Qi, H., Gao, Q., Ma, F., Zhang, C., 2008. Biosensors and Bioelectronics 23(11), 1624-1630.

LifeSpan BioSciences, I., https://www.lsbio.com/elisakits/human-erbb4-her4-elisa-kit-sandwich-elisa-ls-f9465/9465.

Miodek, A., Regan, E., Bhalla, N., Hopkins, N., Goodchild, S., Estrela, P., 2015. Sensors 15(10), 25015.

Mucciarini, C., Rossi, G., Bertolini, F., Valli, R., Cirilli, C., Rashid, I., Marcheselli, L., Luppi, G., Federico, M., 2007. BMC Cancer 7:230(1), 1-7.

Nilsson, B., Bümming, P., Meis-Kindblom, J.M., Odén, A., Dortok, A., Gustavsson, B., Sablinska, K., Kindblom, L.-G., 2005. Cancer 103(4), 821-829.

Pui, T.S., Kongsuphol, P., Arya, S.K., Bansal, T., 2013. Sensors and Actuators B: Chemical 181, 494-500.

Rimmele, M., 2003. ChemBioChem 4(10), 963-971.

Sandvik, O.M., Søreide, K., Kvaløy, J.T., Gudlaugsson, E., Søreide, J.A., 2011. Cancer Epidemiology 35(6), 515-520.

Seigel, R.R., Harder, P., Dahint, R., Grunze, M., Josse, F., Mrksich, M., Whitesides, G.M., 1997. Analytical Chemistry 69(16), 3321-3328.

Song, S., Wang, L., Li, J., Fan, C., Zhao, J., 2008. TrAC Trends in Analytical Chemistry 27(2), 108-117.

Steigen, S.E., Eide, T.J., 2009. APMIS 117(2), 73-86.

Straw, S., Ferrigno, P.K., Song, Q., Tomlinson, D., Galdo, F.D., 2013. J. Biomed. Sci. Eng. 6(8), 32-42.

Sylvia, P., Brehm, S.O., Hoch, H.J.A., 1975. Biochemical and Biophysical Research Communications 63(1), 24-31.

Szymańska, I., Radecka, H., Radecki, J., Kaliszan, R., 2007. Biosensors and Bioelectronics 22(9–10), 1955-1960.

Tebbutt, N., Pedersen, M.W., Johns, T.G., 2013. Nat Rev Cancer 13(9), 663-673.

Tiede, C., Tang, A.A.S., Deacon, S.E., Mandal, U., Nettleship, J.E., Owen, R.L., George, S.E., Harrison, D.J., Owens, R.J., Tomlinson, D.C., McPherson, M.J., 2014. Protein Engineering Design and Selection 27(5), 145-155.

Uchida, K., Otsuka, H., Kaneko, M., Kataoka, K., Nagasaki, Y., 2005. Analytical Chemistry 77(4), 1075-1080.

Woodman, R., Yeh, J.T.H., Laurenson, S., Ferrigno, P.K., 2005. Journal of Molecular Biology 352(5), 1118-1133.

Xu, Y., Cheng, G., He, P., Fang, Y., 2009. Electroanalysis 21(11), 1251-1259.

Zhao, W.-Y., Zhuang, C., Xu, J., Wang, M., Zhang, Z.-Z., Tu, L., Wang, C.-J., Ling, T.-L., Cao, H., Zhang, Z.-G., 2014. American Journal of Cancer Research 4(6), 838-849.

Chapter 6. Conclusions

With the main aim of improving diagnosis and prognosis in the field of cancer detection, the work presented in this thesis is a step towards the development of novel biosensors for multiple protein biomarker detections. Interestingly, research groups around the globe are considering and developing novel synthetic probes for their enhanced application with biosensors to improve both reproducibility and sensitivity coupled with ease of modification and immobilisation. To highlight such an advancement, this dissertation focuses on the alternative probes to their biological counterparts, namely antibodies.

In recent years, there has been a huge turnover in the development of novel bioreceptors, which is mainly due to the emergence of different molecular cloning techniques along with simultaneous accessibility of varied development methods. Whilst antibodies remain the workhorse choice for the molecular recognition for many biosensing devices and laboratory assays, their usage can still impose limitations on technology adoption. For instance, antibodies are often unstable in special conditions such as high temperature or extreme pH. One of the most important parameters of a reliable biosensor is its reproducibility which is significantly affected by the recognition element. Antibodies, which are known to be irreproducible from batch to batch adding on to the disadvantages. Furthermore, limited chemical modification of antibodies further limits their flexibility in the type of immobilisation to various solid supports. To address the drawbacks of antibodies, this thesis will demonstrate the use of synthetic probes like DNA aptamers and affimers for the development of biosensors.

By combining the power of electrochemical detection techniques with novel probes (both DNA aptamers and affimers), modern, label-free and robust biosensors have been developed for cancer diagnostics and prognostic applications. It is worth mentioning that such a biosensor using relatively inexpensive instrumentation could be a step towards a future low-cost point-of-care (POC) device for medical diagnostic applications. One important aspect of the development of a biosensor is its application with clinical samples. The work presented in this thesis will further demonstrate and

evaluate the performance of both DNA aptamer-based and affimer-based biosensor with human serum and plasma samples.

For example, the chapter on the development of PSA-aptasensor presented in this thesis shows how the detection limit of a previously reported methodology using a planar gold surface can be significantly improved with the addition of a simple step to attach AuNPs. In prostate cancer diagnosis, the testing of prostate-specific antigen (PSA) was introduced about 3 decades ago which led to the possibility of early detection of prostate cancer. Although PSA testing reduced the mortality rate, it is also associated with high risk of over diagnosis in patients with and without PCa. Despite the issues associated with PSA testing as a reliable PCa biomarker, this protein biomarker has been chosen for a proof of concept in the project demonstrating a DNA-aptamer based approach for PSA detection. The aptasensor was developed by co-immobilising the anti-PSA aptamer with either FcSH or MCH provides a platform for the amperometric or impedimetric detection of PSA. Due to the combined effect of aptamer and AuNPs modified gold surfaces, we shift the limit of quantification from 60 ng/mL to 10 pg/mL, i.e. nearly 4 orders of magnitude improvement, so that it aligns with the clinically relevant range of 1 to 10 ng/mL. The fabricated aptasensor was successfully tested with spiked human serum samples and a detection of PSA as low as 10 pg/mL was achieved. The real strength of our approach is the simplicity and flexibility of the fabrication process. Simply switching the MCH for FcSH during co-immobilisation of the aptamer probe allows for amperometric detection. Most importantly modifying the planar gold surface with AuNPs can be extended to many other metallic substrates and the simple process of controlling surface coverage of the aptamer probe through co-immobilisation provides mechanisms to achieve robust anti-fouling properties for improved surface chemistry. The aptasensor performed markedly better in its impedimetric guise, with PSA concentrations down to 10 pg/ml detected in diluted human serum with a linear response up to 10 ng/ml. The sensitivity and specificity of the aptasensor make it applicable for clinical analysis of PCa. We believe the simplicity of the fabricated aptasensor offers several advantages compared to other current PCa detection techniques. Moreover, such a dual-detection approach could potentially reduce false positives, providing additional validation of the signals.

Another approach using DNA aptamers have been presented for the detection of breast cancer by capturing Her2 protein (a protein biomarker). In such a device, the planar gold as mentioned in the previous study was replaced with interdigitated Au electrodes. Again, a thiol terminated DNA aptamer with an affinity for Her2 was used to prepare the bio-recognition layer via self-assembly on interdigitated gold surfaces. Non-specific binding was prevented by blocking free spaces on the surface via starting block phosphate buffer saline-tween20 blocker. Non-Faradic EIS measurements were utilised to investigate the sensor performance via monitoring the changes in capacitance. The aptasensor exhibited logarithmically detection for HER2 from 1 pM to 100 nM in the buffer and undiluted serum with limits of detection lower than 1 pM in both buffer and serum, respectively. The biosensor showed excellent selectivity when challenged with other serum protein. The prepared biosensor exhibited linear detection for Her2 at 1 pM to 100 nM range with a high sensitivity of 0.201 μF/ log([Her2] pM) in undiluted serum. Furthermore, the fabrication method is simple and can be applied for detection of other biomarkers in a serum sample, paving the way to a new platform for alternative low-cost and rapid biosensors.

The trend towards the development of aptamer-based sensors for both PSA and her2 requires further research into their usage as an alternative to antibodies. Overall, the expansion of aptasensors for biomarker detection is anticipated to draw increasing interest in the coming years, thanks to its advantages over antibodies.

More recently, developments in the field of biochemistry and molecular biology have led to a deeper understanding of the role of peptide-based probes and demonstrated that the roles they play are far greater than originally expected. This led to the new horizons of biosensing applications, where oligonucleotide-based biosensing could be potentially be replaced by peptide-based approaches which can have an unparalleled impact on molecular diagnostics. The increasing demand for enhanced efficiency and to overcome some of the drawbacks of using oligonucleotides or antibodies, has enabled biochemists to come up with synthetic analogues of antibodies called Affimers, which have further amplified the projections of biosensing approaches.

The last chapter, a new probe (Affimer) has been investigated for the development of a biosensor for stromal tumours, by targeting Her4 protein. Affimer technology has been engineered to overcome many of the problems associated with aptamers or with antibodies and possess a number of unique key benefits. Sensitivity to the assay environment has been solved because the Affimer scaffold has evolved to be resistant to a wide pH range, making it suitable for an equally wide range of assay conditions.

The Affimer scaffold has been engineered so that it no longer binds to proteins found in human cells, serum or plasma. The Biological half-life of Affimer molecules is also superior because they are biologically and biophysically stable. We have demonstrated that the Affimer-based sensor shows better sensitivity as compared to antibody-based assays available commercially (LifeSpan BioSciences). A pre-modified cysteine-terminated Affimer with an affinity for Her4 was utilised to prepare the bio-recognition layer via self-assembly on gold interdigitated electrodes for the sensor fabrication. Again, electrochemical impedance spectroscopy (EIS) in the absence of redox markers was used to evaluate the sensor performance by monitoring the changes in capacitance. The Affimer sensor also showed excellent selectivity when challenged with other serum protein. The prepared electrodes showed the high sensitivity of 0.284 µF/ log cHer4 in undiluted serum with a detection limit lower than 1 pM. The biosensor shows good selective measurement of HER4 in undiluted serum in the concentration range of 1 pM to 100 nM, with very low non-specific response to serum proteins. Furthermore, the fabrication method is simple and can be applied for detection of other biomarkers in a serum sample, paving the way to new platforms for alternative low-cost and rapid biosensors.

In conclusion, the development of both DNA aptamer-based and Affimer-based biosensor devices is an interdisciplinary field and many aspects such as probe design, surface chemistry, sensor design, microfluidics, etc. Several biosensing systems were analysed and practical applications with complex samples (serum and plasma) for cancer biomarker detection have been demonstrated. By a strategic coupling of biological probes to the electrode surfaces together with electrochemical techniques, effective and low-cost biosensors could be realised and could be easily integrated into multiplexed systems. These studies not only demonstrate the enormous potential of

synthetic receptors (DNA apatmers and Affimers) but how they can be used for a wide range of other biomarkers for various diseases that exploit target/probe features like those of the systems here reported. The studies demonstrated in the thesis is a step towards the development of a multiplexed sensing platform by monitoring various biomarkers or a single or multiple diseases. As a result, a more informed and reliable analysis could be attained by reducing the probability of false positives. Furthermore, such devices could be easily represented as a POC device that can give the first assessment of the health of patients which would help the clinician to take immediate actions. Not only these devices could be used for diagnosis and prognosis, it can also be used for surveillance purposes which can be used to monitor patient's health post-treatment.